

การเปรียบเทียบคุณภาพของภาพถ่ายดิจิทัลที่ได้จากเซ็นเซอร์รับภาพต่างกัน



นาย วิริยะ พรกุลวิไล

สถาบันวิทยบริการ
จุฬาลงกรณ์มหาวิทยาลัย

วิทยานิพนธ์นี้เป็นส่วนหนึ่งของการศึกษาตามหลักสูตรปริญญาวิทยาศาสตรมหาบัณฑิต
สาขาวิชาเทคโนโลยีทางภาพ ภาควิชาวิทยาศาสตร์ทางภาพถ่ายและเทคโนโลยีทางการพิมพ์

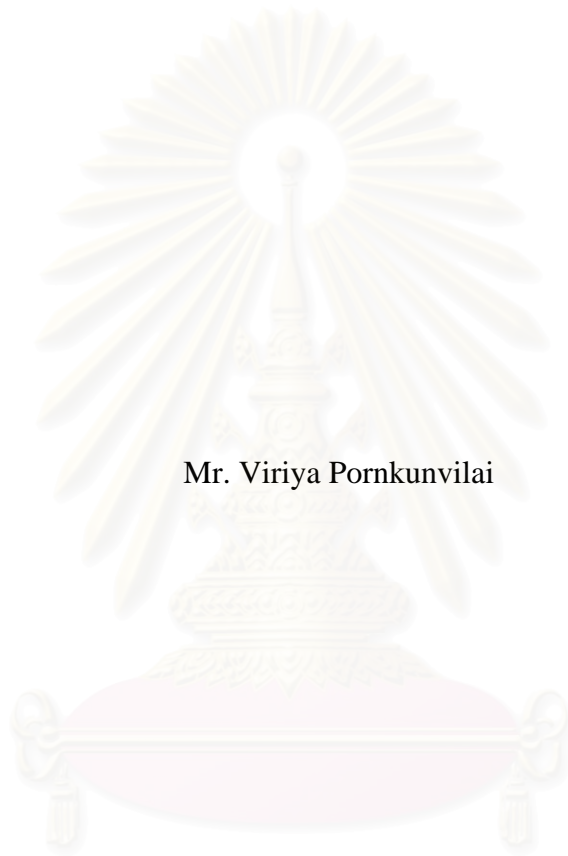
คณะวิทยาศาสตร์ จุฬาลงกรณ์มหาวิทยาลัย

ปีการศึกษา 2547

ISBN 974-53-1931-7

ลิขสิทธิ์ของจุฬาลงกรณ์มหาวิทยาลัย

COMPARISON OF DIGITAL IMAGE QUALITY OBTAINED FROM
DIFFERENT IMAGE SENSORS



Mr. Viriya Pornkunvilai

สถาบันวิทยบริการ
จุฬาลงกรณ์มหาวิทยาลัย

A Thesis Submitted in Partial Fulfillment of the Requirements
for the Degree of Master of Science Program in Imaging Technology
Department of Photographic Science and Printing Technology

Faculty of Science

Chulalongkorn University

Academic Year 2004

ISBN 974-53-1931-7

Thesis Title COMPARISON OF DIGITAL IMAGE QUALITY OBTAINED
FROM DIFFERENT IMAGE SENSORS

By Mr. Viriya Pornkunvilai

Field of Study Photographic Science and Printing Technology

Thesis Advisor Chawan Koopipat, Ph.D.

Accepted by the Faculty of Science, Chulalongkorn University in Partial
Fulfillment of the Requirements for the Master's Degree

..... Dean of the Faculty of Science
(Professor Piamsak Menasveta, Ph.D.)

THESIS COMMITTEE

..... Chairman
(Assistant Professor Aran Hansuebsai, Ph.D.)

..... Thesis Advisor
(Chawan Koopipat, Ph.D.)

..... Member
(Pichayada Katemake, Ph.D.)

..... Member
(Suchitra Sueeprasan, Ph.D.)

วริยะ พรกุลวิไล : การเปรียบเทียบคุณภาพของภาพถ่ายดิจิทัลที่ได้จากเซ็นเซอร์รับภาพต่างกัน (COMPARISON OF DIGITAL IMAGE QUALITY OBTAINED FROM DIFFERENT IMAGE SENSORS) อ. ที่ปรึกษา : ดร. ชวาล คุรุพิพัฒน์, 153 หน้า. ISBN 973-53-1931-7.

กล้องถ่ายภาพนิ่งดิจิทัลได้รับการยอมรับว่าเป็นอุปกรณ์สำหรับการบันทึกภาพที่สำคัญในปัจจุบัน เซ็นเซอร์รับภาพถือว่ามีบทบาทสำคัญอย่างยิ่งในการนำเสนอคุณภาพของภาพถ่ายและของกล้องดิจิทัล ดังนั้นงานวิจัยนี้จึงมีจุดประสงค์เพื่อทำการทดสอบถ่ายภาพด้วยกล้องดิจิทัลที่เกิดจากการเก็บภาพด้วยเซ็นเซอร์รับภาพชนิดต่างๆ ได้แก่ ซีซีดี ซุปเปอร์ซีซีดี ซีมอส และไพโรอนเอ็กซ์ทีรี รวมถึงการนำผลมาเปรียบเทียบคุณภาพของภาพในด้านต่างๆ ได้แก่ ความละเอียด การผลิตน้ำหนักรสี การผลิตสี และการขึ้นเงน/สัญญาณรบกวน สำหรับการทดสอบความละเอียดของภาพ ค่าความละเอียดที่มองเห็นได้ และเอสเอฟอาร์ (SFR, spatial frequency response) ถูกนำมาวิเคราะห์และเปรียบเทียบ สำหรับการทดสอบการผลิตน้ำหนักรสี งานวิจัยนี้ได้ทำการเปรียบเทียบเส้นกราฟแสดงลักษณะของการผลิตน้ำหนักรสีของค่าอิมเมจพิกเซล สำหรับการทดสอบการผลิตสีนั้นค่า ΔE^*_{ab} (ค่าความผิดพลาดของสีของ Macbeth color checker) ถูกนำมาวิเคราะห์และเปรียบเทียบ สำหรับการขึ้นเงน/สัญญาณรบกวน ซึ่งประกอบด้วยสัญญาณรบกวนประเภทต่างๆ อาทิเช่น ดาร์กเคอร์เรนทน้อยส์ แอนพริไฟเออร์น้อยส์ เทอร์มอลน้อยส์ และชอตน้อยส์ เป็นต้น ค่าความเบี่ยงเบนมาตรฐานของค่าอิมเมจพิกเซลที่สีเทากลาง ถูกนำมาวิเคราะห์และเปรียบเทียบ ผลที่ได้จากการทดสอบความละเอียด ของภาพพบว่า ฟุจิเอสทูโปร (ซูเปอร์ซีซีดี) มีค่าแอมป์โซลูชันรีโซลูชัน และค่าเอ็กทินชันรีโซลูชันสูงสุด ในขณะที่ ซิกม่าเอสดีไนย์ (ไพโรอนเอ็กซ์ทีรี) มีค่าเอสเอฟอาร์สูงสุด ผลที่ได้จากการทดสอบโทนรีโปรดักชันพบว่า แคนอนดีซิกตี้ (ซีมอส) มีค่าไดนามิกเรนจ์สูงสุด ซึ่งแสดงให้เห็นว่า ซีมอสสามารถเก็บความสว่างและความมืดของภาพถ่ายได้ดีที่สุดในบรรดาเซ็นเซอร์ทั้งหมดที่ทำการเปรียบเทียบ ผลที่ได้จากการทดสอบคัลเลอร์รีโปรดักชันที่การวิเคราะห์ทุกโทนสีพบว่า นิกอนดีวันฮันเดร็ด (ซีซีดี) มีค่าความผิดพลาดของสีต่ำสุด ซึ่งแสดงให้เห็นว่าซีซีดีสามารถสูงที่สุดในการเก็บรายละเอียดของสีทุกสีได้ใกล้เคียงกับสีธรรมชาติ ผลที่ได้จากการทดสอบเกนนิ่งเนส/น้อยส์พบว่า แคนอนดีซิกตี้ (ซีมอส) มีค่าแอมพริไฟเออร์น้อยส์ต่ำสุดในลูมิเนียสซาแนลที่ค่าไอเอสโอ100 ในขณะที่ฟุจิเอสทูโปร (ซูเปอร์ซีซีดี) มีค่าแอมพริไฟเออร์น้อยส์ต่ำสุดในลูมิเนียสซาแนลที่ค่าไอเอสโอ200ถึงค่าไอเอสโอ1600 ซึ่งแสดงให้เห็นว่าซีมอสมีความแม่นยำสูงที่สุดในการให้สัญญาณภาพที่ค่าไอเอสโอ100 ในขณะที่ซูเปอร์ซีซีดีให้ผลที่ดีกว่าที่ค่าไอเอสโอ200ถึงค่าไอเอสโอ1600 อย่างไรก็ตาม คุณภาพของเซ็นเซอร์รับภาพที่ได้จะขึ้นอยู่กับโปรแกรมการจัดการของกล้องแต่ละยี่ห้อ

ภาควิชา วิทยาศาสตร์ทางภาพถ่ายและเทคโนโลยีทางการพิมพ์ ลายมือชื่อนิสิต

สาขาวิชา เทคโนโลยีทางภาพ ลายมือชื่ออาจารย์ที่ปรึกษา

ปีการศึกษา 2547 ลายมือชื่ออาจารย์ที่ปรึกษาร่วม

4472410023 : MAJOR IMAGING TECHNOLOGY

KEY WORD : IMAGE SENSORS, CCD, SUPER CCD, CMOS, FOVEON X3, IMAGE RESOLUTION, TONE REPRODUCTION, COLOR REPRODUCTION, AND GRANINES/NOISE

VIRIYA PORNKUNVILAI: COMPARISON OF DIGITAL IMAGE QUALITY OBTAINED FROM DIFFERENT IMAGE SENSORS. THESIS ADVISOR: CHAWAN KOOPIPAT, DR., 153 pp. ISBN 974-53-1931-7.

Nowadays, digital still camera is worldwide accepted as a significant input device. Image sensors play a vital role for the image quality of digital still cameras. The purpose of this research is to evaluate and compare the digital image quality generated from four different image sensors, i.e. CCD, Super CCD, CMOS and FOVEON X3, in terms of image resolution, tone reproduction, color reproduction and graininess/noise. For image resolution, visual resolution and spatial frequency response (SFR) were measured and compared. For tone reproduction, comparisons of tone reproduction curve of image pixel values were performed. For color reproduction, Delta E^*_{ab} (color error of Macbeth color checker) were measured and compared. With different kinds of graininess/noise including dark current noise, amplifier noise, thermal noise and shot noise, the standard deviations of image pixel value at middle gray were measured and compared. For the image resolution measurement, Fuji S2pro (Super CCD) had highest absolute and extinction resolution while Sigma SD9 (Foveon X3) had the highest SFR, which represents the best contrast. For the tone reproduction measurement, Canon D60 (CMOS) had the highest dynamic range which means that CMOS could best capture the bright and dark areas. For the color reproduction measurement with all color tones analysis, Nikon D100 (CCD) had lowest color error, which means that CCD could most capture the natural color in all color. For the graininess/noise measurement, Canon D60 (CMOS) had the lowest amplifier noise in luminous channel at ISO100 while Fuji S2pro (Super CCD) had the lowest amplifier noise in luminous channel at ISO200-ISO1600. It means that CMOS had high capacity in providing an accurate image signal at ISO100 while Super CCD was better at ISO200-ISO1600. Nevertheless, the effectiveness of each image sensor could be differently among the management program of each camera.

Department Photographic Science and Printing Technology Student's signature.....

Field of study Imaging Technology Advisor's signature.....

Academic year 2004 Co-advisor's signature.....

ACKNOWLEDGEMENTS

I would like to express the sincere gratitude to my advisor, Dr. Chawan Koopipat, for his helpful guidance and suggestion during the research to make this study successful. As well, I would like to convey my appreciation to the committee members for their constructive comments and suggestions which broaden perspective.

I specially express my sincere thanks to all of institutions and kind sponsors on providing equipments and materials support including Niks (Thailand) Ltd for Nikon D100, Fuji Photo Film (Thailand) Ltd. For Fuji S2pro, Mr. Surat Osathanugrah from The Royal Photographic Society of Thailand under The Royal Patronage of H.M. The King for Broncolor HMI 575, Mr. Somchai Buddha for Minolta Color Meter IIIIF and Mr. Theeradej Singjaroenkun for Sigma Lens 15-30mm F3.5-4.5 of Canon.

Many thanks to my colleagues at Department of Photographic Science and Printing Technology from Chulalongkorn University for their helpfulness and warm encouragement to make this thesis become realized.

Lastly, I am very gratitude to my family and my beloved for their inspiration, understanding and endless encouragement throughout this achievement.

CONTENTS

	PAGE
ABSTRACT (IN THAI).....	iv
ABSTRACT (IN ENGLISH).....	v
ACKNOWLEDGEMENTS.....	vi
CONTENTS.....	vii
LIST OF TABLES.....	xi
LIST OF FIGURES.....	xvii
CHAPTER I : INTRODUCTION.....	4
1.1 Scientific Rationale.....	4
1.2 Objectives of the Research Work.....	5
1.3 Scope of the Research Work.....	5
1.4 Content of the Research work.....	5
CHEAPTER II : THEORY AND LITERATURE REVIEW	7
2.1 Theoretical Background	7
2.1.1 Image Sensors Types.....	7
2.1.1.1 CCD (Charge Coupled Device).....	7
2.1.1.2 Super CCD.....	10
2.1.1.3 CMOS (complementary metal oxide semiconductor).....	11
2.1.1.4 FOVEON X3.....	13
2.1.2 Digital Image Quality Measurement	14
2.1.2.1 Image Resolution	14
2.1.2.2 Toner Reproduction	17
2.1.2.3 Color Reproduction	19

	PAGE
2.1.2.4 Graininess/Noise.....	22
2.2 Literature Reviews.....	28
CHAPTER III : EXPERIMENTAL.....	30
3.1 Material.....	30
3.2 Apparatus.....	30
3.3 Software Application.....	31
3.4 Procudure.....	31
3.4.1 Experiment Setup.....	31
3.4.2 Experimental Procedure.....	31
3.4.2.1 Preparation of Resolution Measurement.....	31
3.4.2.2 Preparation of Tone Reproduction Measurement...	33
3.4.2.3 Preparation of Color Reproduction Measurement...	37
3.4.2.4 Preparation of Graininess/Noise Measurement.....	38
3.4.2.4.1 Preparation of Dark Current Noise Measurement.....	38
3.4.2.4.2 Preparation of Amplifier Noise Measurement.....	38
3.4.2.4.3 Preparation of Shot Noise Measurement.....	39
CHAPTER IV : RESULTS AND DISCUSSION.....	41
4.1 The Image Resolution.....	41
4.1.1 The Preparation and Evaluation of the Image Resolution.....	41
4.1.1.1 Virtual Resolution	42

	PAGE
4.1.1.2 Spatial Frequency Resolution (SFR)	48
4.1.2 The Comparison of the Image Resolution.....	59
4.2 The Tone Reproduction.....	62
4.2.1 The Preparation and Evaluation of the Tone Reproduction....	62
4.2.2 The Comparison of the Tone Reproduction.....	72
4.3 The Color Reproduction.....	74
4.3.1 The Preparation and Evaluation of the Color Production.....	74
4.3.2 The Comparison of the Color Reproduction.....	93
4.4 The Noise and Graininess.....	99
4.3.1 The Preparation and Evaluation of the Noise and Graininess.	99
4.3.2 The Comparison of the Noise and Graininess.....	109
CHAPTER V : CONCLUSIONS AND SUGGESTION.....	121
5.1 Conclusions.....	121
5.1.1 Conclusions of Resolution Measurement.....	121
5.1.2 Conclusions of Tone Reproduction Measurement.....	122
5.1.3 Conclusions of Color Reproduction Measurement.....	123
5.1.4 Conclusions of Graininess/Noise Measurement.....	124
5.2 Suggestions for Future Work.....	129
REFERENCES.....	130
APPENDICES.....	133
Appendix A.....	134
Appendix B.....	140
Appendix C.....	142

VITA..... 153



สถาบันวิทยบริการ
จุฬาลงกรณ์มหาวิทยาลัย

LIST OF TABLES

TABLE	PAGE
4-1 The specification of each image sensor.....	41
4-2 The visual resolution measurement of each image sensor.....	46
4-3 The value of horizontal SFR and vertical SFR from Nikon D100.....	51
4-4 The value of horizontal SFR and vertical SFR from Fuji S2pro.....	53
4-5 The value of horizontal SFR and vertical SFR from Canon D60.....	55
4-6 The value of horizontal SFR and vertical SFR from Sigma SD9.....	57
4-7 Number of observers who can differentiate the shadow detail.....	62
4-8 Color value of Macbeth color checker(24 patches) measured by Gretag Spectrolino under D65.....	76
4-9 Color value and color difference of Macbeth color checker (24 patches) captured by Nikon D10 under D65.....	77
4-10 Color value and color differences of Macbeth color checker (24 patches) captured by Fuji S2pro under D65.....	79
4-11 Color value and color differences of Macbeth color checker (24 patches) captured by Canon D60 under D65.....	81
4-12 Color value and color differences of Macbeth color checker (24 patches) captured by Sigma SD9 under D65.....	83
4-13 Color value and color differences of Macbeth color checker (24 patches) captured by Nikon D100 under daylight illumination and with auto white balance setting	85
4-14 Color value and color differences of Macbeth color checker (24 patches) captured by Fuji S2pro under daylight illumination and with auto white balance setting	87

TABLE	PAGE
4-15 Color value and color differences of Macbeth color checker (24 patches) captured by Canon D60 under daylight illumination and with auto white balance setting	89
4-16 Color value and color differences of Macbeth color checker (24 patches) captured by Sigma SD9 under daylight illumination and with auto white balance setting	91
4-17 Total Delta E^*_{ab} of Macbeth color checker of all digital cameras	93
4-18 The classification of CIE color space in the a^*b^* plane for comparing the color error of normal image sensor	94
4-19 The average Delta E^*_{ab} calculated from all 5 color groups classified in Table 4-18, show the capability of each image sensor in color reproduction once comparing to an ideal color	95
A-1 The relationship between the density and reflectance of Kodak grayscale and the pixel value of image captured by each image sensor.....	133
A-2 The reflectance and pixel value of Kodak grayscale of each image sensor after adjustment.....	135

LIST OF FIGURES

FIGURE	PAGE
2-1 Area scanning.....	8
2-2 Full-frame architecture.....	8
2-3 Frame-transfer architecture.....	9
2-4 Interline architecture.....	9
2-5 Pixel layout comparison.....	11
2-6 CMOS image architecture.....	12
2-7 Typical bayer filter pattern showing the alternative sampling of red, green, and blue pixels.....	13
2-8 Schematic depiction of Foveon X3 image sensor showing stacks of color pixels, which record color depth wise in silicon	14
2-9 Resolution test chart.....	15
2-10 Test chart features.....	16
2-11 Dynamic range in digital images.....	18
2-12 Noise in digital images.....	24
2-13 The Fixed pattern noise from image taken with a digital camera.....	26
2-14 The Amplifier noise from images of a Kodak color patch taken with a digital camera	27
3-1 The Macbeth color checker.....	34
3-2 The dark point test chart of various pixels value from 1-5 with pixels level range between 0-7 each	35

FIGURE	PAGE
3-3 The dark point test chart of various pixels value from 1-5 with pixels level range between 8-15 each.....	36
4-1 The resolution test chart resulting from each image sensor.....	42
4-2 The horizontal LW/PH (line widths per picture height) resulting from each image sensor.....	43
4-3 The vertical LW/PH (line widths per picture height) resulting from each image sensor.....	44
4-4 The 5° diagonal LW/PH (line widths per picture height) resulting from each image sensor.....	45
4-5 The horizontal slant edge (L3) test chart of each image sensor.....	49
4-6 The vertical slant edge (L4) test chart of each image sensor.....	50
4-7 The horizontal SFR and vertical SFR from Nikon D1.....	52
4-8 The horizontal SFR and vertical SFR from Fuji S2pro.....	54
4-9 The horizontal SFR and vertical SFR from Canon D60.....	56
4-10 The horizontal SFR and vertical SFR from Nikon Sigma SD9.....	58
4-11 The horizontal SFR of each image sensor.....	59
4-12 The vertical SFR of each image sensor.....	60
4-13 Tone reproduction at 8 bits per channel from Nikon D100.....	63
4-14 The middle gray patches of various shutter speeds (11.5 stop) captured by Nikon D100.....	64
4-15 Tone reproduction at 8 bits per channel from Fuji S2pro.....	65
4-16 The middle gray patches of various shutter speeds (11.5 stop) captured by Fuji S2pro.....	66

FIGURE	PAGE
4-17 Tone reproduction at 8 bits per channel from Canon D60.....	67
4-18 The middle gray patches of various shutter speeds (11.5 stop) captured by Canon D60.....	68
4-19 Tone reproduction at 8 bits per channel from Sigma SD9.....	69
4-20 The middle gray patches of various shutter speeds (11.5 stop) captured by Sigma SD9.....	71
4-21 The luminosity of tone reproduction at 8 bits per channel from all image sensors	72
4-22 The 24 assigned numbers to each color patch of the Macbeth Color Checker.....	74
4-23 Color error in the a*b*plane of the CIELAB color space captured by Nikon D10 under D65.....	78
4-24 Color error in the a*b*plane of the CIELAB color space captured by Fuji S2pro under D65.....	80
4-25 Color error in the a*b*plane of the CIELAB color space captured by Canon D60 under D65.....	82
4-26 Color error in the a*b*plane of the CIELAB color space captured by Sigma SD9 under D65.....	84
4-27 Color error in the a*b*plane of the CIELAB color space captured by Nikon D100 under daylight illumination and with auto white balance setting.....	86
4-28 Color error in the a*b*plane of the CIELAB color space captured by Fuji S2pro under daylight illumination and with auto white balance setting.....	88

FIGURE	PAGE
4-29 Color error in the a*b*plane of the CIELAB color space captured by Canon D60 under daylight illumination and with auto white balance setting.....	90
4-30 Color error in the a*b*plane of the CIELAB color space captured by Sigma SD9 under daylight illumination and with auto white balance setting.....	92
4-31 Dark current noise- from Nikon D100.....	100
4-32 Dark Current Noise- from Fuji S2pro.....	100
4-33 Dark Current Noise- from Canon D60.....	101
4-34 Dark Current Noise- from Sigma SD9.....	101
4-35 Amplifier Noise from Nikon D100.....	102
4-36 Amplifier Noise from Fuji S2pro.....	103
4-37 Amplifier Noise from Canon D60.....	103
4-38 Amplifier Noise from Sigma SD9.....	104
4-39 Shot Noise from Nikon D100.....	105
4-40 Shot Noise from Fuji S2pro.....	106
4-41 Shot Noise from Canon D60.....	107
4-42 Shot Noise from Sigma SD9.....	108
4-43 Dark current noise of all image sensors in red, green, and blue channel.....	109
4-44 Dark current noise of all image sensors in luminance channel.....	111
4-45 Amplifier noise of all image sensors in red, green, and blue channel.....	114
4-46 Amplifier noise of all image sensors in luminance channel.....	115
4-47 Shot noise of all image sensors in red, green, and blue channel.....	118
4-48 Shot noise of all image sensors in luminance channel.....	119
A-1 Tonal response curves for Nikon D100 (CCD).....	135

FIGURE	PAGE
A-2 Tonal response curve for Nikon D100 (CCD) after adjusting the reflectance and pixel value.....	137
A-3 Tonal response curves for Nikon D100 (CCD) – Set Data 1 after adjusting the reflectance and pixel value of Kodak grayscale.....	138
A-4 Tonal response curves for Nikon D100 (CCD) – Set Data 2 after adjusting the reflectance and pixel value of Kodak grayscale.....	138
A-5 Tonal response curves for Nikon D100 (CCD) – Set Data 3 after adjusting the reflectance and pixel value of Kodak grayscale.....	137
A-6 Tonal response curves for Nikon D100 (CCD) – Set Data 4 after adjusting the reflectance and pixel value of Kodak grayscale.....	137
B-1 The dynamic range from calculating tone reproduction at luminosity channel of Canon D60.....	140

CHAPTER I

INTRODUCTION

1.1 Scientific Rationale

Nowadays, a digital still camera is worldwide accepted as a significant input device. Image sensors play a vital role for the image quality of digital still cameras; therefore, suppliers have extensively developed new technology and generated various new types of image sensors in the market for customizing different using purposes. For example, one may pay most attention on sharpness while another may concentrate to color reproduction.

Generally, image quality measurement is determined by sharpness, graininess, tone and color reproduction (1). The purpose of this research is to compare the digital image quality generated from four different image sensors, i.e. CCD, Super CCD, CMOS and FOVEON X3.

The result of this experiment will give not only the comparable advantages and disadvantages, but also an overview of efficiency of each image sensor. This information can be used for decision making with respect to the needs of the individuals when purchasing a digital camera.

1.2 Objectives of Research Work

To evaluate and compare the image quality in terms of resolution, tone reproduction, color reproduction and graininess/noise obtained from different image sensors.

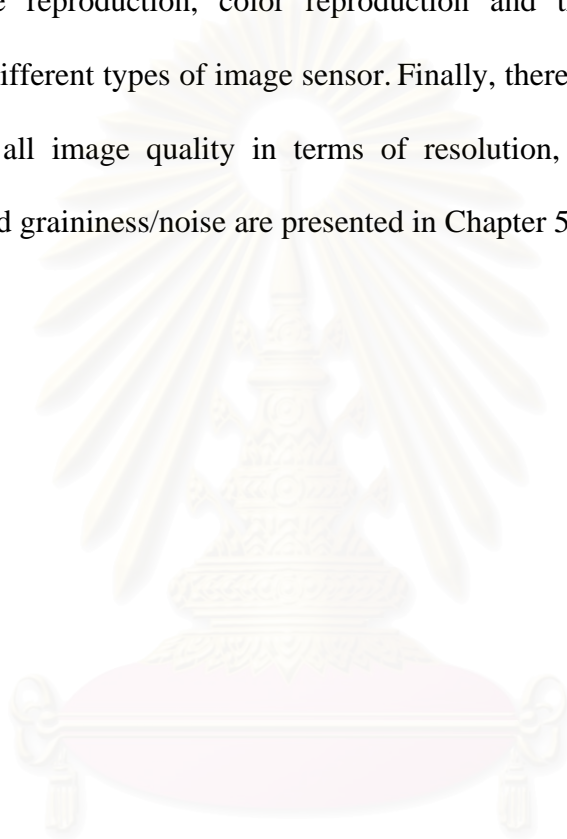
1.3 Scope of the Research Work

To evaluate and compare the image quality generated from four different image sensors, i.e. CCD, Super CCD, CMOS and FOVEON X3, in terms of image resolution, tone reproduction, color reproduction and graininess/noise. For resolution, visual resolution and spatial frequency response (SFR) are measured and compared. For tone reproduction, the comparison will be made in terms of tone reproduction curve of image pixel values. For color reproduction, Delta E^*_{ab} (color error of macbeth color checker) will be measured and compared. The last measurement in terms of graininess/noise will be calculated from different kinds of noise such as dark current noise, amplifier noise, thermal noise and shot noise.

1.4 Contents of the Research Work

This thesis consists of 5 chapters including introduction, theoretical background and literature review, experimental, results and discussion, and conclusion and suggestions. Chapter 1 is an introduction of this thesis. Chapter 2 concerns a brief description of the type of image sensors, CCD (charge-coupled

device), Super CCD, CMOS (complementary metal oxide semiconductor), FOVEON X3, the digital image quality measurement in terms of image resolution, tone reproduction, color reproduction, graininess/noise and the short literature review of previous studies. Chapter 3 is the experimental materials and the experimental apparatus of the research. Chapter 4 interprets the results and discussion of image resolution, tone reproduction, color reproduction and the noise and graininess obtained from different types of image sensor. Finally, there will be an evaluation and comparison of all image quality in terms of resolution, tone reproduction, color reproduction and graininess/noise are presented in Chapter 5.



สถาบันวิทยบริการ
จุฬาลงกรณ์มหาวิทยาลัย

CHAPTER II

THEORY AND LITERATURE REVIEWS

1.1.Theoretical Background

2.1.1 Image Sensors Types

Image sensors are silicon chips containing 'photosensitive diode'. This photosensitive diode are generally known as 'photosite' where are sorted as a mesh and have similar function to a film in photography. Image sensors are like the human's retina and also can produce the slight electricity inside once the light has collided with the chips. More captured light will generate more electricity that could be converted to digital numeric by A/D converter and later be transformed to digital image.

2.1.1.1 CCD (Charge-Coupled Device)

CCDs (2) can take on various architectures. The primary CCDs in use today are called full-frame transfer and frame-transfer devices, which use MOS photocapacitors as detectors, and interline transfer devices that use photodiodes and photocapacitors as the detector. Each is described below as applied to area CCD sensors but the concepts also apply to linear CCDs. Other image sensing architectures,

which will not be discussed here, include frame-interline transfer, accordion, charge injection and MOS XY addressable among others.

- **Full-frame**

Full-frame CCDs have the simplest architecture and are the easiest to fabricate and operate. They consist of a parallel CCD shift register, a serial CCD shift register and a signal sensing output amplifier. (See Figure 2-4) Images are optically projected onto the parallel array that acts as the image plane. The device takes the scene information and partitions the image into discrete elements that are defined by the number of pixels thus "sampling" the scene. The resulting rows of scene information are then shifted in a parallel fashion to the serial register that subsequently shifts the row of information to the output as a serial stream of data. The process repeats until all rows are transferred off chip. The image is then reconstructed as dictated by the system. Since the parallel register is used for both scene detection and readout, a mechanical shutter or synchronized strobe illumination must be used to preserve scene integrity. The simplicity of the full-frame design yields CCD imagers with the highest resolution and highest density.

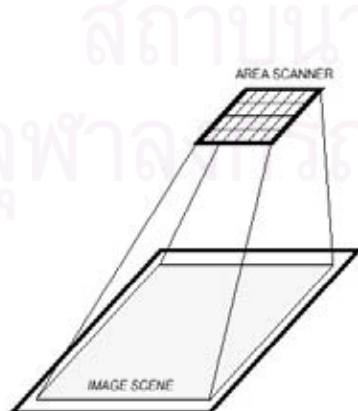


Figure 2-1 Area scanning.

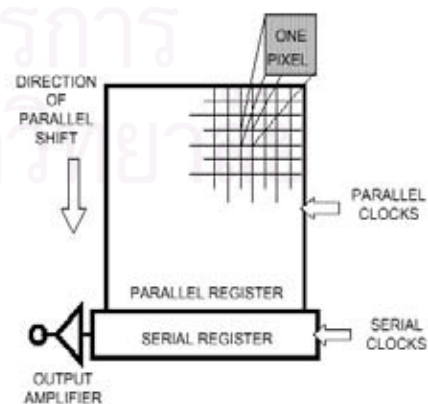


Figure 2-2 Full-frame architecture.

- **Frame-transfer**

Frame-transfer CCDs are very much like full-frame architectures. (See Figure 2-5.) The difference is that a separate and identical parallel register, called a storage array, is added which is not light sensitive. The idea is to shift a captured scene from the photosensitive, or image array, very quickly to the storage array. Readout off chip from the storage register is then performed as previously described in the full-frame device while the storage array is integrating the next frame. The advantage of this architecture is that a continuous or shutterless/strobeless operation is achieved resulting in faster frame rates. The resulting performance is compromised, however, because integration is still occurring during the image dump to the storage array resulting in image "smear". Since twice the silicon area is required to implement this architecture, frame-transfer CCDs have lower resolutions and much higher costs than full-frame CCDs.

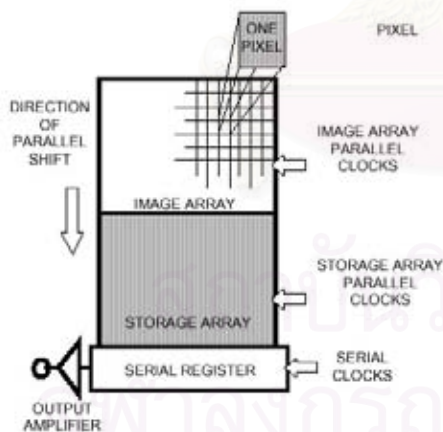


Figure 2-3 Frame-transfer architecture.

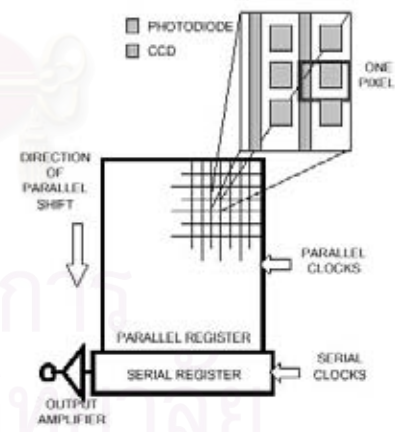


Figure 2-4 Interline architecture.

- **Interline**

Interline CCDs are incorporated to address the shortcomings of the frame-transfer devices. (See Figure 2-6.) This is achieved by separating the photo-detecting and readout functions by forming isolated photosensitive regions in between lines of non-sensitive or lightshielded parallel readout CCDs. After integrating a scene, the signal collected in every pixel is transferred, all at once, into the light shielded parallel CCD. Transfer to the output is then carried out similarly to full-frame and frame-transfer CCDs. During readout, like the frame-transfer CCD, the next frame is being integrated thus achieving a continuous operation and a higher frame rate. This architecture significantly improves the image smear during readout when compared to frame-transfer CCDs.

The major disadvantages of interline CCD architectures are their complexity that leads to higher unit costs, and lower sensitivity. Lower sensitivity occurs because less photosensitive area (i.e. a reduced aperture) is present at each pixel site due to the associated light shielded readout CCD. Furthermore, sampling errors are greater because of the reduced aperture. Lastly, some interline architectures using photodiodes suffer image "lag" as a consequence of charge transfer from photodiode to CCD.

2.1.1.2 Super CCD

Super CCD (3) features unique octagonal-shaped photodiodes in an interwoven arrangement that realizes a larger photo-diode for each pixel. The sensor shape and arrangement of the super CCD increases sensitivity, improves S/N ratio and

offers a much wider dynamic range, an attribute that produces digital sparkling clarity. Further, the innovative interwoven pixel arrangement increases resolution in the vertical and horizontal directions, resulting in higher overall resolutions. The super CCD capture data at 12 bits for each RGB and records it at an optimal 8 bits, depending on the situation.

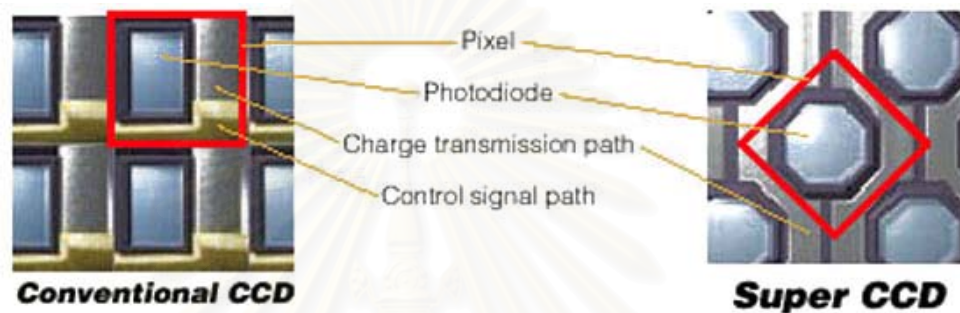


Figure 2-5 Pixel layout comparison.

2.1.1.3 CMOS (Complementary Metal Oxide Semiconductor)

CMOS (4) image sensors are silicon chips that capture and read light. High-performance CMOS image sensors use “active-pixel” architectures invented at NASA’s Jet Propulsion Laboratory in the mid 1990s.

The CMOS imager architecture (5) is arranged more like a memory cell or a flat-panel display. Each pixel contains a photodiode, which converts light to electrons, charge-to-voltage conversion section; reset and select transistor; and amplifier section. Overlaying the entire pixel array is a grid of metal interconnects, which applies timing and readout signals, and output signal metal interconnects for

each column. The column output signal is connected to a set of decode and readout electronics, which are arranged for each column outside the pixel array. This architecture allows the pixel signals from the entire array, from subsections to individual pixels, to be read by a simple X,Y. (See Figure 2-6)

The first of CMOS innovation is the on-chip noise-removal technology, which permits the sensor to scan signals with a high S/N ratio through a built-in circuit that subtracts at the final stage the noise components previously scanned.

Another innovation is the internal charge full transfer system, which allows a complete transfer of charges in the pixels. This system eliminates random noise caused by irregular fluctuation at the molecular level. In addition, these sensors have low energy consumption, contributing to smaller and lighter digital SLR cameras.

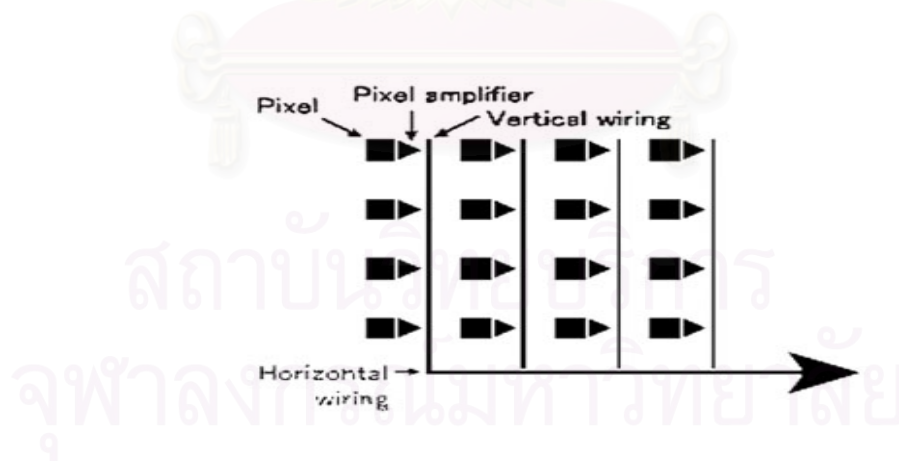
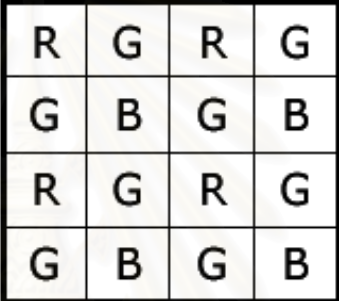


Figure 2-6 CMOS image architecture.

2.1.1.4 Foveon X3

In their native state, the image sensors used in digital image capture devices are black-and-white. To enable color capture, small color filters are placed on top of each photodiode. The filter pattern most often used is derived in some way from the Bayer pattern⁶, a repeating array of red, green, and blue pixels that lie next to each other in the image plane.



R	G	R	G
G	B	G	B
R	G	R	G
G	B	G	B

Figure 2-7 Typical bayer filter pattern showing the alternate sampling of red, green and blue pixels.

Foveon X3 (7) is a new technology used exclusively in Foveon X3 direct image sensors. Foveon X3 direct image sensors are the only image sensors that directly capture in three layers, just like color film. Foveon pioneered the development of the direct image sensor using the most advanced developments in semiconductor design, image processing, and signal processing.

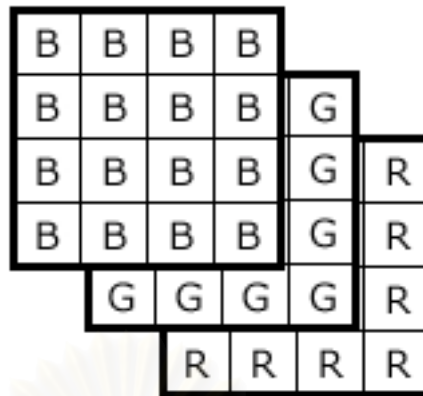


Figure 2-8 Schematic depiction of Foveon X3 image sensor showing stacks of color pixels, which record color depth wise in silicon.

2.1.2 Digital Image Quality Measurement

As indicated by Miyake (1), image quality measurement can be determined by its sharpness, tone reproduction, color reproduction and graininess. Therefore, this study will use all four qualifications for evaluating the image quality. These four qualifications are discussed below

2.1.2.1 Image Resolution

Sharpness is directly related to the image resolution; therefore this study will measure resolution of the captured images. Resolution is the ability of a camera system, or a component of a camera system, in depicting picture detail. A method for measurement of image resolution, using the spatial frequency response (SFR) analysis, was adopted by the ISO.

The ISO 12233 (8) standard procedure for digital camera resolution measurement uses the resolution test chart and test chart features, as shown in figure 2-9 and 2-10 respectively, as the experimental material.

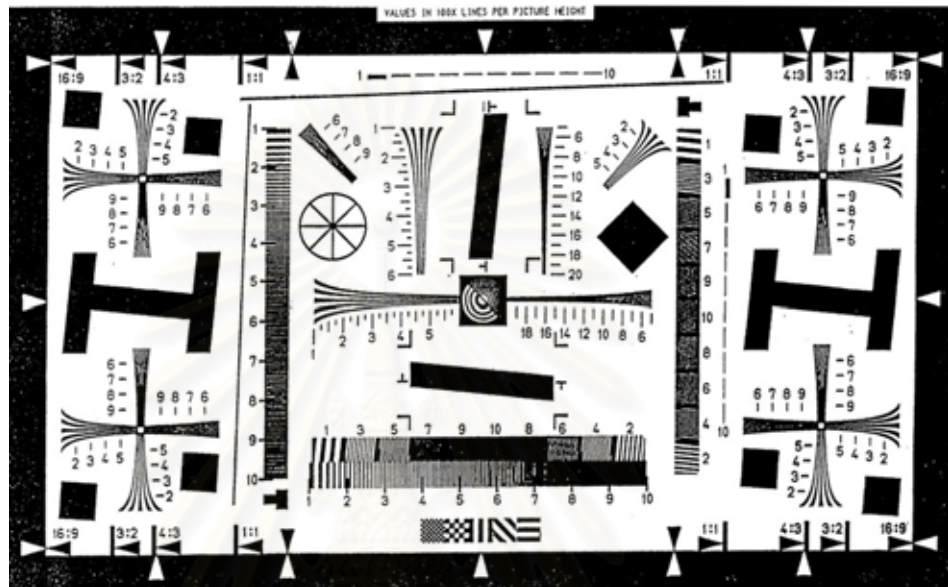


Figure 2-9 Resolution test chart.

Visual resolution is the spatial frequency (SFR) at which the individual black and white line of the test pattern image can no longer be distinguished by the viewer. From the figure 2-10, the wedges of each bar are used to measure the different type of resolution. The horizontal visual resolution is measure by using the wedges of K1 and J1 bar. The vertical visual resolution is measured by using the wedges of K2 and J2 bar. The 5° diagonal resolution is measured by using the wedges of KD and KJ bar.

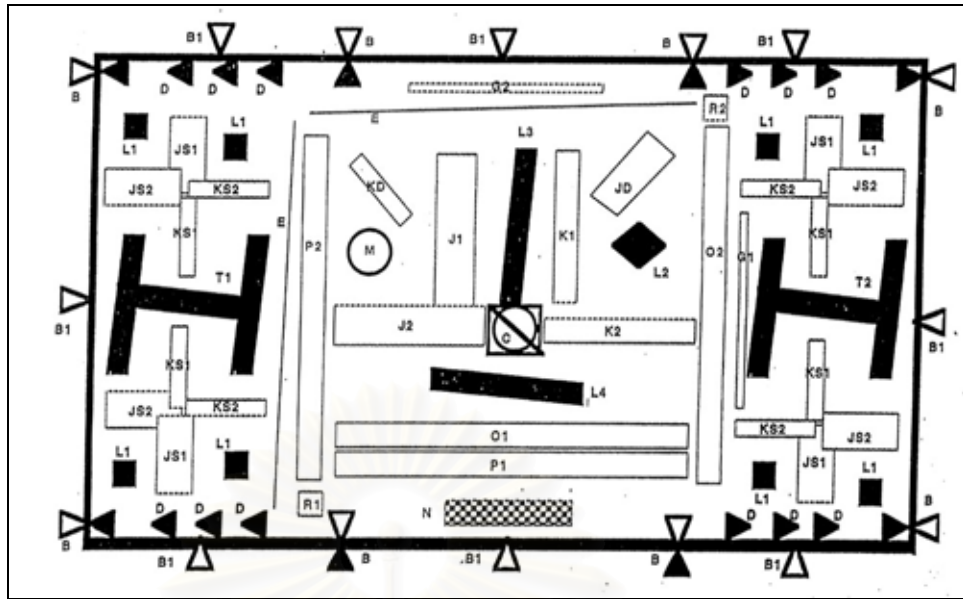


Figure 2-10 Test chart features.

The spatial frequency response (SFR) of an electronic still camera picture is measured by analyzing the camera data near a slanted black to white edge. For the target shown in figure 2-10, the black L3 bar is used to measure the horizontal SFR and the black L4 bar is used to measure the vertical SFR, in the center of the image. The diagonal black square L2 is used to measure the diagonal SFR near the center of the image. The L1 black squares and L4 H-shaped features are used to measure the SFR at other locations in the image. The SFR measurement can be performed automatically by image processing software. To perform the measurement, the digital camera output data in the region of specific black to white and white to black edges on the test chart are analyzed by a computer algorithm. If the camera provides only analog output signals, the signals should be digitized by a suitable analog to digital converter and stored in a suitable memory to allow the data to be analyzed by the computer algorithm.

2.1.2.2 Tone Reproduction

Tone reproduction **(9)** is the matching, modifying, or enhancing of output tones relative to the tones of the original document. It refers to the degree to which an image conveys the luminance ranges of an original scene (or, in the case of reformatting, of an image to be reproduced). It is the single most important aspect of image quality.

In tone reproduction measurement, opto-electronic conversion function (OECF) **(10)**, dynamic range, and flare can be all characterized by capturing and analyzing neutral gray-scale patches that vary from dark to light.

Generally, camera sensor has difficulty in capturing bright and dark areas at the same time. Those with a large dynamic range are able to capture subtle tonal gradations in the shadow, midtone, and highlight areas of the scene. In technical terms, dynamic range is defined by the ratio of the highest non-white value and smallest non-black value a sensor can capture at the same time.

The dynamic range is used to measure capability in compressing the actual scaling luminance values into limited capability devices like digital cameras. If the result of the measurement shows that the dynamic range of the luminance values is high, such device is identified as giving the good tone reproduction capability, or vice versa.

To measure a dynamic range of all sensors, we must take a series of gray patch with different exposure, usually 10-11 stops. Then, plot a graph between average pixels value of gray patch with the exposure in stops as shown in Figure 2-11.

The dynamic range calculate from the shadow and highlight of captured image. The shadow pixel is determined from the lowest value that just see the different from blackest point.

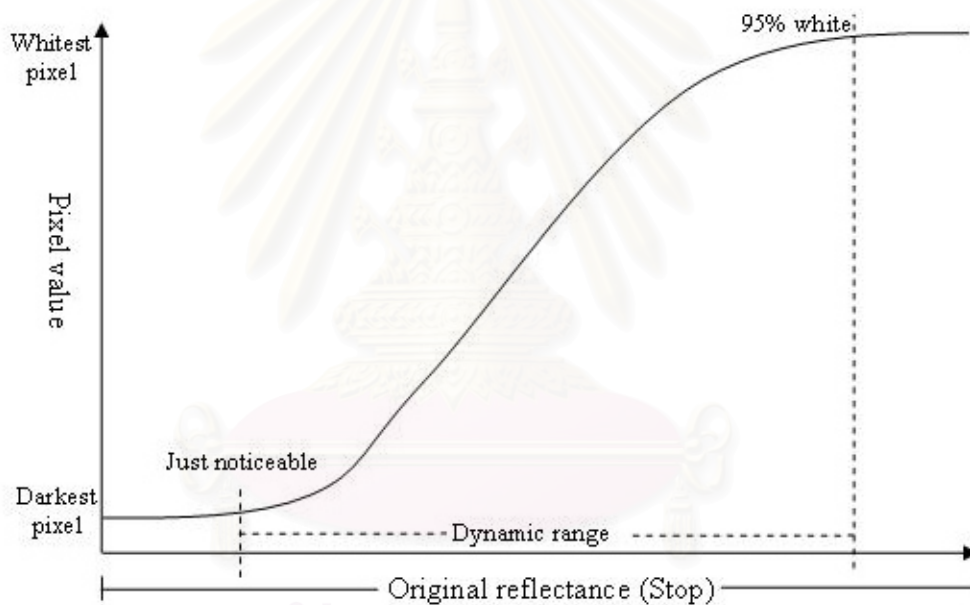


Figure 2-11 Dynamic range in digital images.

2.1.2.3 Color Reproduction

Three color reproduction intents (9) can apply to a digital image: perceptual intent, relative colorimetric intent, and absolute colorimetric intent. The perceptual intent is to create a pleasing image on a given medium under given viewing conditions. The relative colorimetric intent is to match, as closely as possible, the colors of the reproduction to the colors of the original, taking into account output media and viewing conditions. The absolute colorimetric intent is to reproduce colors as exactly as possible, independent of output media and viewing conditions. This terminology is often associated with the International Color Consortium (ICC).

The more accurate term of color reproduction has been coined for the potential color performance or fidelity of a digital capture: the metamerism index. A metamerism index of zero would indicate equivalence between the digital camera's color performance and that of a human observer. A suitable surrogate for color capture fidelity, called average Delta E^*_{ab} , or ΔE^*_{ab} , is often used.

ΔE^*_{ab} makes use of a standardized perceptual color space called CIELAB. This color space, characterized by three variables L^* , a^* , and b^* is one in which equal distances in the space represent approximately equal perceptual color differences. L^* , a^* , and b^* can be measured for any color and specified illuminant. By knowing these values for color patches of a target and comparing them with their digitized values, a color fidelity index, ΔE^*_{ab} , can be measured.

Finally, gray-scale uniformity may be considered a form of color fidelity. Gray-scale uniformity is a measure of how well neutral tones are detected equivalently by each color channel of digital cameras. Although it can also be measured with the CIELAB metric, there are often occasions where the L*a*b* values are not available. In such cases, a first step in measuring color fidelity is to examine how well the average count value of different density neutral patches matches across color channels.

The color reproduction is measured from the color difference (ΔE^*_{ab}) by comparing colors between original images and reproductions from digital cameras. Firstly, transforming the color format of RGB to CIEXYZ (D65) under sRGB color space (11) by using linear transformation matrix, as shown in Equation (2-1). Secondly, transforming CIEXYZ to CIELAB and compare with CIELAB of the original image color.

$$\begin{bmatrix} X \\ Y \\ Z \end{bmatrix} = \begin{bmatrix} 0.4124 & 0.3576 & 0.1805 \\ 0.2126 & 0.7152 & 0.0722 \\ 0.0193 & 0.1192 & 0.9505 \end{bmatrix} \begin{bmatrix} R_{sRGB} \\ G_{sRGB} \\ B_{sRGB} \end{bmatrix} \quad (2-1)$$

a. CIELAB

The CIE 1976 (L*a*b*) color space, is defined by Equations (2-2) – (2-6)

for tristimulus values normalized to the white that are greater than 0.008856.

$$L^* = 116 (Y/Y_n)^{1/3} - 16 \quad (2-2)$$

$$a^* = 500 \{ (X/X_n)^{1/3} - (Y/Y_n)^{1/3} \} \quad (2-3)$$

$$b^* = 200 \{ (Y/Y_n)^{1/3} - (Z/Z_n)^{1/3} \} \quad (2-4)$$

$$C^*_{ab} = \sqrt{(a^{*2} + b^{*2})} \quad (2-5)$$

$$h^0_{ab} = \tan^{-1}(b^*/a^*) \quad (2-6)$$

X,Y,Z are the tristimulus values of the stimulus.

X_n, Y_n, Z_n are the tristimulus values of the reference white.

L* represents the lightness,

a* approximate redness-greenness,

b* approximate yellowness-blueness,

C*_{ab} chroma,

h⁰_{ab} hue angle,

The L*, a*, and b* coordinates are used to construct a Cartesian color space.

The L*, C*_{ab}, and h⁰_{ab} coordinates are the cylindrical representation of the same space.

b. Color Difference

Color differences are measured in the CIELAB space as the Euclidean distance between the coordinates of the two stimuli. This is expressed in terms of a CIELAB ΔE^*_{ab} , which can be calculated using Equation (2-7). It can also be expressed in terms of lightness, chroma, and hue differences, as illustrated in Equation (2-8) using the combination of Equations (2-7) – (2-9)

$$\Delta E^*_{ab} = [\Delta L^{*2} + \Delta a^{*2} + \Delta b^{*2}]^{1/2} \quad (2-7)$$

$$\Delta E^*_{ab} = [\Delta L^{*2} + \Delta C^{*2}_{ab} + \Delta H^{*2}_{ab}]^{1/2} \quad (2-8)$$

$$\Delta H^*_{ab} = [\Delta E^{*2}_{ab} - \Delta L^{*2} - \Delta C^{*2}_{ab}]^{1/2} \quad (2-9)$$

In rectangular coordinates:

- The lightness difference on the L^* axis, expressed by ΔL^*
- The red – green color difference on the a^* axis, expressed by Δa^*
- The yellow – blue color difference on the b^* axis, expressed by Δb^*

In cylindrical coordinates:

- The lightness difference on the L^* axis, expressed by ΔL^*
- The chroma difference on the C^* radius, expressed by ΔC^*
- The hue angle difference on h° , expressed by Δh° , in degrees. It will be transformed into a unit of length. This hue difference will then be represented by ΔH^*

2.1.2.4 Graininess/Noise

In photography, the grainy effect (**12**) is caused by developed silver halide crystals that clump together in the processed negative. Upon printing, the grain clumps are enlarged, becoming reality visible as a random pattern distributed over the whole image. Graininess can be a nuisance but is often used as an artistic effect to create a rough feel to the image. Gain in photographs is also effect to create a rough feel that Photoshop offers an option to create the effect. Though often used for effect, generally grain is not pleasant in a photographic image, and most photographers attempt to reduce its presence. One route to grain-free images is slow film. The emulsion in lower speed film has very small fine grain.

In digital imaging, noise exists as a random background fluctuation. It is measured as base and fog in photographic film and as dark noise in CCD images. For an image to be detected, the image signal needs to be larger than the background noise variations. If the signal is not very bright, it can get lost in the noise variations. In astronomy, a very faint star may get lost in the background noise and not be detected. In everyday digital imaging, there is usually enough light to create a signal significantly larger than the background noise. In general, the ratio of signal-to-background noise must be such that it is possible to see the image. This occurs with either a very low noise level or a relatively high signal level or, if possible, both. It is important to meet this condition for good quality imaging.

Noise in digital images is seen as random background pixel value fluctuations. To be detected, the image/signal needs to be above this background level. Area A is too dim and is lost in the noise. Area B is just detected, while Area C forms a good image as it has a very high signal to noise ratio. (See Figure 2-12)

สถาบันวิทยบริการ
จุฬาลงกรณ์มหาวิทยาลัย

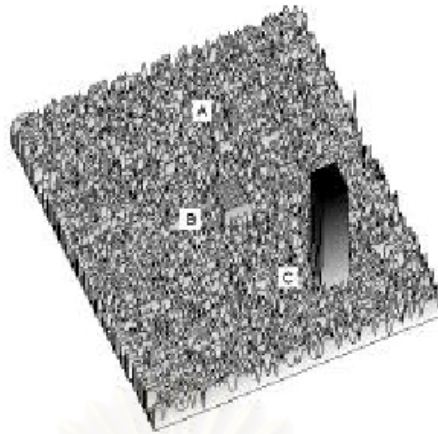


Figure 2-12 Noise in digital images.

Figure 2-12 is seen as random background pixel value fluctuations. To be detected, the image signal needs to be above this background level. Area A is too dim and is lost in the noise. Area B is just detected, while Area C forms a good image as it has a very high signal to noise ratio.

a. Dark Current Noise

There are many sources of noise in digital imaging. The first is dark current, also called 'dark current noise'. This type of noise is caused by CCD pixels acquiring pixel values without any exposure. Electrons recreated in a pixel by thermal agitation and are indistinguishable from exposure-generated electrons. The number of electrons generated in each pixel is a random number, resulting in random pixel values. It is important to ensure that the unwanted dark noise is not too large as there won't be any room for the electrons from the camera exposure.

Dark current is highly temperature dependent and drops by half for every 10°C fall in temperature. For CCDs used in astronomy and scientific imaging, dark noise is significantly reduced by cooling. Typically, a CCD will be cooled to about -60°C or less. In commercial digital cameras, it isn't practical to cool the camera, so dark noise is dealt with in another way. Circuitry that measures the average level of dark noise compensates for it. The camera's CCD has shielded pixels at the edge of the sensor that are used to establish the average dark current level at the time of exposure. This average is used as a reference, and subtracted from the imaging pixels creating a corrected image free from the effects of dark noise. (Note that camera companies include the calibration pixels in the total quoted pixel number, even though they are not actively used for imaging.) Despite this correcting mechanism, one should avoid leaving a digital camera in front of very hot studio lights. The heat from the lights will raise the temperature of the camera back where the sensor is located, which will increase the dark noise level.

b. Fixed Pattern Noise

Digital cameras produce a pattern of noise that is identical in every frame called "fixed pattern noise". It is caused by individual pixels having a different response to the same input. This response difference is due to small underlying variations in pixel size or spacing, or non-uniformities in the silicon semiconductor. The fixed pattern is normally mixed in with the camera exposure; to see it you have to make an exposure without any image.

For instance, these images were taken with a digital camera. The shutter was kept open for 30 seconds with the lens cap on. The images show two types of noise: the random background dark noise that changes between frames, and the fixed pattern noise that is clearly visible as prominent spikes that repeat in both frames. (See Figure 2-13)

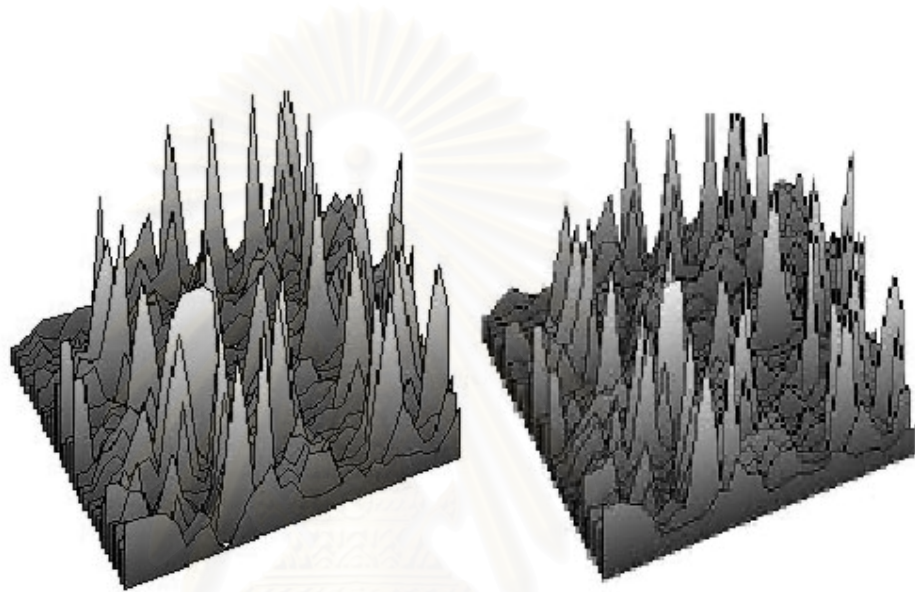


Figure 2-13 The Fixed pattern noise from image taken with a digital camera.

c. Amplifier Noise

The final source of digital image noise comes at the readout stage and is due to the amplifier circuits. When charge is read out from the CCD, it is amplified, which is controlled by the ISO setting on a digital camera. In digital cameras, there is no film to change when altering the ISO setting; the effective speed change is caused by more amplification in the readout circuitry.

Amplifier noise gets added to the image during readout, and varies with amplification. An effect is very similar to a photograph, where low amplification (100 ISO setting) gives low noise, and a high amplification setting (6400 ISO setting) gives high noise. In some digital cameras there is another amplifier problem. It is not able to operate linearly for all pixel values at all ISO settings, so along with the noise effects; digital cameras also produce a color (usually blue) shift at higher ISO settings.

For instance, these images of a Kodak color patches were taken with a camera. The ISO setting was altered for each. Notice how the amplifier noise increases at higher ISO levels.



Figure 2-14 The Amplifier noise from images of a Kodak color patch taken with a digital camera.

สถาบันวิทยบริการ
จุฬาลงกรณ์มหาวิทยาลัย

2.2 Literature Reviews

Uschold (13) studied the current capabilities of digital cameras and the comparison of the classical architecture of digital cameras based on 35 mm SLR-systems and a digital optimized architecture. The study concluded that the current high end digital cameras' features were equivalent to silver halide film. There is a quantitative analysis of lenses based on the classical 35 mm SLR architecture and of a full digital designed modern camera model.

Burns and Williams (14) studied the improved evaluation of image resolution for digital cameras and scanner. Their study indicated that a method for measurement of image resolution for digital cameras using slanted-edge gradient analysis was adopted by the ISO. More recently, this method has been applied to the spatial frequency response and MTF of film and print scanners and CRT displays. As a result of this study, detection of clipped-image data, which causes bias error, is recommended. Spatial image distortion caused by optical aberration or position errors can reduce the measured SFR.

Roberts and Kelley (15) studied the appearance of noise on a display and stated that it is an important usability issue. They suggested that sources of noise are electrical interference, display driver artifacts, resampling artifacts, transmission artifacts, compression artifacts, and any intrinsic noise artifacts produced within a display device. They investigated the intricacies of using a digital camera to accurately measure noise in a static image on a flat panel display (FPD). The electrooptical transfer function of the FPD was measured. A known noise pattern was

displayed and measured using the digital camera whereby the predicted noise was compared to the measured noise.

Baer (16) studied the performance of a digital camera. The study result was largely determined by the capabilities of its CCD. The CCD characteristics required to produce digital cameras that compared favorably with film cameras were presented. The result indicated that various CCD characteristics such as resolution, quantum efficiency and charge capacity are related to their eventual effect on image quality or camera capability.



สถาบันวิทยบริการ
จุฬาลงกรณ์มหาวิทยาลัย

CHAPTER III

EXPERIMENTAL

3.1 Materials

- Resolution Test Chart
- Macbeth Color Checker
- Kodak Gray Scale

3.2 Apparatus

- Digital Camera Single Lens Reflect (DSLR)
 - Nikon D100 (CCD) Serial No: 2004690
 - Fuji S2Pro (Super CCD) Serial No: 22L00422
 - Canon D60 (CMOS) Serial No: 0930500547
 - Sigma SD9 (FOVEON X3) Serial No: 1003545
- SIGMA Lens 15-30 mm. F3.5-4.5 for Nikon, Fuji, Canon and Sigma
- LCD Monitor Display
- Fuji ND Filter
- Minolta Color Meter IIIF
- Tripod
- Broncolor HMI 575
- Compact Flash Memory Cards

3.3 Software Application

- Adobe Photoshop 7
- Nikon Capture 3
- Nikon View 5
- Raw File Converter EX
- FinePixViewer
- RAW Image Converter 2
- SIGMA Photo Pro 2.1
- SFRwin 1.0

3.4 Procedures

3.4.1 Experimental Setup

Four digital still cameras were used in this experiment with having different type of image sensors (CCD, Super CCD, CMOS and FOVEON X3). In order to eliminate the variation of image quality caused by various lens used, only SIGMA lens 15-30 mm. F3.5-4.5 were applied.

3.4.2 Experimental Procedure

3.4.2.1 Preparation of Resolution Measurement

- Measurement condition

- Daylight flash illumination

- Sensitivity setting

Nikon D100 = ISO200

Fuji S2Pro = ISO100

Canon D60 = ISO100

Sigma SD9 = ISO100

- Noise reduction setting : Off

- Convert raw file to tiff file with following conditions

White balance = Daylight

Sharpening = None

Color mode = sRGB

Saturation = Normal

- Set environmental condition according to the ISO/DIS 12233.
- Capture the resolution test chart using all digital cameras.
- To measure the visual resolution of each image sensor types, the horizontal LW/PH, vertical LW/PH and diagonal LW/PH from resolution test chart evaluated
- Capture Kodak gray scale chart using all digital cameras and calculate the relative reflectance and pixel value and linearize the data with opto-electronic conversion function (OECF) (10)..
 - Transform data from OECF to the lookup table (LUT).
 - Capture the slant edge test chart using all digital cameras
 - Evaluate the spatial frequency resolution (SFR) via SFRwin1.0 programming using data from both the lookup table (LUT) and the image from slant edge test chart (L3-L4).

- Analyze the output.

3.4.2.2 Preparation of Tone Reproduction Measurement

- Measurement condition
 - Daylight flash illumination
 - Sensitivity setting

Nikon D100	=	ISO200
Fuji S2Pro	=	ISO100
Canon D60	=	ISO100
Sigma SD9	=	ISO100
 - Noise reduction setting : Off
 - Convert raw file to tiff file with following conditions

White balance	=	Daylight
Sharpening	=	None
Color mode	=	sRGB
Saturation	=	Normal
- Capture the Macbeth color checker with the highest to lowest shutter speed with half-stop intervals. Then, crop the middle gray areas at 100x100 pixels value. (Figure 3-1)



Figure 3-1 The Macbeth color checker.

- Measure the average of pixels value in Red, Green, Blue and Luminosity by using the middle gray value through Adobe Photo Shop and plot the graph.
- Because average pixels value is not sufficient for evaluation, therefore, subjective measurement added. Observers are asked to judge just noticeable dark point differences of pixels value in test chart displaying on a LCD (Figures 3-2 and 3-3). This will demonstrate how well the image sensor distinguish the shadow detail. Then, use the observed result to measure the minimum dynamic range and use 5 percentage of above fog to evaluate the maximum dynamic range.
- Compare and analyze the output.

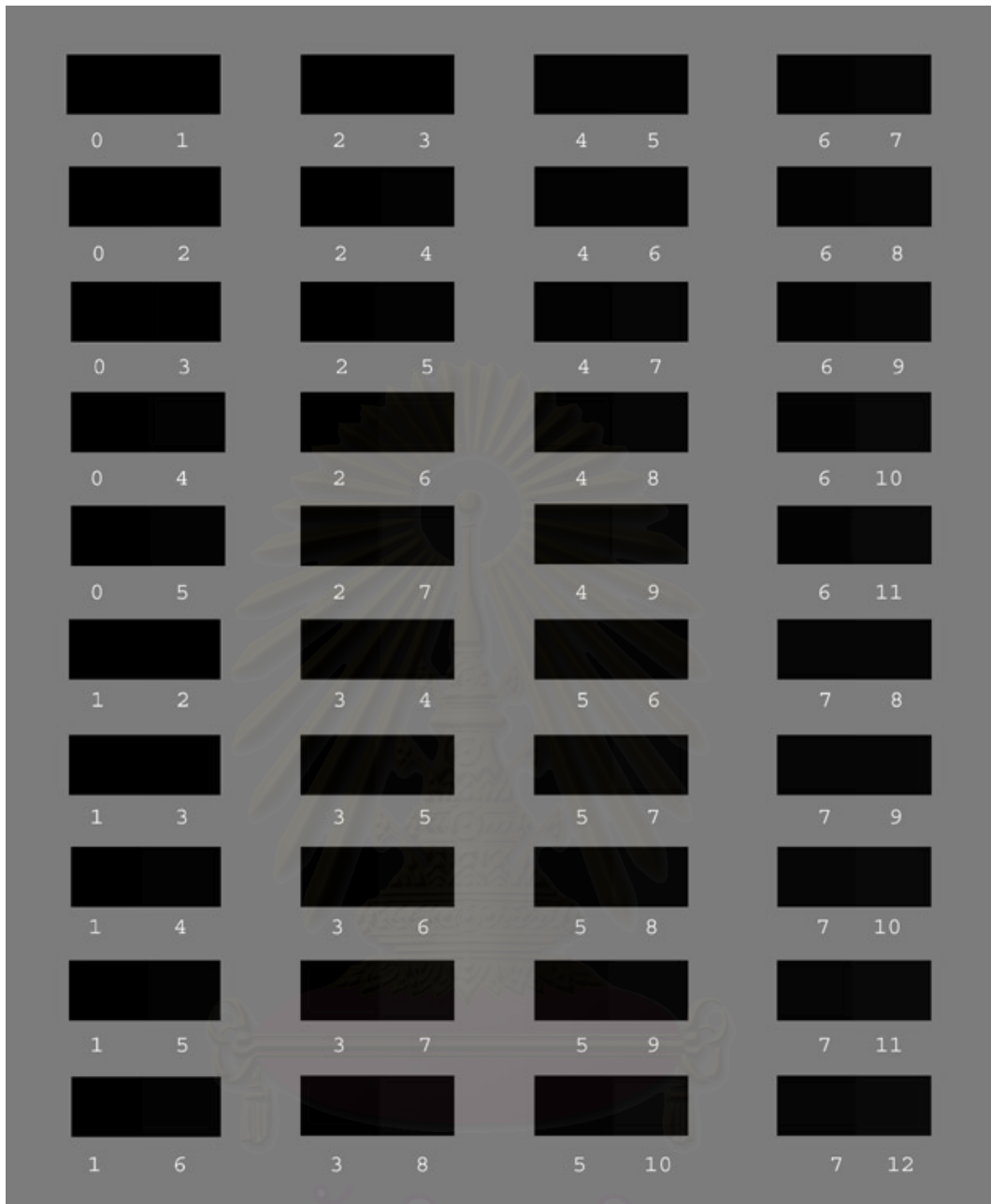


Figure 3-2 The dark point test chart of various pixel values from 1-5 with pixels level between 0-7.

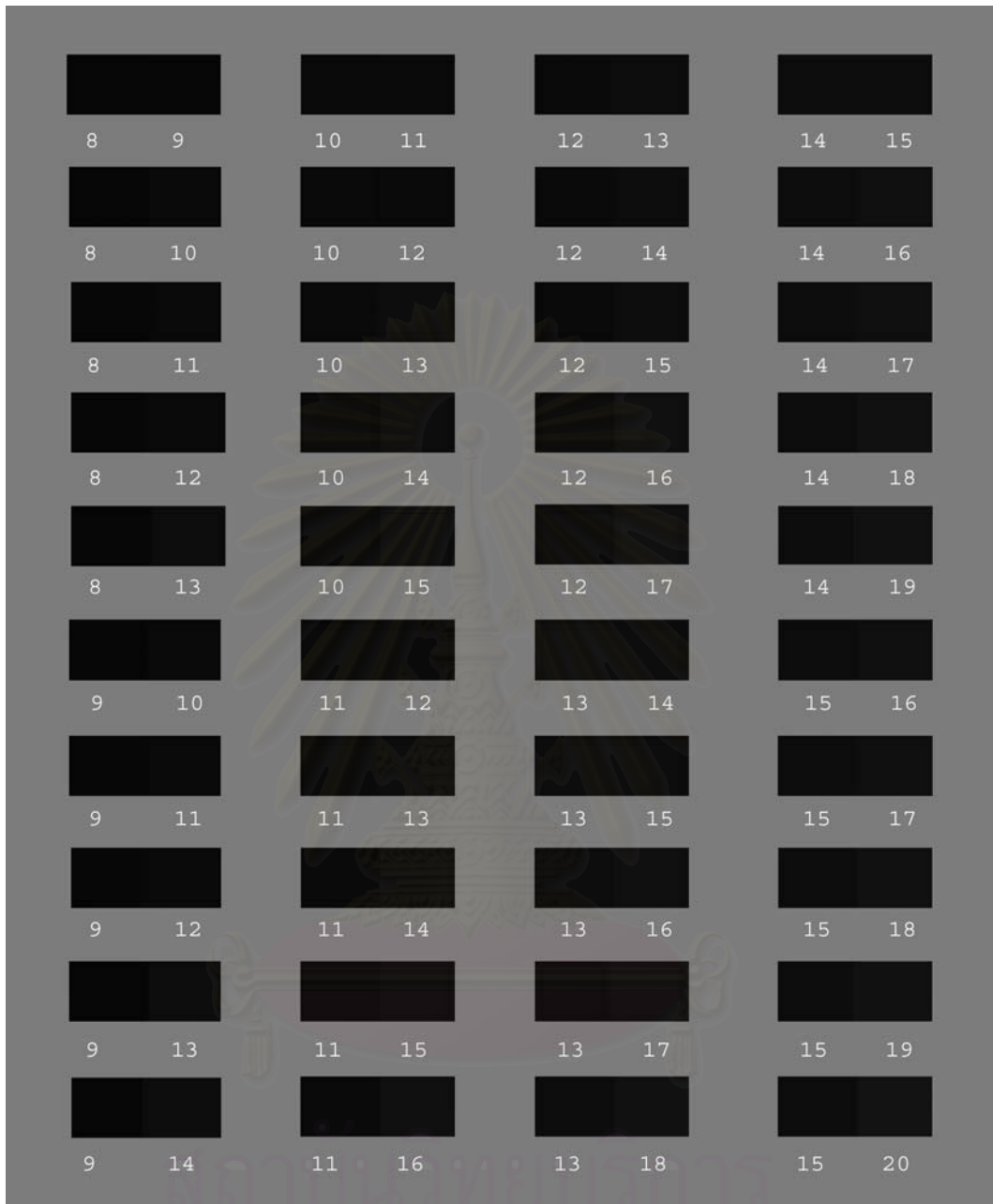


Figure 3-3 The dark point test chart of various pixel values from 1-5 with pixels level between 8-15.

3.4.2.3 Preparation of Color Reproduction Measurement

- Measurement condition
 - Daylight flash illumination
 - Sensitivity setting

Nikon D100	=	ISO200
Fuji S2Pro	=	ISO100
Canon D60	=	ISO100
Sigma SD9	=	ISO100
 - Noise reduction setting : Off
 - Convert raw file to tiff file with following conditions

White balance	=	Daylight
Sharpening	=	None
Color mode	=	sRGB
Saturation	=	Normal
- Capture the Macbeth color checker with the highest to lowest shutter speed with half-stop intervals. Then, crop the middle gray areas at 100x100 pixels value. (Figure 3-1)
- Apply equation 2-1 to transform the color value in sRGB to CIEXYZ by using linear transformation matrix. Then, transform CIEXYZ to CIELAB
 - Calculate ΔE^*_{ab} between original and captured images.
 - Analyze the output.

3.4.2.4 Preparation of Graininess/Noise Measurement

3.4.2.4.1 Preparation of Dark Current Noise Measurement

- Measurement conditions
 - Daylight illumination
 - Camera compression = off
 - Noise reduction setting : Off
 - Convert raw file to tiff file with following conditions
 - White balance = Daylight
 - Sharpening = None
 - Color mode = sRGB
 - Saturation = Normal
- Close the lens' cap and capture images with different ISOs at highest shutter speed.
- Crop the Macbeth color checker at 100x100 pixels of the middle gray.
- Calculate the average pixel value and the standard deviation.
- Use the standard deviation to analyze the output.

3.4.2.4.2 Preparation of Amplifier Noise Measurement

- Measurement conditions
 - Daylight illumination
 - Camera compression = off
 - Noise reduction setting : Off

- Convert raw file to tiff file with following conditions

White balance = Daylight

Sharpening = None

Color mode = sRGB

Saturation = Normal

- Capture the Macbeth color checker with standard ISO setting and increase the ISO from 1-3 stops respectively for all digital cameras.
- Crop the Macbeth color checker at 100x100 pixels of the middle gray.
- Measure the average pixel value and the standard deviation.
- Use the standard deviation to analyze the output.

3.4.2.4.3 Preparation of Shot Noise Measurement

- Measurement conditions
 - Daylight illumination
 - Camera compression = off
 - Noise reduction setting : Off
 - Convert raw file to tiff file with following conditions
 - White balance = Daylight
 - Sharpening = None
 - Color mode = sRGB
 - Saturation = Normal
- Capture the Macbeth color checker with various exposure times with lowest ISO by all digital cameras.

- Crop the Macbeth color checker at 100x100 pixels of the middle gray.
- Measure the average pixel value and the standard deviation.
- Use the standard deviation to analyze the output



สถาบันวิทยบริการ
จุฬาลงกรณ์มหาวิทยาลัย

CHAPTER IV

RESULTS AND DISCUSSION

4.1 The Image Resolution

4.1.1 The Preparation and Evaluation of the Image Resolution

Among the different types of image sensors (CCD, Super CCD, CMOS and Foveon X3), Foveon X3 has the effective pixels at 3 million pixels lesser than other image sensors. (see Table 4-1). Therefore, all images captured from Foveon X3 must be interpolated to have the comparative resolution with other different types of image sensors at 6 million pixels.

Table 4-1 The specification of each image sensor.

Cameras	Nikon D100	Fuji S2pro	Canon D60	Sigma SD9
Sensor manufacturer	Sony	Fujifilm	Canon	Foveon
Sensor type	CCD	Super CCD	CMOS	CMOS (Foveon X3)
Color filter array	RGB	RGB	RGB	None
Pixel pitch	7.8 x 7.8 μm	N/A	7.4 x 7.4 μm	9.12 x 9.12 μm
Sensor size	23.7 x 15.5 mm	23 x 15.5 mm	22.7 x 15.1 mm	20.7 x 13.8 mm
Resolution max	3008 x 2000	4256 x 2848 (interpolated)	3072 x 2048	2268 x 1512 (x3-Foveon X3)
Resolution test	3008 x 2000	3024 x 2016	3072 x 2048	3024 x 2016 (interpolated)
Effective pixels locations	6.0 million	6.1 million	6.4 million	3.4 million
Photo detectors	6.0 million	6.1 million	6.4 million	10.6 million

4.1.1.1 Visual Resolution

The horizontal LW/PH, vertical LW/PH and diagonal LW/PH from resolution test chart are evaluated to measure the visual resolution of each image sensors. (Figures 4-1 to 4-4)

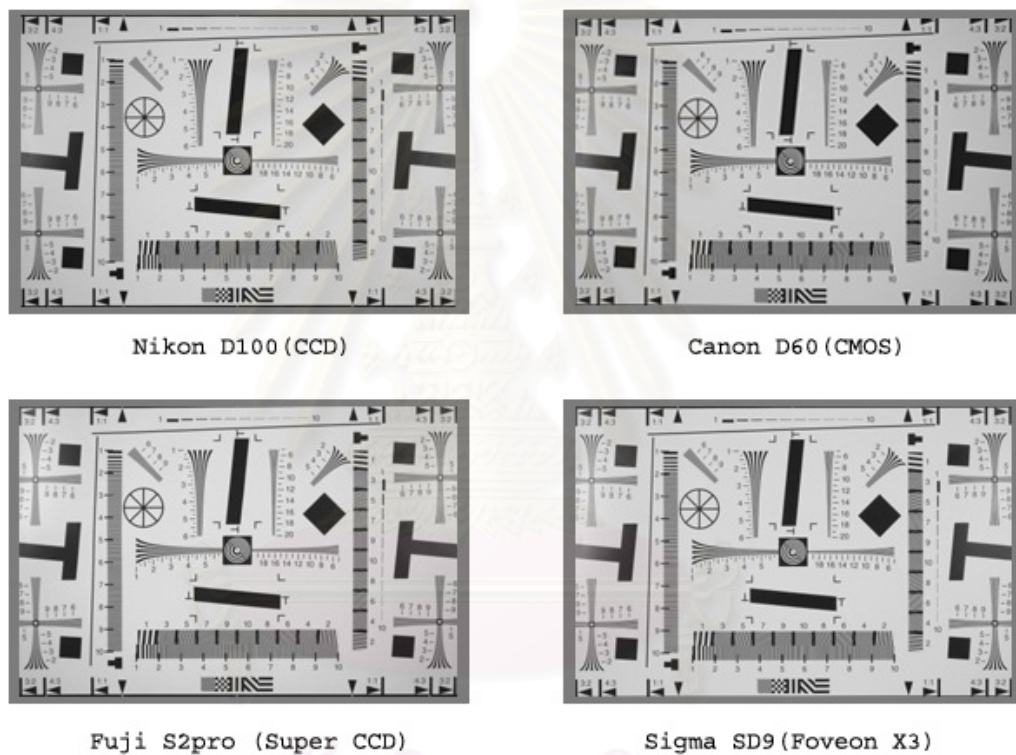
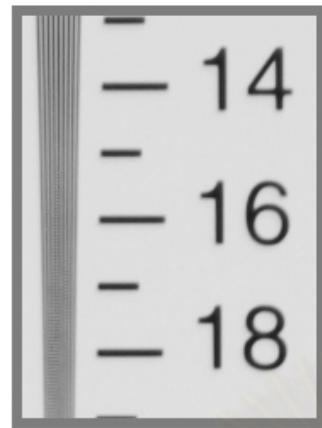
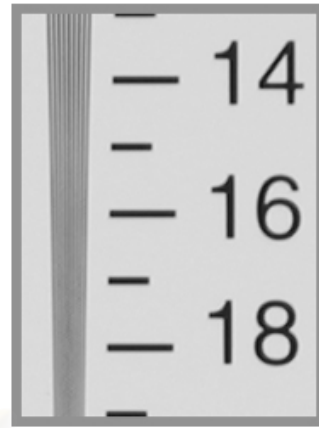


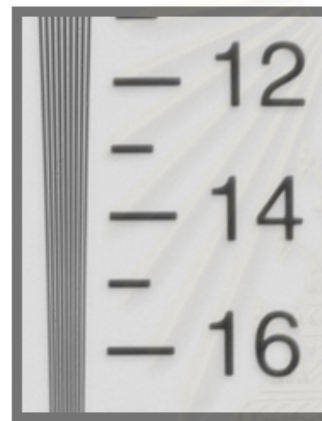
Figure 4-1 The resolution test chart resulting from each image sensor.



Nikon D100 (6.1mp)



Canon D60 (6.3mp)



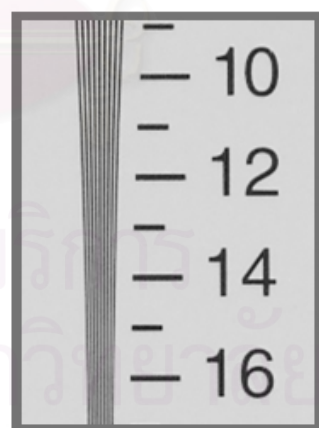
Fuji S2pro (6.1mp)



Sigma SD9 (6.1mp)



Fuji S2pro (12.2mp)



Sigma SD9 (3.4mp)

Figure 4-2 The horizontal LW/PH (line widths per picture height) resulting from each image sensor.

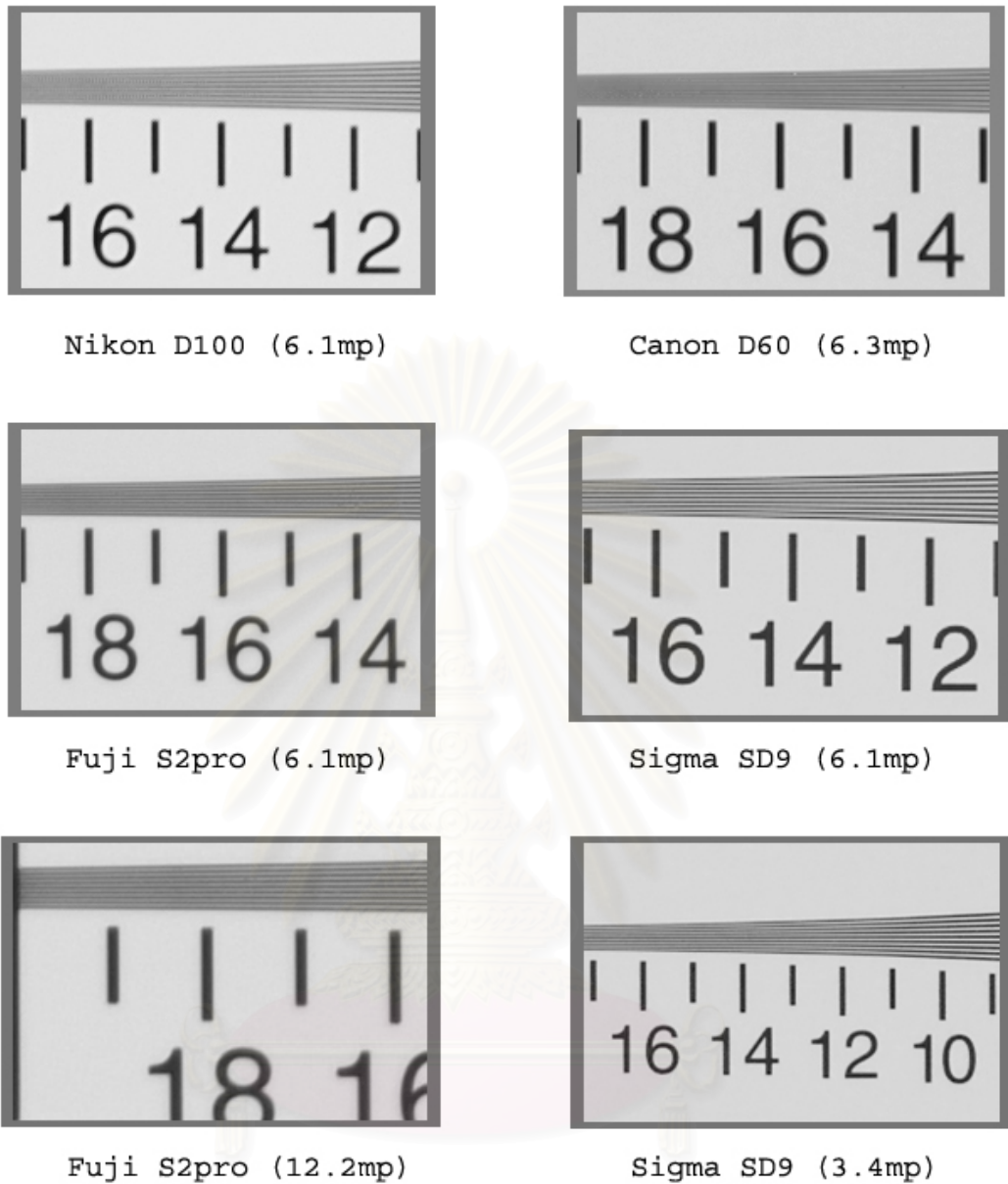


Figure 4-3 The vertical LW/PH (line widths per picture height) resulting from each image sensor types.



Figure 4-4 The 5° diagonal LW/PH (line widths per picture height) resulting from each image sensor.

Table 4-2 The visual resolution measurement of each image sensor

Camera	Measurement	Absolute Res.	Extinction Res.
Nikon D100 (6.0 mp)	Horizontal LW/PH	1400	*1600
	Vertical LW/PH	1350	*1600
	5° Diagonal LW/PH	+1000	n/a
Fujifilm S2 Pro (6.1 mp)	Horizontal LW/PH	1550	*1700
	Vertical LW/PH	1450	*1700
	5° Diagonal LW/PH	+1000	n/a
Fujifilm S2 Pro (12 mp)	Horizontal LW/PH	1800	+2000
	Vertical LW/PH	1700	+2000
	5° Diagonal LW/PH	+1000	n/a
Canon D60 (6.4 mp)	Horizontal LW/PH	1450	*1650
	Vertical LW/PH	1350	*1600
	5° Diagonal LW/PH	+1000	n/a
Sigma SD9 (6.1 mp)	Horizontal LW/PH	1300	*1800
	Vertical LW/PH	1300	*1800
	5° Diagonal LW/PH	+1000	n/a
Sigma SD9 (3.4 mp)	Horizontal LW/PH	1200	*1800
	Vertical LW/PH	1200	*1800
	5° Diagonal LW/PH	+1000	n/a

Where,

* : Moiré is visible

+ : Chart maximum

LW/PH : Line widths per picture height (to allow for different aspect ratios the measurement is the same for horizontal and vertical)

5° Diagonal : Lines set at 5° diagonal

Absolute res : Point at which all lines of a resolution bar are still visible and defined, beyond this resolution loss of detail occurs (below Nyquist frequency).

Extinction res : Detail beyond camera's definition (becomes aliased)

n/a : Not Available (above the capability of the test chart)

Figures 4-2 and 4-3 are summarized in table 4-2, when considering absolute resolution in both horizontal and vertical the Fuji S2pro (Super CCD 6 million pixels) has the highest value followed by Canon D60 (CMOS), Nikon D100 (CCD) and Sigma SD9 (Foveon X3).

This result shows the advantage of arranging photosite at 45° diagonal that caused the high absolute resolution to Fuji S2pro (Super CCD) because of lacking of aliasing filter in Sigma SD9 (Foveon X3) caused the low absolute.

Calculated resolutions of the all image sensor type.

From image size, pixels size and number of pixels, it is possible to calculate the ideal line width per pixel height. The following are the results of the calculations:

- Nikon D100, CMOS size 23.4x15.6mm, 3008 x 2000 pixels (6.1mp), 7.8 μm
Resolution: $1/(2 \times 0.0078) = 64.1$ lp/mm, 1500 line widths per picture height
- Canon D60, CMOS size 22.7x15.1mm, 3072 x 2048 pixels (6.4mp), 7.4μm
Resolution: $1/(2 \times 0.0074) = 67.57$ lp/mm, 1534 line widths per picture height
- Fuji S2Pro, Super CCD size 23.0x15.5, 4256 x 2848 pixels (12.2mp) (with spatial approximation)
Resolution: $4288/23.0/2/1 = 93.22$ lp/mm, 2144 line widths per picture height
- Fuji S2Pro, Super CCD size 23.0x15.5, 3024 x 2016 pixels (6.1mp) (with spatial approximation)
Resolution: $3024/23.0/2/1 = 65.74$ lp/mm, 1512 line widths per picture height

- Sigma SD9 , CMOS (Foveon X3) size 20.7 x 13.8, 2268 x 1512 pixels (3.4mp),
9.12 μm
Resolution: $1/(2 \times 0.00912) = 54.82$ lp/mm, 1135 line widths per picture height
- Sigma SD9 , CMOS (Foveon X3) size 20.7 x 13.8, 3024 x 2016 pixels(6.1mp),
(interpolated)
Resolution: $3024/20.7/2/1 = 73.04$ lp/mm, 1512 line widths per picture height

The theoretical of line width per picture height is not fully applied to visual resolution because many factors are not taken into account, for example lens quality, image processing etc. It is obvious that the value of absolute resolution always lower than theoretical one.

4.1.1.2 Spatial Frequency Response (SFR)

To evaluate the spatial frequency response (SFR), two data are needed, the first data is lookup table (LUT) and the second data is the slant edge that come from test chart (Figures 4-5 and 4-6).

To generate the lookup table (LUT), the neutral gray-scale patches captured and data were then processed through opto-electronic conversion function (OECF). (See Appendix A1)

The slant edges were captured by each camera described in 3.4.2 then, consolidating data from two sources are used to measure the spatial response via program SFRwin 1.0 (17).

Generally, the spatial frequency responses (SFRs) show the contrast characteristic of each image sensor, where contrast is the capability to differentiate the dark and white areas.

The slanted-edge method was applied for spatial frequency response (SFR) analysis, the result of horizontal spatial frequency response and vertical spatial frequency response of Nikon D100 (CCD), Fuji S2pro (Super CCD), Canon D60 (CMOS) and Sigma SD9 (Foveon X3) are represented in figure 4-3 to figure 4-6.

Both horizontal and vertical spatial frequency responses are displayed in Figure 4-7 to 4-10. The x axis is the spatial frequency response (SFR) value while the x axis is the cycle per pixel location where the nyquist frequency is calculated at 0.5 cycle per pixel location.

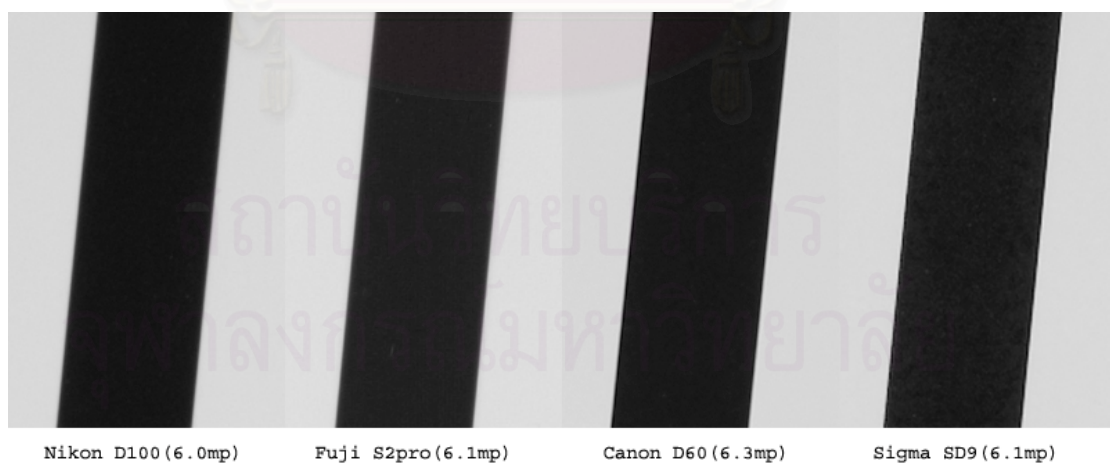


Figure 4-5 The horizontal slant edge (L3) test chart of each image sensor.



Figure 4-6 The vertical slant edge (L4) test chart of each image.

สถาบันวิทยบริการ
จุฬาลงกรณ์มหาวิทยาลัย

Table 4-3 The value of horizontal SFR and vertical SFR from Nikon D100.

Frequency (Cycles/pixel location)	Nikon D100 Horizontal SFR(L3)	Nikon D100 Vertical SFR (L4)
0.0000	1.0000	1.0000
0.0200	0.9756	0.9772
0.0400	0.9275	0.9270
0.0600	0.8728	0.8673
0.0800	0.8089	0.7985
0.1000	0.7416	0.7220
0.1200	0.6779	0.6440
0.1400	0.6189	0.5692
0.1600	0.5609	0.4952
0.1800	0.5078	0.4230
0.2000	0.4580	0.3574
0.2200	0.4107	0.2967
0.2400	0.3659	0.2414
0.2600	0.3261	0.1945
0.2800	0.2904	0.1562
0.3000	0.2560	0.1216
0.3200	0.2264	0.0924
0.3400	0.1990	0.0685
0.3600	0.1710	0.0514
0.3800	0.1466	0.0420
0.4000	0.1272	0.0338
0.4200	0.1088	0.0297
0.4400	0.0951	0.0268
0.4600	0.0781	0.0270
0.4800	0.0605	0.0291
0.5000	0.0476	0.0353
0.5200	0.0410	0.0346
0.5400	0.0380	0.0341
0.5600	0.0363	0.0387
0.5800	0.0386	0.0420
0.6000	0.0358	0.0429
0.6200	0.0337	0.0380
0.6400	0.0320	0.0342
0.6600	0.0268	0.0289
0.6800	0.0231	0.0259
0.7000	0.0242	0.0253
0.7200	0.0204	0.0260
0.7400	0.0228	0.0233
0.7600	0.0276	0.0151
0.7800	0.0299	0.0167
0.8000	0.0248	0.0184
0.8200	0.0203	0.0195
0.8400	0.0226	0.0143
0.8600	0.0293	0.0057
0.8800	0.0301	0.0189
0.9000	0.0267	0.0275
0.9200	0.0251	0.0265
0.9400	0.0210	0.0138
0.9600	0.0136	0.0036
0.9800	0.0192	0.0103
1.0000	0.0291	0.0144

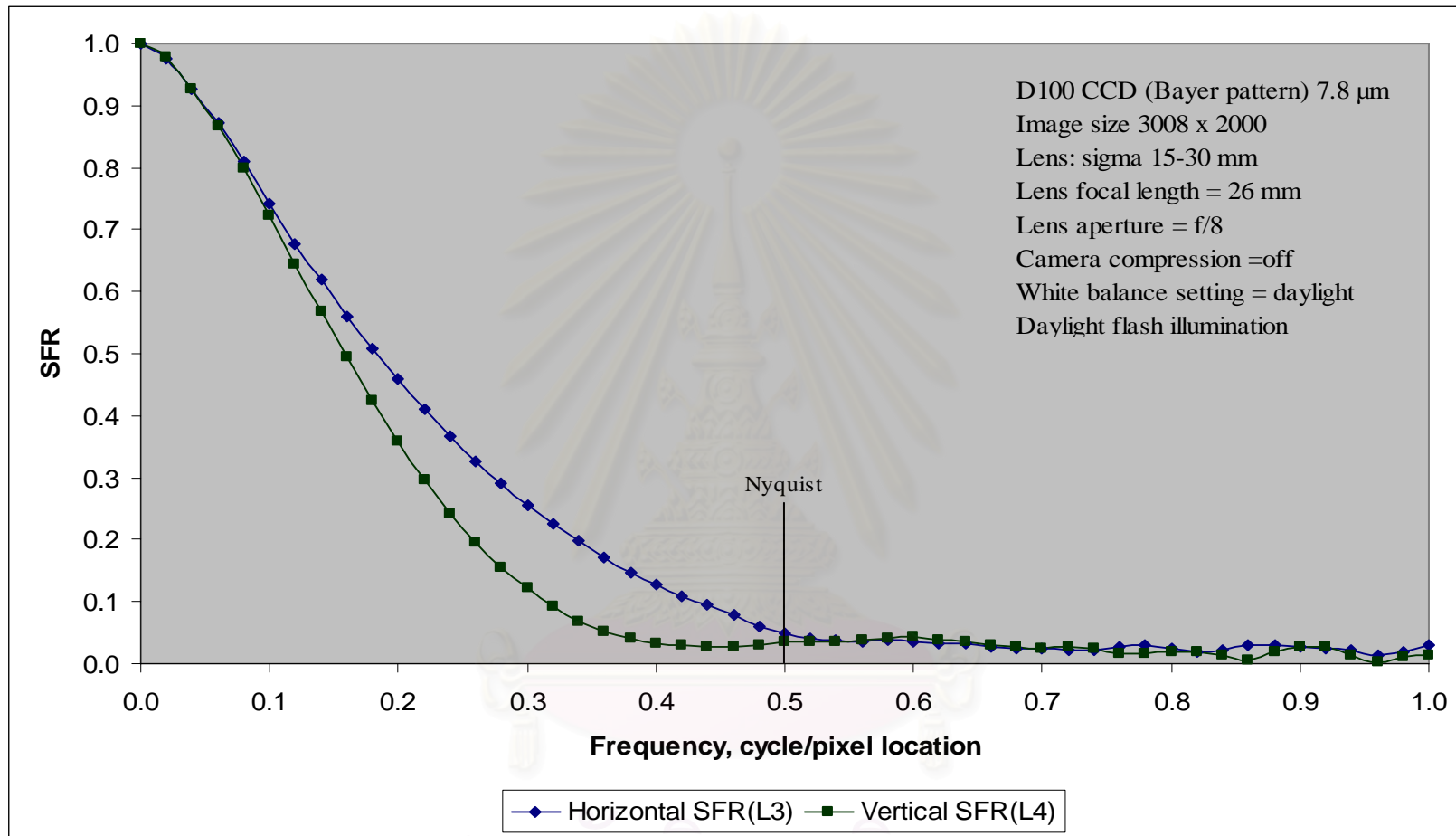


Figure 4-7 The horizontal SFR and vertical SFR from Nikon D100.

Table 4-4 The value of horizontal SFR and vertical SFR from Fuji S2pro.

Frequency (Cycles/pixel location)	Fuji S2pro Horizontal SFR(L3)	Fuji S2pro Vertical(L4)
0.0000	1.0000	1.0000
0.0200	0.9804	0.9805
0.0400	0.9346	0.9327
0.0600	0.8793	0.8746
0.0800	0.8176	0.8125
0.1000	0.7589	0.7505
0.1200	0.7053	0.6903
0.1400	0.6603	0.6373
0.1600	0.6224	0.5886
0.1800	0.5896	0.5427
0.2000	0.5563	0.5004
0.2200	0.5217	0.4589
0.2400	0.4918	0.4182
0.2600	0.4625	0.3830
0.2800	0.4314	0.3509
0.3000	0.3977	0.3166
0.3200	0.3613	0.2810
0.3400	0.3240	0.2489
0.3600	0.2941	0.2203
0.3800	0.2649	0.1924
0.4000	0.2382	0.1673
0.4200	0.2141	0.1467
0.4400	0.1924	0.1277
0.4600	0.1682	0.1101
0.4800	0.1467	0.0926
0.5000	0.1300	0.0794
0.5200	0.1135	0.0684
0.5400	0.1006	0.0626
0.5600	0.0895	0.0535
0.5800	0.0811	0.0448
0.6000	0.0682	0.0392
0.6200	0.0601	0.0379
0.6400	0.0551	0.0342
0.6600	0.0500	0.0264
0.6800	0.0494	0.0255
0.7000	0.0406	0.0240
0.7200	0.0340	0.0265
0.7400	0.0375	0.0215
0.7600	0.0324	0.0091
0.7800	0.0281	0.0175
0.8000	0.0260	0.0215
0.8200	0.0224	0.0217
0.8400	0.0301	0.0202
0.8600	0.0337	0.0100
0.8800	0.0246	0.0105
0.9000	0.0200	0.0179
0.9200	0.0184	0.0147
0.9400	0.0079	0.0068
0.9600	0.0133	0.0127
0.9800	0.0177	0.0140
1.0000	0.0058	0.0069

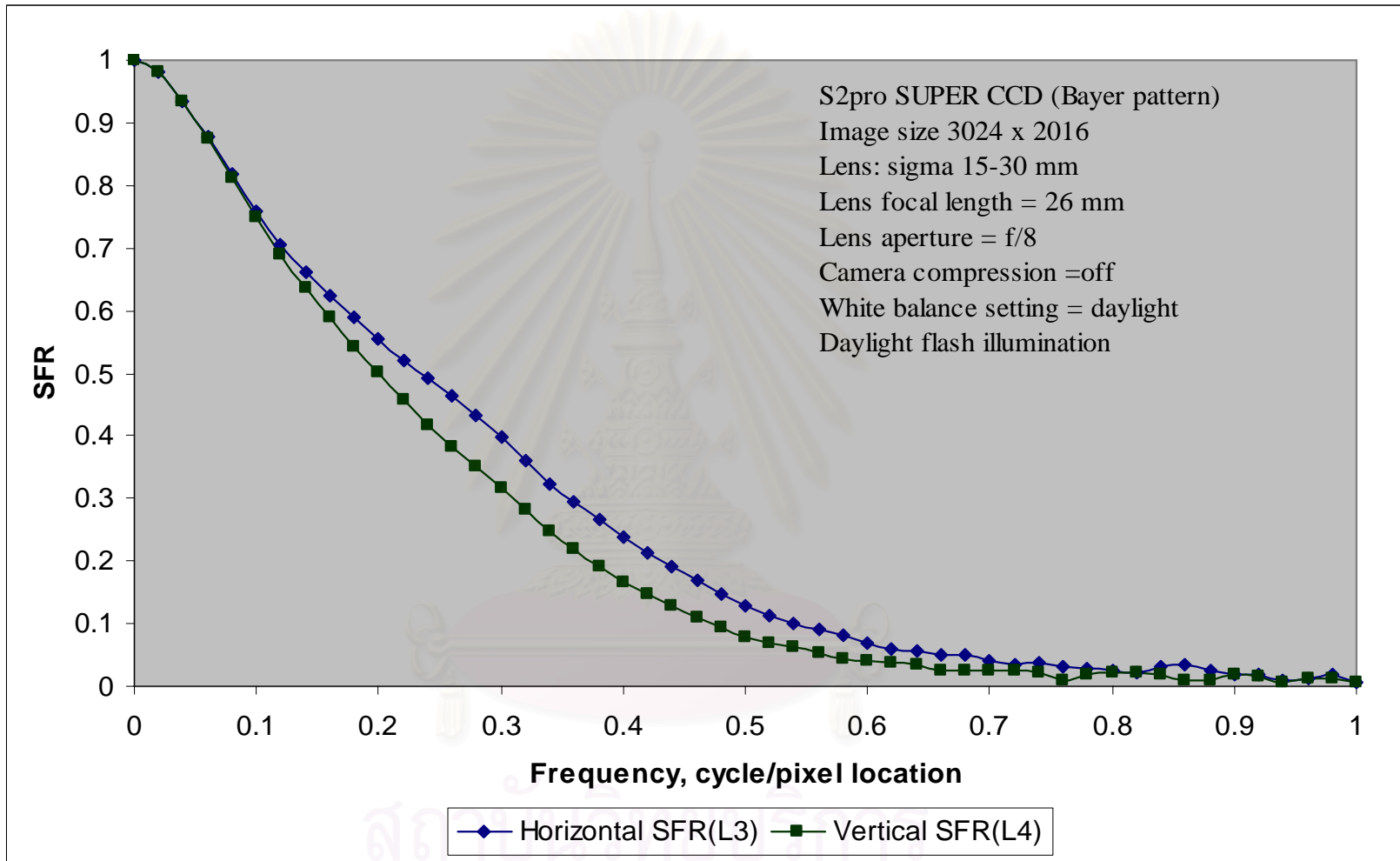


Figure 4-8 The horizontal SFR and vertical SFR from Fuji S2pro.

Table 4-5 The value of horizontal SFR and vertical SFR from Canon D60.

Frequency (Cycles/pixel location)	Canon D60 Horizontal SFR(L3)	Canon D60 Vertical SFR(L4)
0.0000	1.0000	1.0000
0.0200	0.9910	0.9898
0.0400	0.9755	0.9600
0.0600	0.9640	0.9249
0.0800	0.9507	0.8876
0.1000	0.9359	0.8460
0.1200	0.9186	0.7998
0.1400	0.8944	0.7488
0.1600	0.8661	0.6955
0.1800	0.8297	0.6366
0.2000	0.7805	0.5756
0.2200	0.7227	0.5148
0.2400	0.6586	0.4544
0.2600	0.5871	0.3895
0.2800	0.5125	0.3278
0.3000	0.4325	0.2762
0.3200	0.3504	0.2275
0.3400	0.2773	0.1830
0.3600	0.2201	0.1449
0.3800	0.1720	0.1151
0.4000	0.1290	0.0902
0.4200	0.0986	0.0690
0.4400	0.0792	0.0532
0.4600	0.0688	0.0408
0.4800	0.0627	0.0365
0.5000	0.0528	0.0338
0.5200	0.0488	0.0322
0.5400	0.0491	0.0403
0.5600	0.0450	0.0527
0.5800	0.0525	0.0615
0.6000	0.0661	0.0694
0.6200	0.0719	0.0738
0.6400	0.0747	0.0783
0.6600	0.0729	0.0775
0.6800	0.0661	0.0733
0.7000	0.0609	0.0724
0.7200	0.0581	0.0673
0.7400	0.0556	0.0553
0.7600	0.0514	0.0466
0.7800	0.0417	0.0417
0.8000	0.0375	0.0377
0.8200	0.0471	0.0373
0.8400	0.0518	0.0335
0.8600	0.0525	0.0275
0.8800	0.0605	0.0292
0.9000	0.0642	0.0224
0.9200	0.0590	0.0101
0.9400	0.0482	0.0197
0.9600	0.0307	0.0249
0.9800	0.0324	0.0218
1.0000	0.0403	0.0138

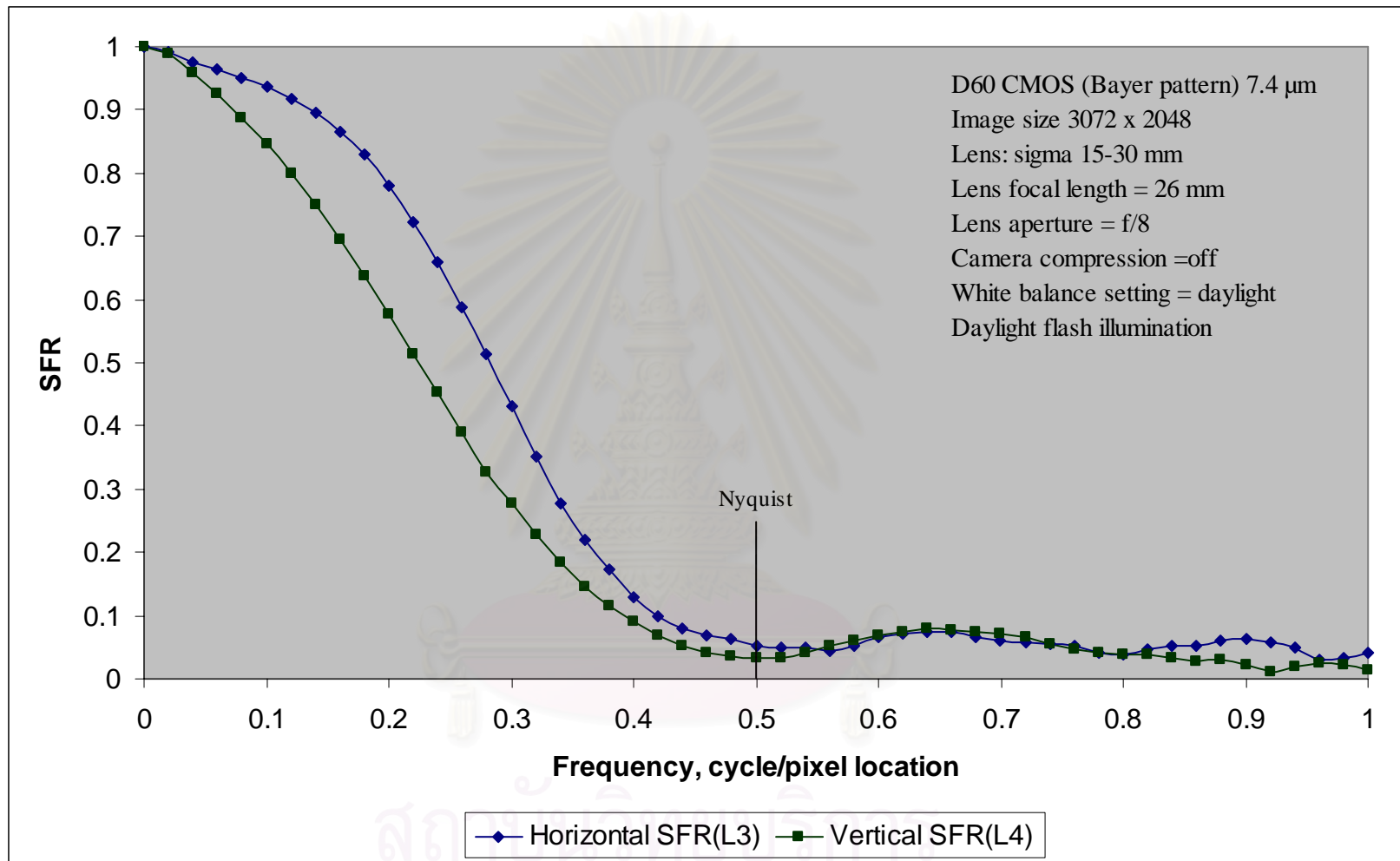


Figure 4-9 The horizontal SFR and vertical SFR from Canon D60.

Table 4-6 The value of horizontal SFR and vertical SFR from Sigma SD9.

Frequency (Cycles/pixel location)	Sigma SD9 Horizontal SFR(L3)	Sigma SD9 Vertical SFR (L4)
0.0000	1.0000	1.0000
0.0200	0.9852	0.9863
0.0400	0.9609	0.9576
0.0600	0.9453	0.9298
0.0800	0.9352	0.9071
0.1000	0.9284	0.8881
0.1200	0.9257	0.8671
0.1400	0.9229	0.8453
0.1600	0.9153	0.8150
0.1800	0.9038	0.7781
0.2000	0.8829	0.7356
0.2200	0.8465	0.6827
0.2400	0.8045	0.6180
0.2600	0.7510	0.5518
0.2800	0.6842	0.4861
0.3000	0.6187	0.4201
0.3200	0.5501	0.3598
0.3400	0.4790	0.3041
0.3600	0.4088	0.2524
0.3800	0.3427	0.2074
0.4000	0.2840	0.1680
0.4200	0.2367	0.1349
0.4400	0.1987	0.1092
0.4600	0.1667	0.0874
0.4800	0.1406	0.0714
0.5000	0.1221	0.0629
0.5200	0.1075	0.0561
0.5400	0.0921	0.0511
0.5600	0.0815	0.0462
0.5800	0.0705	0.0426
0.6000	0.0576	0.0394
0.6200	0.0529	0.0363
0.6400	0.0436	0.0275
0.6600	0.0291	0.0264
0.6800	0.0159	0.0315
0.7000	0.0116	0.0259
0.7200	0.0051	0.0128
0.7400	0.0115	0.0165
0.7600	0.0150	0.0119
0.7800	0.0134	0.0032
0.8000	0.0237	0.0144
0.8200	0.0234	0.0200
0.8400	0.0196	0.0187
0.8600	0.0210	0.0201
0.8800	0.0284	0.0078
0.9000	0.0271	0.0211
0.9200	0.0359	0.0218
0.9400	0.0404	0.0202
0.9600	0.0249	0.0167
0.9800	0.0093	0.0265
1.0000	0.0161	0.0354

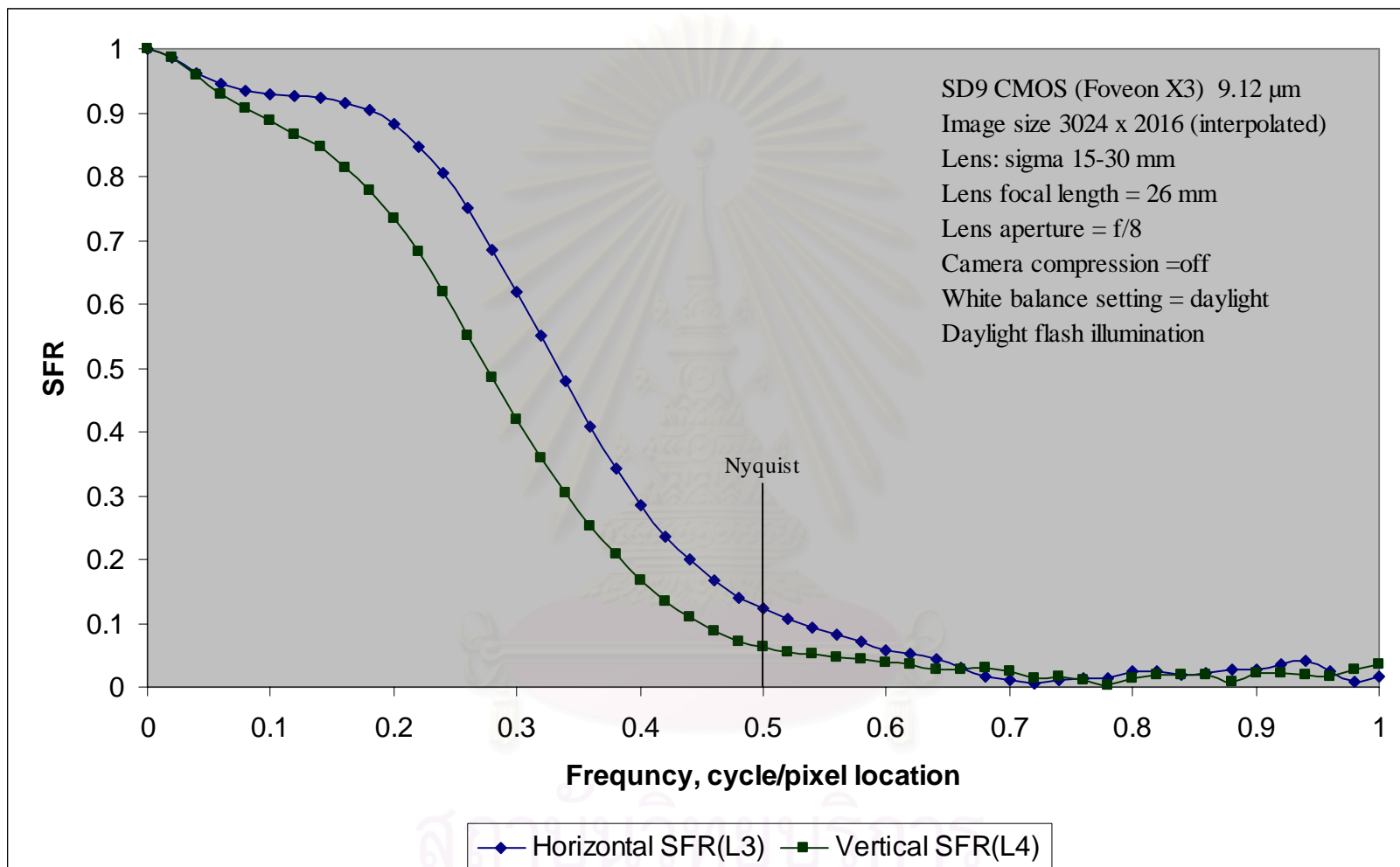


Figure 4-10 The horizontal SFR and vertical SFR from Nikon Sigma SD9.

4.1.2 The Comparison of the Image Resolution

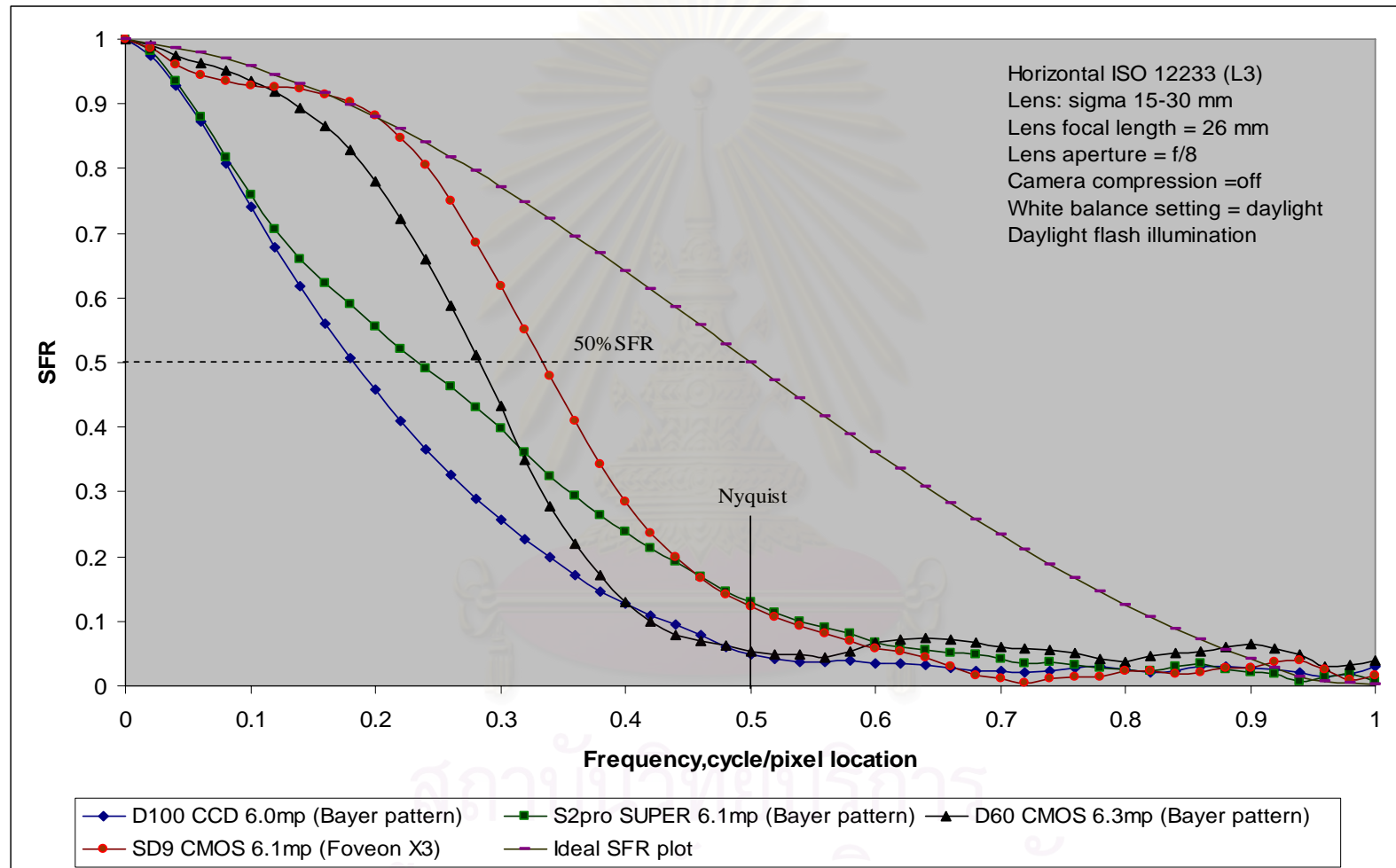


Figure 4-11 The horizontal SFR of each image sensor.

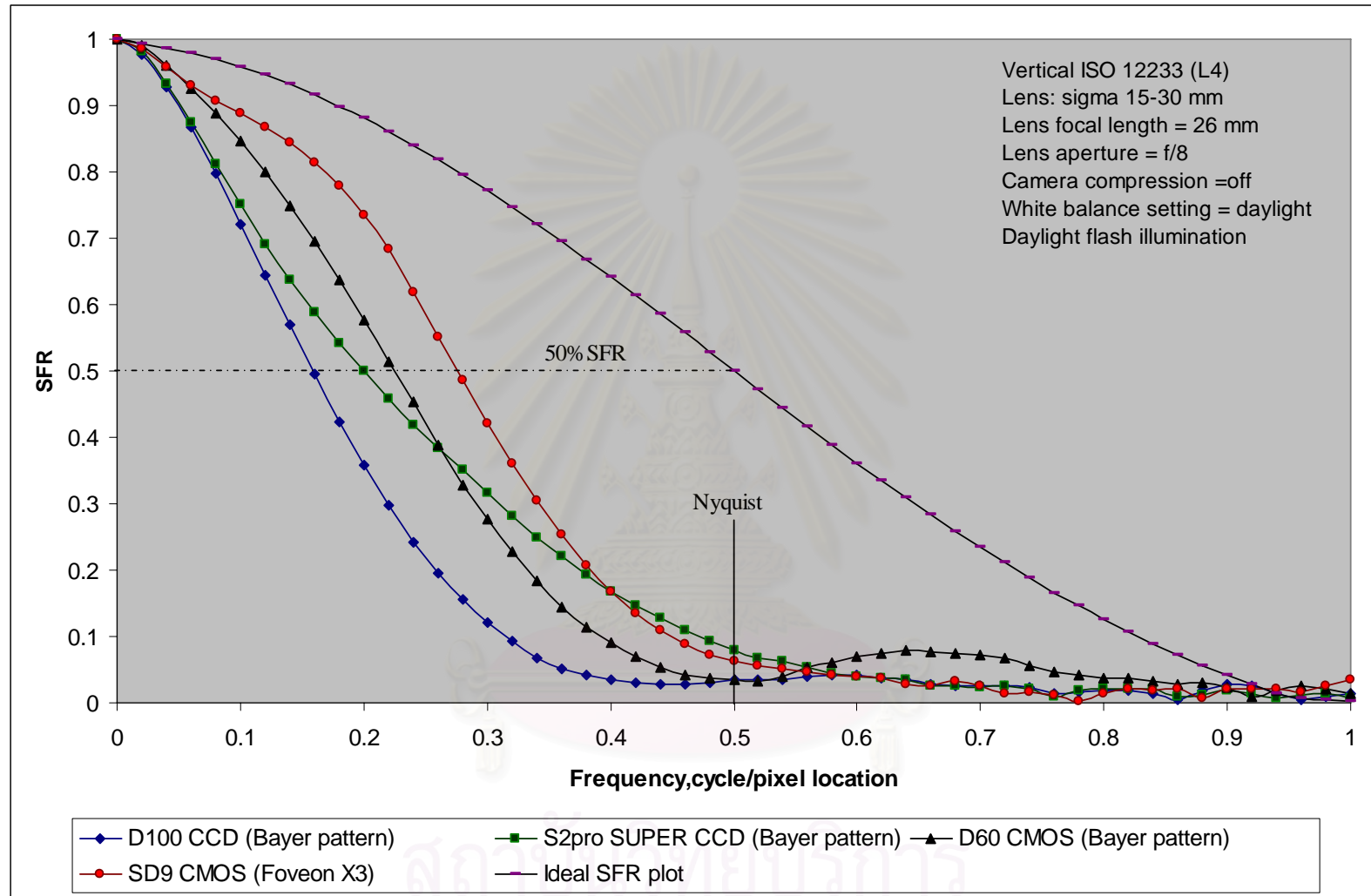


Figure 4-12 The vertical SFR of each image sensor.

From Figures 4-11 and 4-12, when considering the 50% SFR, the result shows that Sigma SD9 (Foveon X3) can provide an image at 50% SFR at spatial frequency higher than Canon D60 (CMOS), Fuji S2proZ (Super CCD) and Nikon D100 (CCD) respectively. This implies that overall image sharpness will be better in Sigma SD9 (Foveon X3).

To evaluate moiré and color artifact, the SFR just above nyquist frequency or 0.5 cycle per pixel location must be compared. This can indicate the beginning of moiré and color artifact. The results of horizontal and vertical slant edge show that Fuji S2pro (Super CCD), shows the highest contrast followed by Sigma SD9 (Foveon X3), Canon D60 (CMOS) and Nikon D100 (CCD).

Nyquist frequency can indicate the SFR of moiré and color artifact occurred. This SFR just nyquist frequency showing the contrast of image sensors, lower value will be higher chance of moiré and color artifact occurred. From Figures 4-11-4-12, when considering the nyquist frequency, the result shows that Nikon D100 (CCD) has highest chance of moiré and color artifact occurred, followed by Canon D60 (CMOS), Sigma SD9 (Foveon X3) and Fuji S2pro (Super CCD). However, when considering the visual resolution, Sigma SD9 (Foveon X3) has the lowest value of absolute resolution because of no anti aliasing filter.

4.2 The Tone Reproduction

4.2.1 The Preparation and Evaluation of the Tone Reproduction

Since tone reproduction were evaluated in terms of dynamic range. The first result shown in Table 4-7 are the value of shadow.

Table 4-7 Number of observers who can differentiate the shadow detail.

First pixels value/ Δ pixels value	0	1	2	3	4	5	6	7	8	9	10	11	12	13	14	15
1	0	0	0	0	0	0	0	0	0	0	0	0	0	0	0	0
2	0	0	0	0	0	0	0	0	0	0	0	0	0	0	0	0
3	0	0	0	0	0	0	0	0	0	0	0	0	0	0	0	0
4	3	3	3	3	3	3	3	3	3	3	3	3	3	3	3	3
5	3	3	3	3	3	3	3	3	3	3	3	3	3	3	3	3

Table 4-7 shows the number of observer who can see the differentiation of shadow details from Figures 3-3 and 3-4. The data are obtained from 3 observers.

สถาบันวิทยบริการ
จุฬาลงกรณ์มหาวิทยาลัย

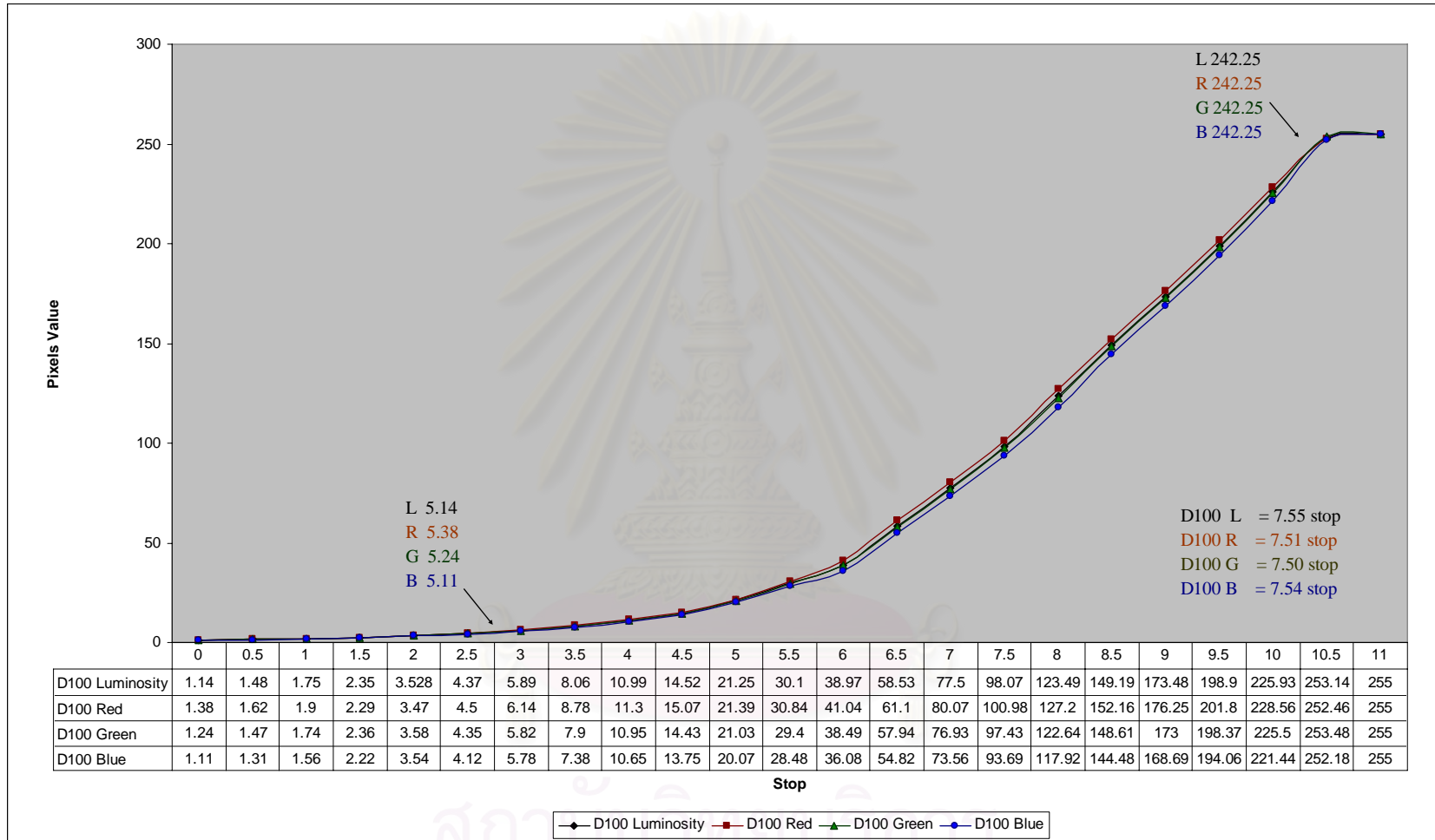


Figure 4-13 Tone reproduction at 8 bits per channel from Nikon D100.



Figure 4-14 The middle gray patches of various shutter speeds (11.5 stop) captured by Nikon D100.

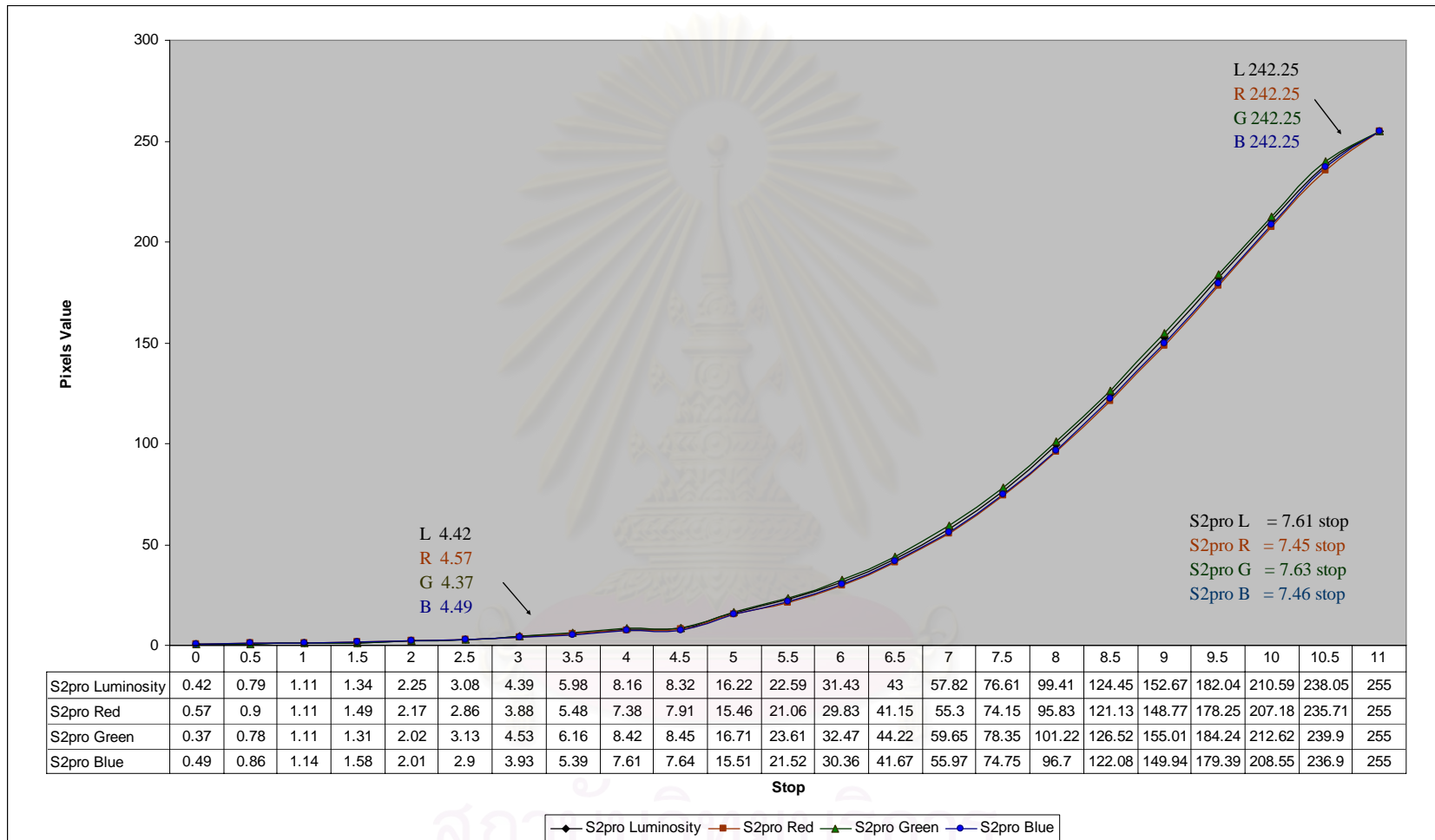


Figure 4-15 Tone reproduction at 8 bits per channel from Fuji S2pro.



Figure 4-16 The middle gray patches of various shutter speeds (11.5 stop) captured by Fuji S2pro.

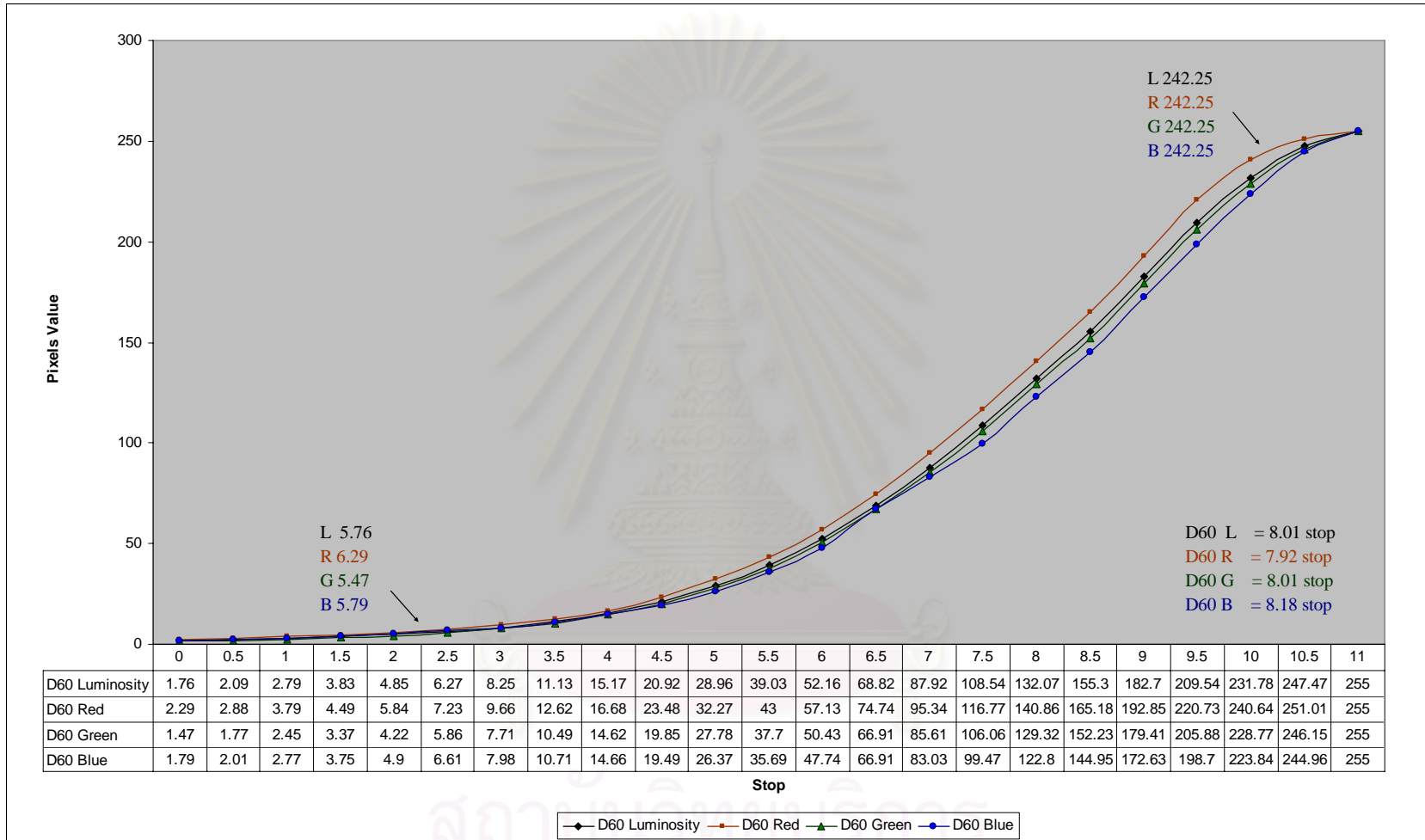


Figure 4-17 Tone reproduction at 8 bits per channel from Canon D60.



Figure 4-18 The middle gray patches of various shutter speeds (11.5 stop) captured by Canon D60.

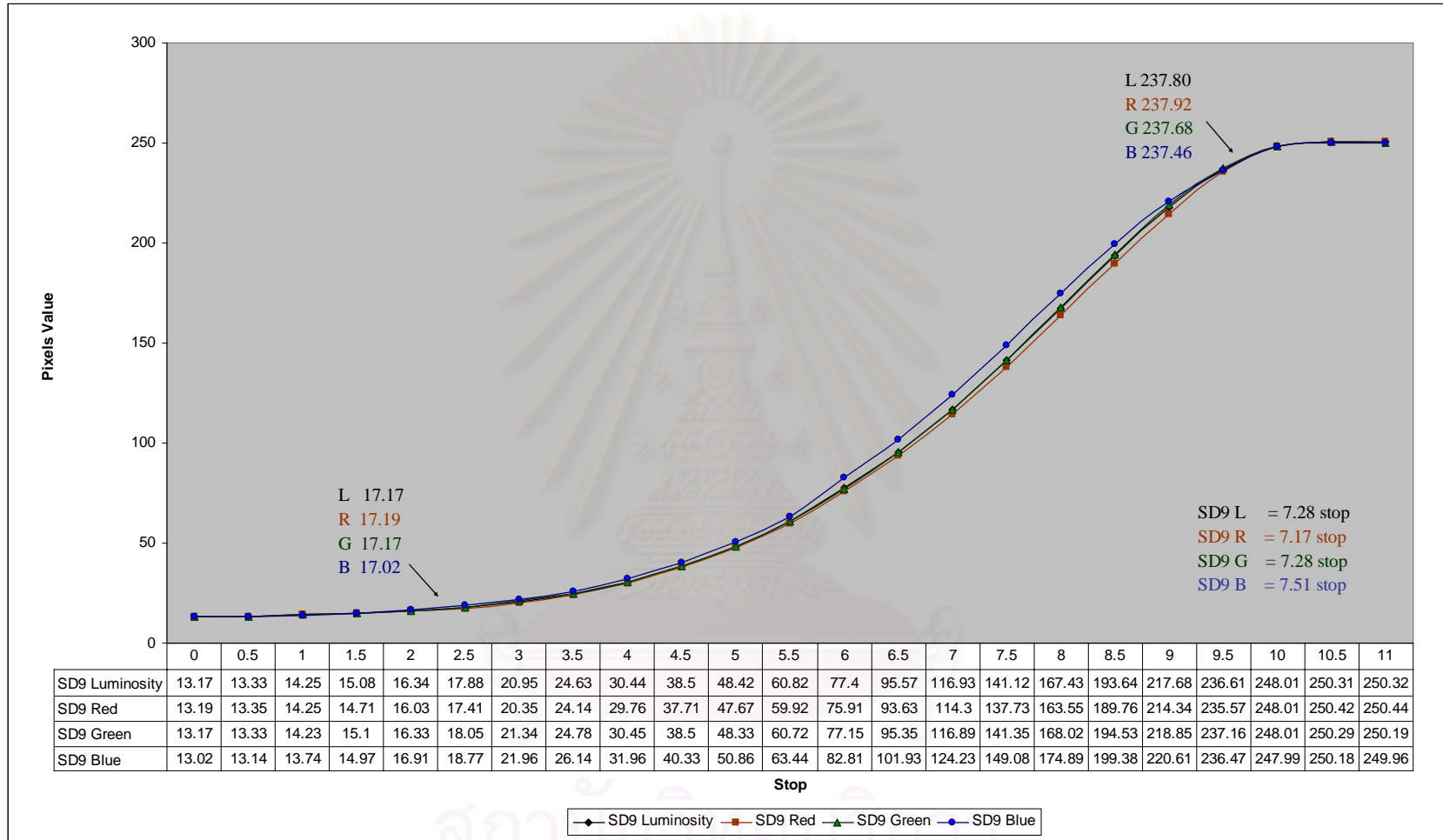


Figure 4-19 Tone reproduction at 8 bits per channel from Sigma SD9.

Figures 4-13, 4-15, 4-17 and 4-19 show tone reproduction at different channels of each image sensor. The y axis represents the pixel values from 0 – 255 at 8 bits per channel, while the x axis represents the change of luminance in 0.5 stop intervals. (tone reproduction calculation is shown in Appendix A).



สถาบันวิทยบริการ
จุฬาลงกรณ์มหาวิทยาลัย



Figure 4-20 The middle gray patches of various shutter speeds (11.5 stop) captured from Macbeth color checker by Sigma SD9.

4.2.2 The Comparison of the Tone Reproduction

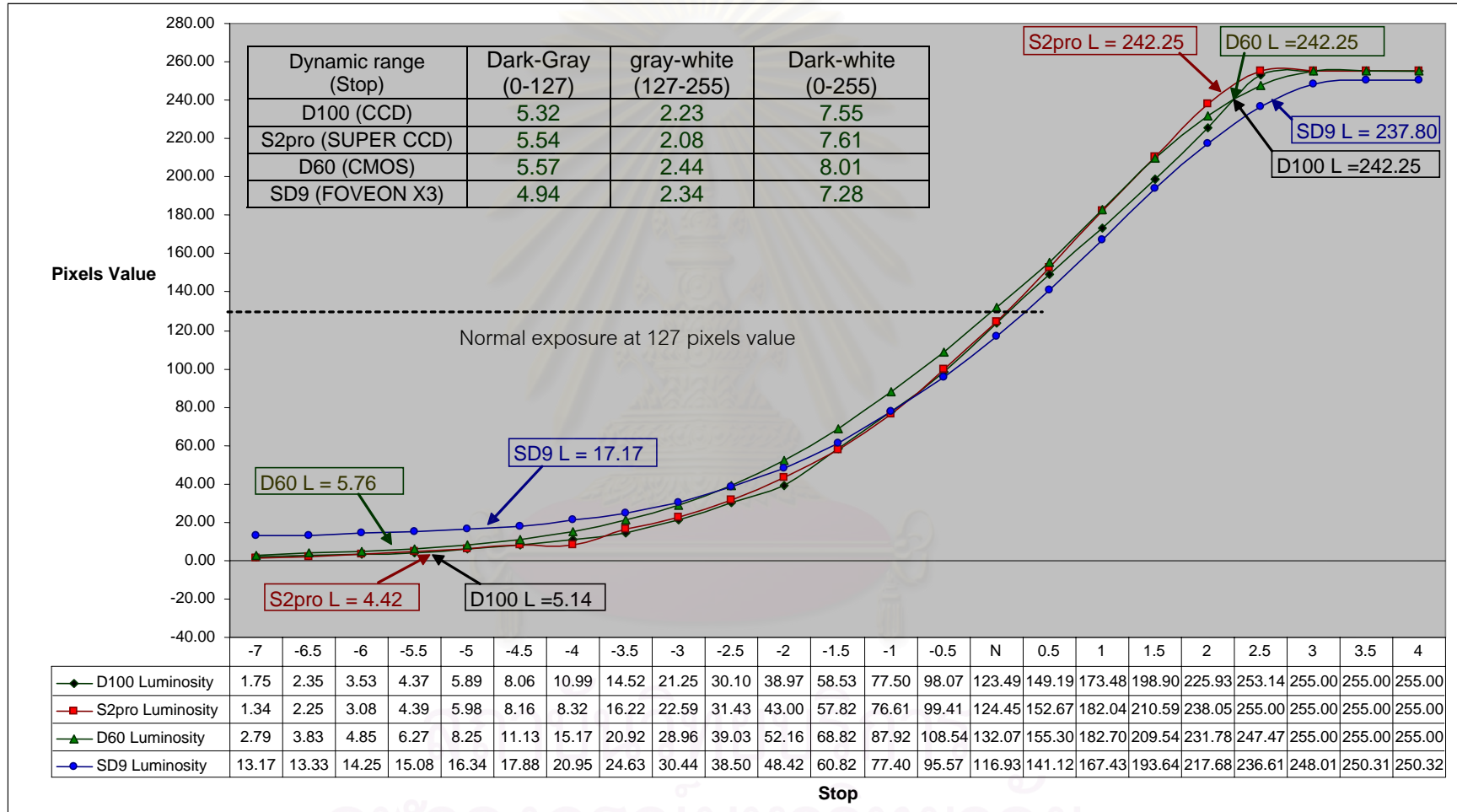


Figure 4-21 The luminosity of tone reproduction at 8 bits per channel from all image sensors.

Figure 4-21 shows tone reproductions in luminance channel. All image sensor types including Nikon D100 (CCD), Fuji S2pro Z (Super CCD), Canon D60 (CMOS) and Sigma SD9 (Foveon X3) were set at the pixels value 127 and there are two parts of tone to be analyzed.

The first part is the gray to dark tone pixel values from 0-127. The dynamic ranges of Nikon D100 (CCD), Fuji S2pro (Super CCD), Canon D60 (CMOS) and Sigma SD9 (Foveon X3) are 5.32, 5.54, 5.57 and 4.94, respectively. Therefore, each image sensor type has similar tone reproduction in the gray to dark tone. The second part is the gray to white tone pixel values from 127-255. Canon D60 (CMOS) has the best dynamic range at 2.4 stop while Sigma SD9 (Foveon X3), Nikon D100 (CCD) and Fuji S2pro (Super CCD) have 2.44, 2.34, 2.23 and 2.08, respectively.

Comparing the overall dynamic range of each image sensor type, Canon D60 (CMOS) has the best dynamic range at 8.01 stop while Fuji S2Pro (Super CCD), Nikon D100 (CCD) and Sigma SD9 (Foveon X3) have lower dynamic range respectively. Therefore, Canon D60 (CMOS) has the best tone reproduction for overall dynamic range comparison.

As a result, Canon D60 (CMOS) has the highest dynamic range which means that CMOS will be able to capture subtle tonal gradation in the shadow, midtone, and highlight details of the scene. Fuji S2pro (Super CCD), Nikon D100 (CCD) and Sigma SD9 (Foveon X3) also have lower dynamic range subsequently.

4.3 The Color Reproduction

4.3.1 The Preparation and Evaluation of the Color Reproduction

The color differences (ΔE^*_{ab}) of Macbeth color checker in sRGB mode are measured. The images were captured under daylight and auto white balance setting of each camera were controlled to guarantee day light illumination.

1	2	3	4	5	6
7	8	9	10	11	12
13	14	15	16	17	18
19	20	21	22	23	24

Figure 4-22 The 24 assigned numbers to each color patch of the Macbeth Color Checker.

From the experiment, the color of Gretag Macbeth of original color reproduction from each image sensor are shown in Table 4-8.

Table 4-9 to Table 4-12 show the color value of Macbeth Color Checker after adjusting the white to be equal to the light source. The average RGB values was measured by cropping the color patch (at 100x100) in sRGB Color Spaces of Macbeth

Color Checker prior to measure CIEXYZ values using Eq. (2-1). Then, the CIELAB values were calculated using Eq. (2-2) – Eq. (2-6) and the ΔE^*_{ab} values were lastly calculated using Eq (2-7)

Figure 4-23 to Figure 4-26 show the color error in the a^*b^* plane of the CIELAB color space from each image sensor. The value from Table 4-9 to Table 4-12 were used to compare with the references color. The Red–Green color values were plotted in the a^* axis (X axis) and the Yellow–Blue color values were plotted in the b^* axis (Y axis).

Table 4-13 to Table 4-16 show the color value of Macbeth Color Checker after adjusting the white to be equal to the auto white balance. The average RGB values was measured by cropping the color patch (at 100x100) in sRGB Color Spaces of Macbeth Color Checker prior to measure CIEXYZ values using Eq. (2-1). Then, the CIELAB values were calculated using Eq. (2-2) – Eq. (2-6) and the ΔE^*_{ab} values were lastly calculated using Eq (2-7)

Figure 4-27 to Figure 4-30 show the color error in the a^*b^* plane of the CIELAB color space from each image sensor. The value from Table 4-13 to Table 4-16 were used to compare with the references color. The Red–Green color values were plotted in the a^* axis (X axis) and the Yellow–Blue color values were plotted in the b^* axis (Y axis).

Table 4-8 Color value of Macbeth color checker (24 patches) measured by Gretag Spectrolino under D65.

No	Color name	X Y Z (CIE)			L* a* b* (CIE D65)		
		X	Y	Z	L*	a*	b*
1	dark skin	11.28	10.06	6.61	37.95	13.21	14.42
2	light skin	37.74	35.03	25.42	65.77	15.10	17.81
3	blue sky	18.22	19.49	34.28	51.25	-1.53	-20.13
4	foliage	10.56	13.52	7.13	43.53	-16.17	22.00
5	blue flower	25.33	24.17	45.30	56.26	10.35	-24.76
6	bluish green	31.56	43.52	44.79	71.91	-32.65	2.80
7	orange	36.12	28.74	5.98	60.55	32.25	55.97
8	purplish blue	13.48	11.94	37.30	41.12	14.58	-41.49
9	moderate red	27.91	18.98	14.12	50.66	45.07	13.69
10	purple	8.47	6.59	14.44	30.85	21.45	-21.23
11	yellow green	33.67	43.99	10.58	72.22	-26.43	60.16
12	orange yellow	45.26	41.69	8.18	70.66	16.97	65.00
13	blue	8.69	6.49	31.20	30.61	24.40	-51.51
14	green	14.93	23.70	9.57	55.79	-39.65	34.83
15	red	19.73	11.46	5.06	40.35	53.21	25.25
16	yellow	56.07	58.86	9.35	81.22	0.35	79.38
17	magenta	28.08	18.54	30.14	50.15	47.92	-16.32
18	cyan	14.46	20.07	39.27	51.92	-25.81	-25.29
19	white 9.5 (0.05D)	82.07	86.78	90.41	94.65	-0.74	2.75
20	white 8 (0.23D)	54.67	57.63	61.90	80.53	-0.23	0.73
21	white 6.5 (0.44D)	33.67	35.48	38.50	66.12	-0.17	0.15
22	white 5 (0.70D)	17.95	18.85	20.50	50.51	0.22	0.03
23	white 3.5 (1.05D)	8.31	8.76	9.61	35.52	-0.13	-0.23
24	white 1.5 (1.5D)	3.78	3.93	4.26	23.43	0.74	0.08

Table 4-9 Color value and color difference of Macbeth color checker (24 patches) captured by Nikon D10 under D65.

No	sRGB			X Y Z (CIE)			L* a* b* (CIE D65)			ΔE
	R	G	B	X	Y	Z	L*	a*	b*	
1	119	67	41	9.90	7.90	2.70	33.74	21.02	27.46	15.77
2	207	155	130	42.10	39.00	26.80	68.76	15.87	20.78	4.28
3	112	140	163	23.10	25.30	39.00	57.38	-4.43	-15.57	8.17
4	93	109	50	10.50	13.50	4.70	43.57	-16.87	32.61	10.63
5	149	148	183	32.10	31.60	50.00	63.03	7.76	-18.07	9.86
6	149	204	189	43.90	54.10	57.10	78.49	-20.85	1.64	13.56
7	223	123	23	38.00	30.20	4.30	61.87	32.61	66.07	10.19
8	76	103	175	15.60	14.40	43.30	44.77	12.01	-42.30	4.54
9	214	85	86	32.90	21.50	11.10	53.49	51.45	26.43	14.53
10	86	58	97	7.30	5.60	12.00	28.27	21.73	-19.50	3.12
11	184	197	75	41.60	51.40	14.10	76.93	-20.91	58.94	7.36
12	234	170	49	49.30	47.10	9.00	74.26	12.57	68.46	6.66
13	36	69	166	9.60	7.10	37.70	32.10	25.49	-57.48	6.25
14	92	160	70	18.30	28.30	10.00	60.20	-39.93	41.09	7.66
15	196	37	30	23.80	13.00	2.10	42.76	61.75	47.58	24.03
16	242	201	64	58.80	61.70	13.30	82.74	0.41	70.94	8.58
17	193	89	145	31.10	20.70	29.70	52.58	48.87	-11.45	5.52
18	70	158	190	24.30	30.00	54.10	61.64	-17.16	-24.49	13.04
19	235	231	223	76.70	80.70	82.00	92.00	-0.08	4.24	3.11
20	207	203	195	57.70	60.80	61.10	82.25	-0.08	4.40	4.06
21	173	168	161	38.40	40.30	40.20	69.65	0.48	4.24	5.44
22	130	123	116	19.70	20.50	19.60	52.39	1.36	4.90	5.34
23	80	76	71	6.80	7.10	6.70	31.99	0.66	3.82	5.43
24	40	37	33	1.40	1.50	1.30	12.39	0.59	3.69	11.62

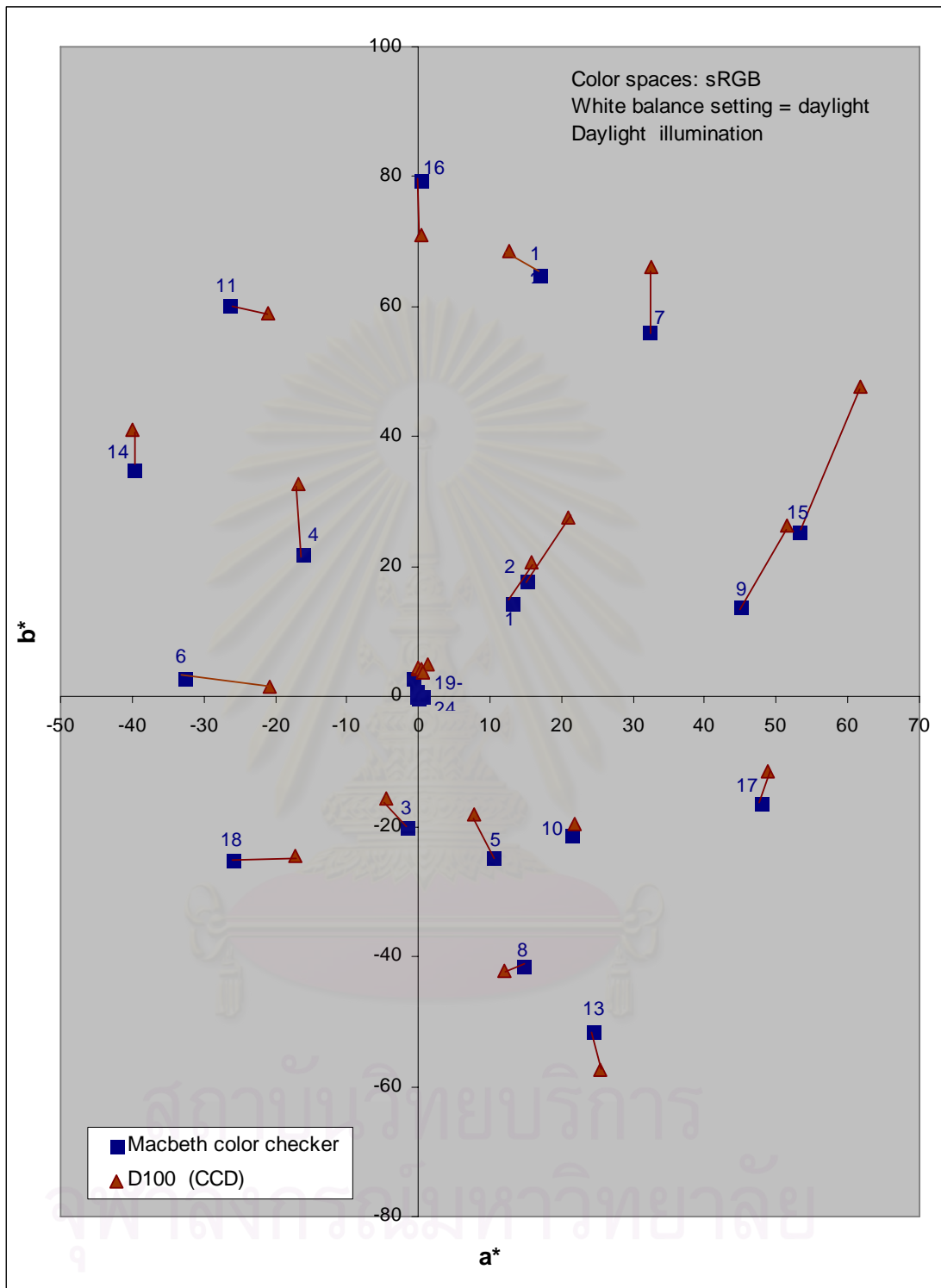


Figure 4-23 Color error in the a^*b^* plane of the CIELAB color space captured by Nikon D100 under D65.

Table 4-10 Color value and color differences of Macbeth color checker (24 patches) captured by Fuji S2pro under D65.

No	sRGB			X Y Z (CIE)			L* a* b* (CIE D65)			ΔE
	R	G	B	X	Y	Z	L*	a*	b*	
1	141	83	62	15.00	12.10	5.80	41.45	22.71	23.93	13.89
2	236	173	150	55.60	50.60	36.30	76.46	19.65	20.74	11.98
3	111	141	174	24.10	26.00	44.60	58.00	-2.41	-20.91	6.85
4	88	105	57	9.70	12.50	5.40	41.96	-16.03	26.45	4.72
5	145	141	187	30.70	29.20	51.90	60.98	11.44	-23.47	5.01
6	122	197	186	37.40	48.40	54.60	75.06	-25.95	-1.94	8.79
7	254	150	48	52.40	43.50	8.00	71.91	31.22	67.66	16.33
8	83	108	187	18.00	16.30	50.00	47.31	14.34	-45.17	7.21
9	240	96	96	42.30	27.80	14.20	59.69	55.62	29.16	20.79
10	87	49	98	7.00	4.80	12.10	26.09	28.39	-23.59	8.74
11	175	192	76	38.40	48.10	13.90	74.90	-22.08	56.11	6.52
12	235	163	39	48.10	44.60	7.60	72.63	16.40	70.48	5.85
13	43	73	174	10.90	8.10	41.80	34.20	26.49	-58.82	8.41
14	87	164	88	19.20	29.80	13.90	61.47	-40.77	32.99	6.07
15	226	44	40	32.70	17.90	3.30	49.39	68.33	50.10	30.46
16	252	209	75	64.50	67.40	16.00	85.70	0.97	69.76	10.63
17	212	87	145	36.00	23.00	29.90	55.03	55.69	-7.49	12.73
18	32	137	174	17.30	21.60	44.10	53.58	-16.33	-27.99	10.00
19	255	254	253	94.40	99.30	107.20	99.73	0.11	0.56	5.60
20	225	219	220	69.90	72.60	78.70	88.24	2.13	0.21	8.08
21	178	173	173	41.60	43.20	46.50	71.68	1.74	0.62	5.90
22	122	116	117	17.70	18.10	19.60	49.68	2.54	0.27	2.48
23	62	61	62	4.20	4.30	4.80	24.78	0.70	-0.51	10.78
24	28	27	27	0.70	0.70	0.80	6.23	-0.58	-0.20	17.25

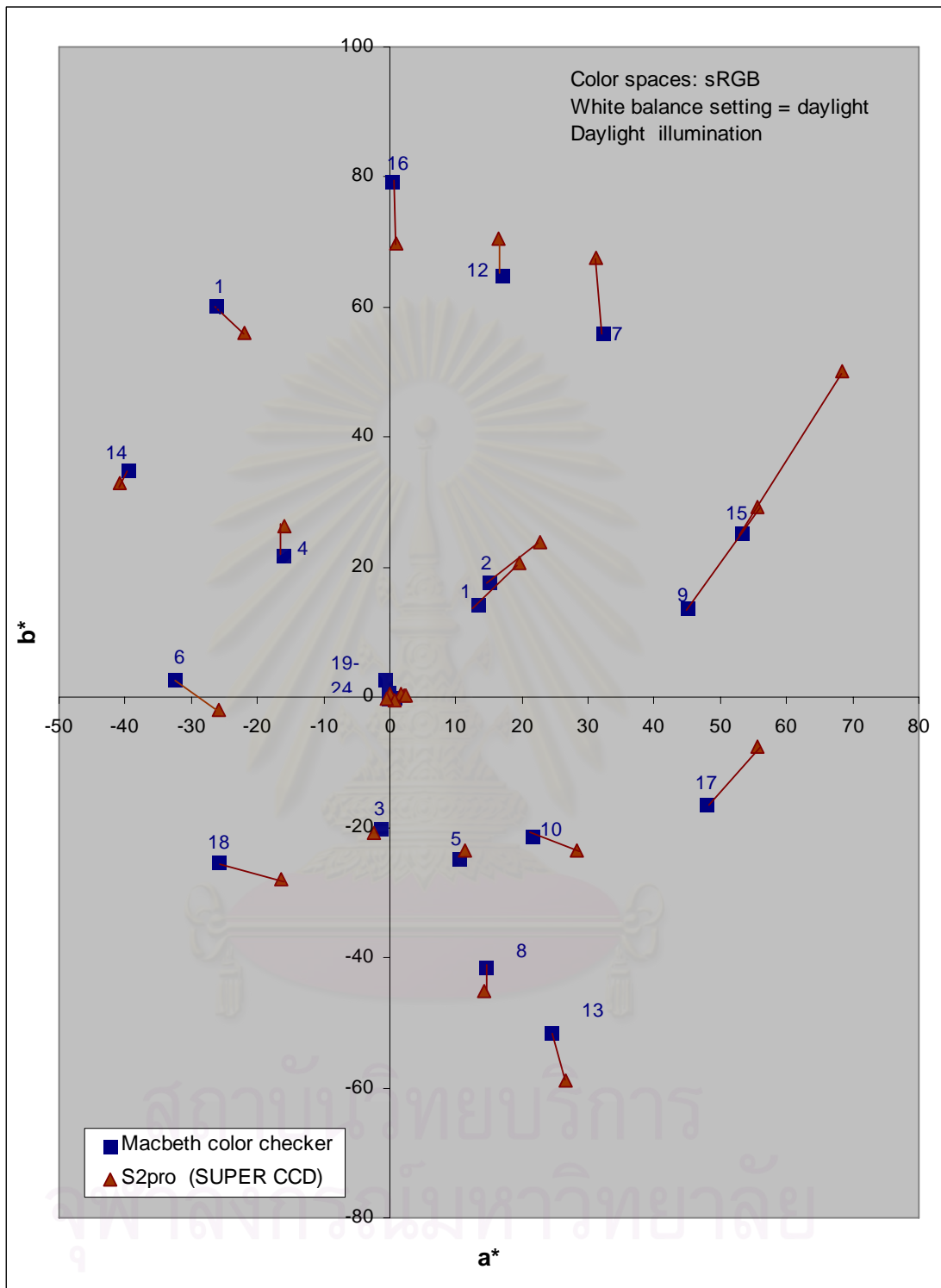


Figure 4-24 Color error in the a^*b^* plane of the CIELAB color space captured by Fuji S2pro under D65.

Table 4-11 Color value and color differences of Macbeth color checker (24 patches) captured by Canon D60 under D65.

No	sRGB			X Y Z (CIE)			L* a* b* (CIE D65)			ΔE
	R	G	B	X	Y	Z	L*	a*	b*	
1	132	78	45	12.70	10.40	3.50	38.62	20.44	30.40	17.55
2	221	166	133	48.30	45.10	28.80	72.94	15.69	25.02	10.19
3	123	149	179	27.50	29.50	47.70	61.25	-2.07	-18.71	10.11
4	98	126	54	13.20	18.00	5.90	49.50	-23.34	37.29	17.91
5	149	150	194	33.70	32.70	56.40	63.95	9.16	-22.78	8.03
6	144	215	199	46.80	59.40	63.90	81.51	-25.55	0.71	12.12
7	233	138	32	43.20	36.00	5.70	66.55	28.77	67.67	13.60
8	92	112	194	20.10	17.90	54.30	49.40	16.10	-45.80	9.46
9	217	97	93	35.10	24.20	13.10	56.31	47.15	25.90	13.61
10	95	64	113	9.40	7.00	16.70	31.91	24.87	-24.37	4.76
11	187	213	91	46.80	59.70	18.90	81.65	-26.12	56.88	9.99
12	229	172	45	48.00	47.00	8.60	74.21	9.29	69.61	9.64
13	60	76	185	13.10	9.40	47.00	36.81	30.76	-61.00	13.00
14	105	184	92	25.20	38.70	16.20	68.53	-43.03	39.79	14.08
15	196	51	44	24.50	14.10	3.40	44.43	57.81	41.08	16.98
16	246	217	83	64.70	70.40	18.20	87.20	-5.01	67.78	14.11
17	193	87	144	30.80	20.30	29.20	52.16	49.74	-11.48	5.55
18	66	160	199	25.40	30.90	59.50	62.46	-16.09	-28.23	14.64
19	245	244	240	86.00	90.70	95.80	96.30	-0.40	1.96	1.86
20	225	224	216	70.70	75.00	76.40	89.37	-1.09	3.93	9.44
21	186	186	178	46.60	49.60	50.00	75.84	-1.48	4.01	10.54
22	138	138	132	24.20	25.70	25.90	57.79	-1.20	3.20	8.07
23	87	89	85	9.00	9.70	9.80	37.30	-1.76	2.15	3.39
24	43	43	42	1.90	2.00	2.10	15.52	0.24	0.92	7.97

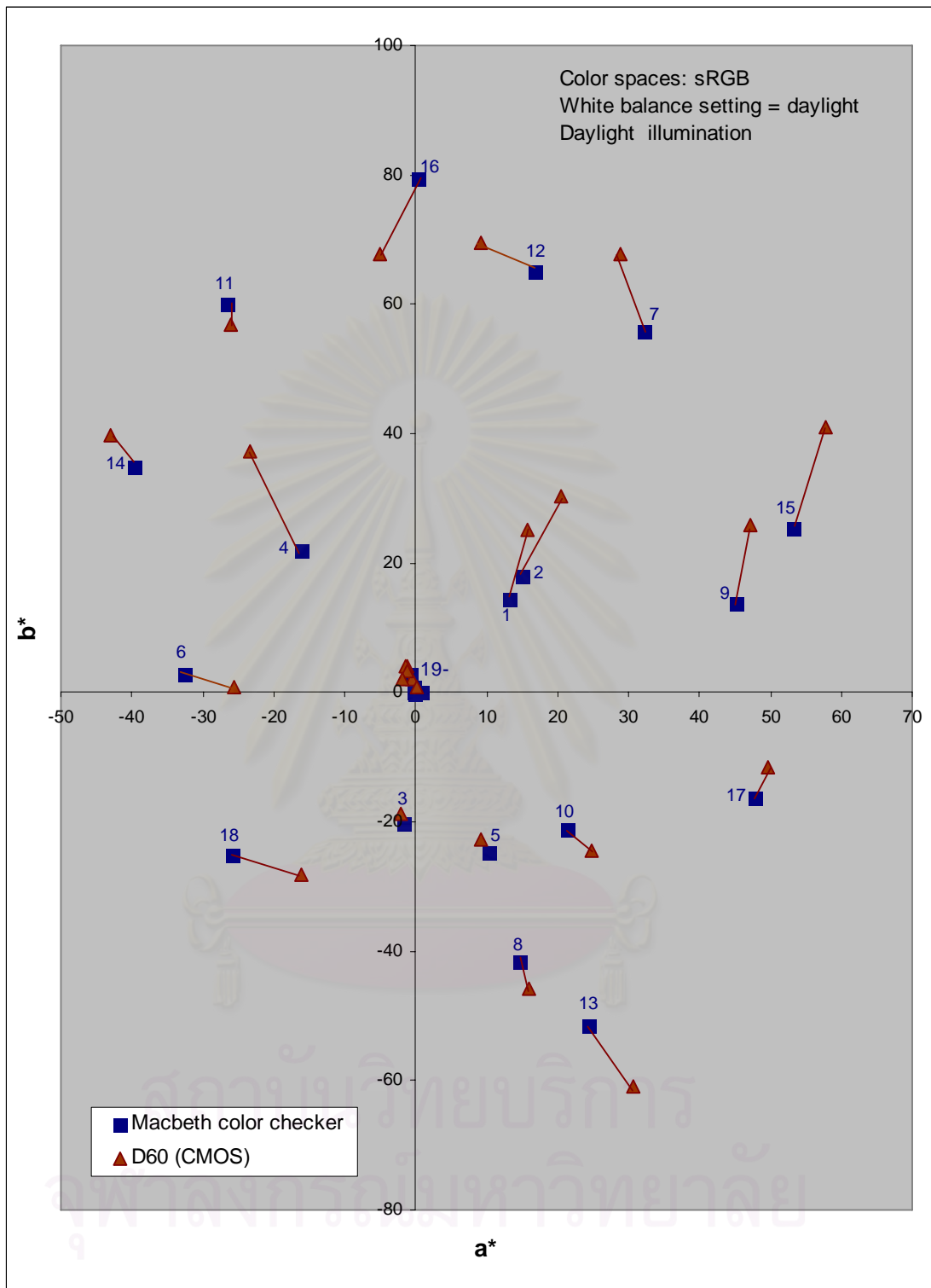


Figure 4-25 Color error in the a*b*plane of the CIELAB color space captured by Canon D60 under D65.

Table 4-12 Color value and color differences of Macbeth color checker (24 patches) captured by Sigma SD9 under D65.

No	sRGB			X Y Z (CIE)			L* a* b* (CIE D65)			ΔE
	R	G	B	X	Y	Z	L*	a*	b*	
1	119	75	61	10.90	9.10	5.30	36.23	17.82	17.23	5.67
2	201	156	123	40.20	38.30	24.30	68.25	12.11	23.93	7.25
3	77	113	149	14.50	15.70	31.30	46.55	-2.67	-24.13	6.28
4	84	91	50	7.80	9.50	4.00	36.86	-10.65	24.42	8.99
5	117	107	162	19.40	17.10	37.20	48.36	16.85	-28.80	11.00
6	103	175	149	26.80	36.40	34.60	66.80	-29.12	6.24	7.10
7	217	143	43	39.30	35.10	6.60	65.82	19.77	62.54	15.06
8	52	77	159	10.20	8.30	34.60	34.67	19.23	-49.06	10.98
9	222	110	108	38.70	28.00	17.70	59.90	53.56	21.78	14.93
10	92	41	115	8.10	4.80	16.90	26.13	38.86	-34.86	22.61
11	165	173	48	31.50	38.80	8.20	68.62	-18.67	61.32	8.63
12	205	153	36	37.40	36.50	6.40	66.90	8.96	65.37	8.86
13	20	68	173	9.80	7.10	41.20	31.95	27.77	-61.94	11.04
14	91	145	64	15.50	23.20	8.20	55.29	-34.31	38.50	6.50
15	188	43	60	22.50	12.60	5.20	42.14	58.87	27.83	6.47
16	226	190	30	50.50	53.80	8.60	78.35	-1.75	76.93	4.32
17	205	71	157	33.90	19.90	34.60	51.75	62.40	-19.69	14.95
18	23	116	140	11.40	14.70	27.50	45.20	-17.51	-20.96	11.52
19	222	219	213	68.10	71.70	74.00	87.84	-0.08	3.22	6.86
20	191	186	186	48.70	50.60	54.50	76.44	1.70	0.60	4.52
21	149	146	146	28.40	29.60	32.00	61.32	1.08	0.38	4.97
22	100	98	99	11.90	12.30	13.60	41.75	1.02	-0.31	8.80
23	56	55	56	3.30	3.50	3.90	21.81	0.72	-0.53	13.74
24	28	26	27	0.70	0.70	0.80	6.06	1.47	-0.42	17.39

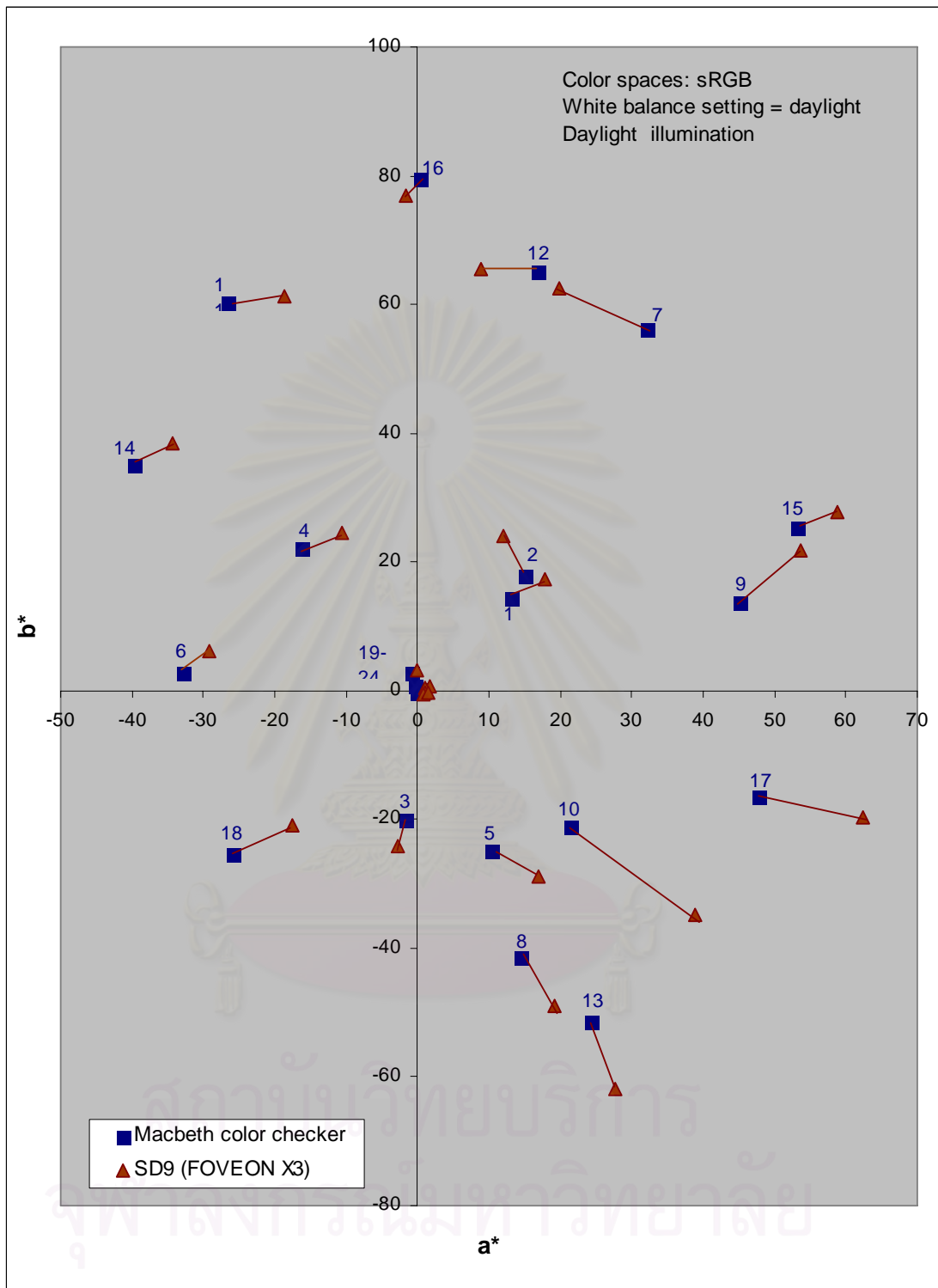


Figure 4-26 Color error in the a^*b^* plane of the CIELAB color space captured by Sigma SD9 under D65.

Table 4-13 Color value and color differences of Macbeth color checker (24 patches) captured by Nikon D100 under daylight illumination and with auto white balance setting.

No	sRGB			X Y Z (CIE)			L* a* b* (CIE D65)			ΔE
	R	G	B	X	Y	Z	L*	a*	b*	
1	105	68	52	8.40	7.10	3.80	32.13	14.83	17.61	6.83
2	192	157	145	39.60	38.10	32.60	68.09	11.01	11.17	8.14
3	97	140	177	22.60	24.90	46.00	56.98	-4.95	-24.25	7.84
4	80	110	62	9.60	13.20	6.30	43.12	-21.56	24.72	6.05
5	135	149	197	31.40	31.30	58.00	62.74	6.15	-26.39	7.89
6	132	205	204	42.90	53.70	66.00	78.28	-22.92	-6.74	15.04
7	208	125	33	34.00	28.60	4.80	60.40	25.59	61.18	8.46
8	64	102	189	16.10	14.30	50.90	44.64	15.15	-50.65	9.83
9	200	96	99	30.60	21.70	14.40	53.70	42.15	18.32	6.26
10	74	58	109	6.90	5.30	15.20	27.47	20.89	-28.90	8.40
11	168	198	90	38.80	50.20	17.20	76.21	-26.58	50.82	10.16
12	218	172	62	45.00	45.50	10.60	73.20	5.35	61.73	12.34
13	30	68	179	10.60	7.40	44.30	32.73	30.74	-64.20	14.34
14	76	168	82	18.60	30.70	12.70	62.21	-46.57	37.04	9.69
15	182	73	39	22.20	14.80	3.20	45.36	43.43	44.02	21.75
16	226	202	75	54.30	59.60	15.10	81.64	-6.11	64.91	15.85
17	180	90	158	29.10	19.60	35.30	51.42	46.28	-21.12	5.23
18	57	160	203	25.30	30.80	61.90	62.36	-16.15	-30.60	15.18
19	220	231	236	73.80	79.00	91.20	91.25	-2.70	-3.61	7.47
20	192	204	210	55.80	59.90	70.40	81.78	-2.91	-4.33	5.86
21	158	169	175	36.70	39.50	47.00	69.13	-2.69	-4.42	6.02
22	113	123	131	18.20	19.60	24.70	51.39	-2.04	-5.77	6.29
23	68	76	82	6.20	6.70	8.80	31.22	-1.90	-4.97	6.64
24	33	36	40	1.20	1.30	1.80	11.44	-0.32	-3.62	12.59

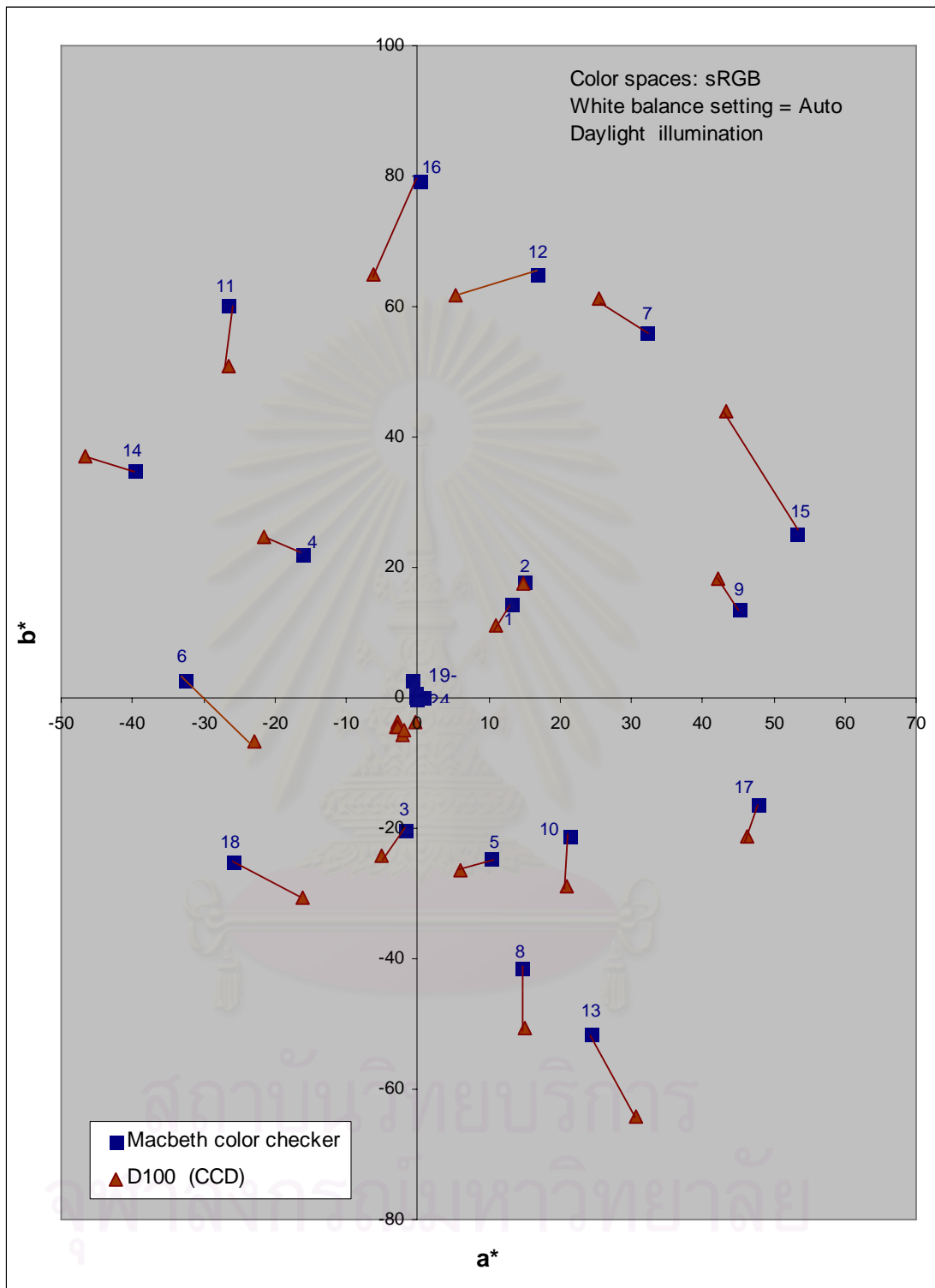


Figure 4-27 Color error in the a^*b^* plane of the CIELAB color space captured by Nikon D100 under daylight illumination and with auto white balance setting.

Table 4-14 Color value and color differences of Macbeth color checker (24 patches) captured by Fuji S2pro under daylight illumination and with auto white balance setting.

No	sRGB			X Y Z (CIE)			L* a* b* (CIE D65)			ΔE
	R	G	B	X	Y	Z	L*	a*	b*	
1	131	84	56	13.30	11.40	4.90	40.22	17.07	25.94	12.36
2	226	174	141	51.90	49.10	32.50	75.53	14.26	24.21	11.70
3	101	141	164	21.90	24.90	39.50	57.02	-8.07	-16.75	9.35
4	79	106	52	8.90	12.20	4.80	41.54	-21.29	28.79	8.73
5	135	143	177	28.30	28.50	46.40	60.36	4.67	-18.85	9.17
6	113	199	177	35.70	48.30	49.80	74.99	-31.41	2.75	3.32
7	243	151	43	48.70	41.90	7.40	70.77	26.16	67.99	16.91
8	75	109	177	16.40	15.70	44.60	46.59	8.56	-40.58	8.18
9	239	98	89	41.90	27.90	12.50	59.77	53.90	33.40	23.44
10	80	51	91	6.10	4.50	10.40	25.20	22.86	-20.24	5.91
11	164	193	69	36.00	47.20	12.60	74.33	-27.57	58.41	2.97
12	223	164	34	44.40	43.00	7.10	71.56	10.69	70.52	8.41
13	39	74	164	9.90	7.80	36.80	33.52	21.41	-53.96	4.84
14	79	165	81	18.30	29.70	12.40	61.36	-44.66	36.56	7.69
15	216	46	37	29.70	16.50	3.00	47.63	64.99	49.46	27.89
16	242	210	67	61.00	66.00	14.50	85.00	-3.98	71.94	9.40
17	200	88	136	32.10	21.20	26.10	53.12	50.37	-5.13	11.83
18	27	138	165	16.50	21.50	39.60	53.45	-20.46	-23.01	6.01
19	250	254	244	91.30	97.80	100.00	99.16	-3.01	4.17	5.24
20	215	220	210	61.10	61.20	70.40	82.51	6.82	-3.06	8.25
21	167	174	163	38.40	41.90	41.40	70.83	-4.56	4.78	7.93
22	111	117	108	15.80	17.40	16.80	48.75	-4.25	4.32	6.44
23	56	62	56	3.70	4.20	4.00	24.33	-4.30	3.12	12.40
24	25	28	25	0.60	0.70	0.70	6.47	-2.66	1.93	17.40

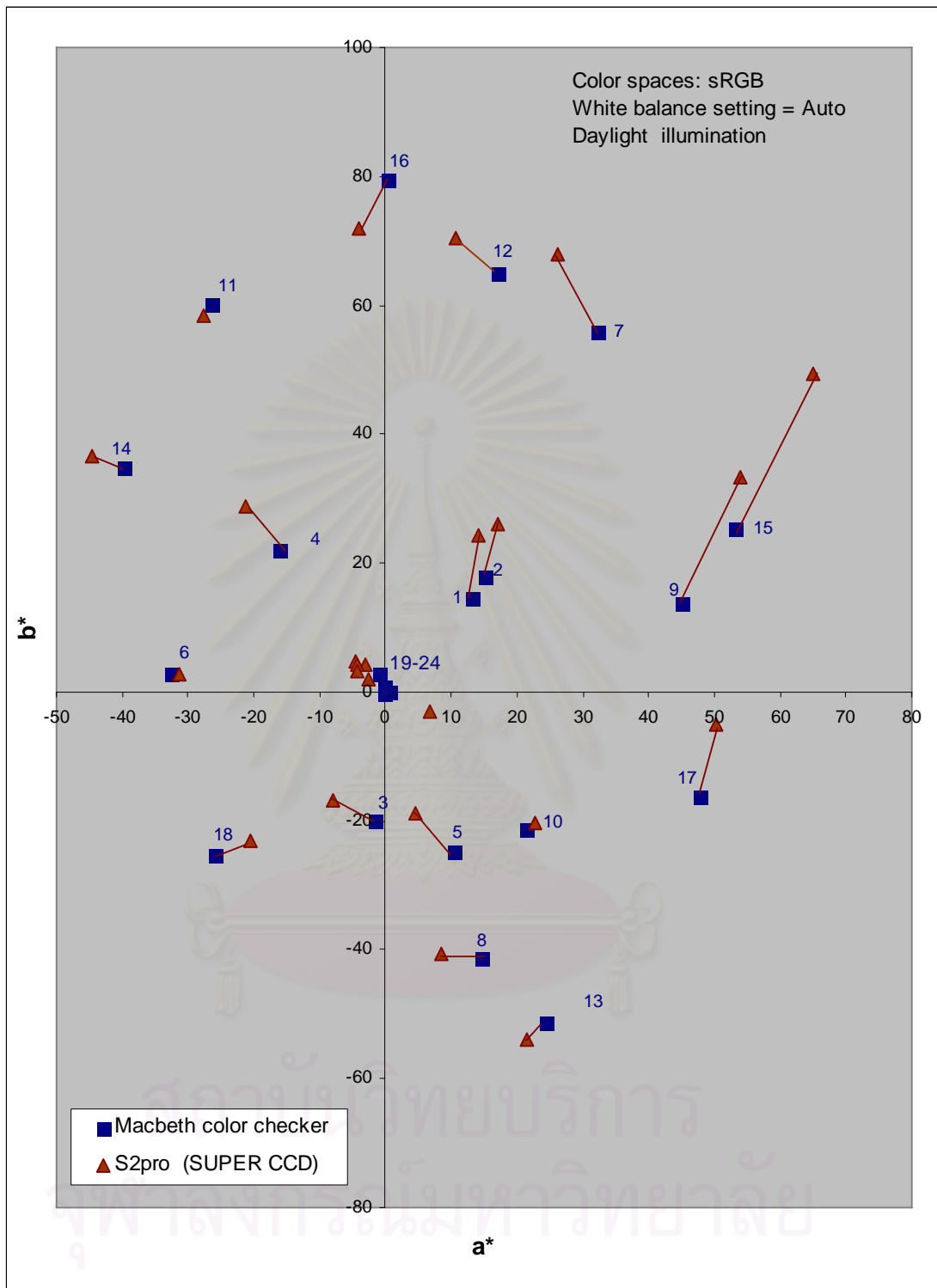


Figure 4-28 Color error in the a*b*plane of the CIELAB color space captured by Fuji S2pro under daylight illumination and with auto white balance setting.

Table 4-15 Color value and color differences of Macbeth color checker (24 patches) captured by Canon D60 under daylight illumination and with auto white balance setting.

No	sRGB			X Y Z (CIE)			L* a* b* (CIE D65)			ΔE
	R	G	B	X	Y	Z	L*	a*	b*	
1	134	80	46	13.20	10.90	3.60	39.43	20.11	31.40	18.39
2	222	168	134	49.10	46.00	29.30	73.54	15.12	25.30	10.79
3	123	150	180	27.80	29.90	48.30	61.57	-2.38	-18.79	10.44
4	99	127	55	13.50	18.30	6.10	49.90	-23.32	37.23	17.99
5	151	151	195	34.30	33.30	57.10	64.41	9.45	-22.62	8.47
6	149	204	189	43.90	54.10	57.10	78.49	-20.85	1.64	13.56
7	223	139	31	40.30	34.70	5.50	65.53	24.12	66.65	14.32
8	92	113	195	20.40	18.20	54.90	49.74	15.79	-45.84	9.73
9	216	94	91	34.50	23.50	12.50	55.54	48.14	26.09	13.67
10	93	62	112	9.00	6.70	16.30	31.07	25.27	-25.05	5.41
11	187	213	89	46.70	59.60	18.40	81.63	-26.28	57.78	9.71
12	229	172	45	48.00	47.00	8.60	74.21	9.29	69.61	9.64
13	59	76	186	13.20	9.40	48.40	36.83	30.96	-61.56	13.52
14	103	183	89	24.60	38.10	15.40	68.09	-43.66	40.79	14.24
15	196	47	41	24.30	13.80	3.10	43.91	59.09	42.37	18.45
16	246	217	82	64.70	70.40	18.00	87.20	-5.07	68.19	13.80
17	194	87	144	31.10	20.40	29.20	52.31	50.05	-11.25	5.91
18	62	160	199	25.10	30.80	59.50	62.34	-16.72	-28.42	14.18
19	246	245	242	86.90	91.60	97.50	96.66	-0.23	1.50	2.42
20	226	225	217	71.40	75.70	77.20	89.72	-1.09	3.92	9.77
21	188	187	178	47.30	50.30	50.10	76.26	-1.31	4.63	11.14
22	138	138	131	24.10	25.70	25.60	57.76	-1.40	3.80	8.33
23	87	88	83	8.80	9.50	9.40	36.92	-1.55	2.92	3.73
24	44	44	42	2.00	2.10	2.10	15.91	-0.54	1.47	7.75

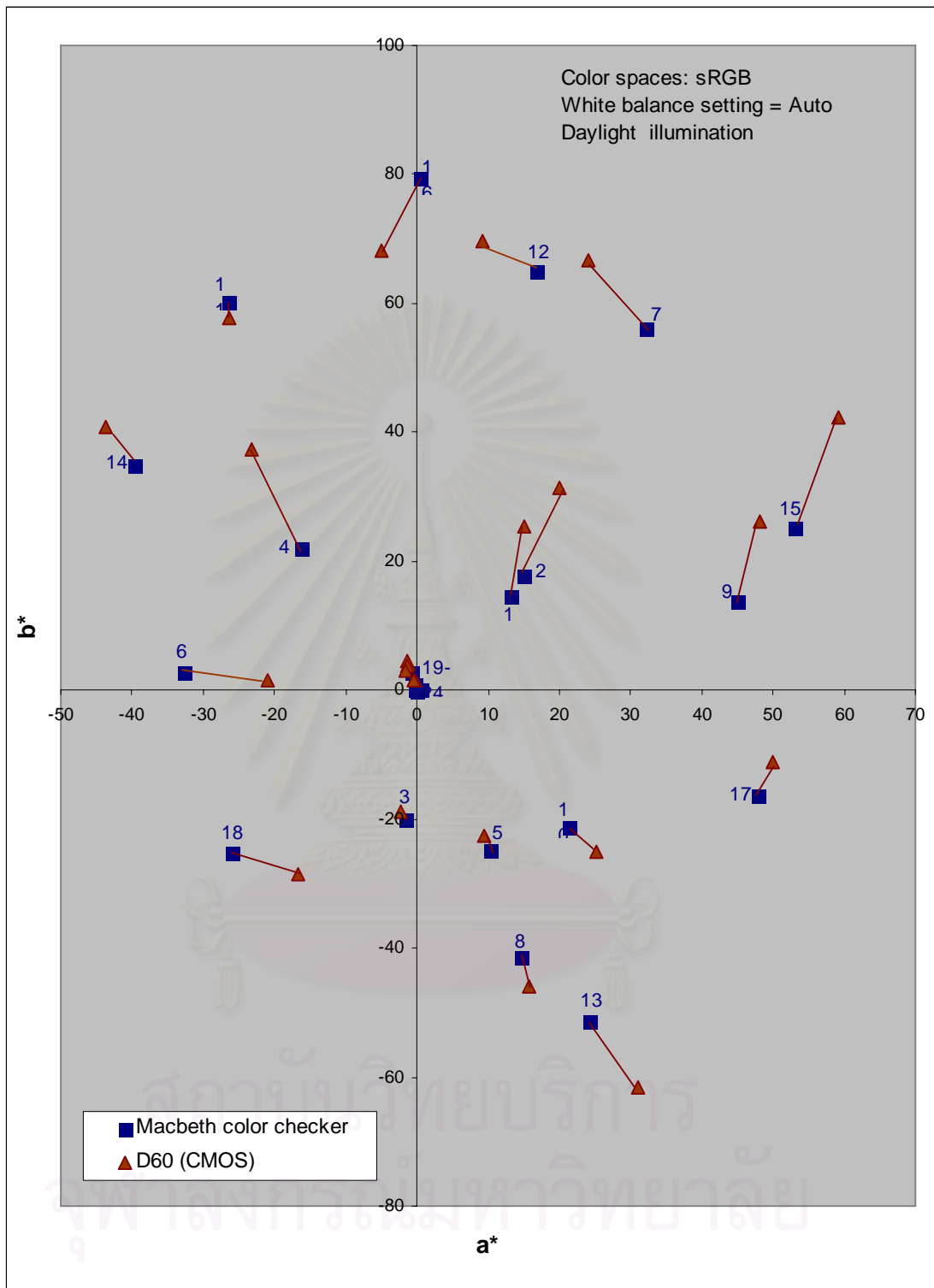


Figure 4-29 Color error in the a^*b^* plane of the CIELAB color space captured by Canon D60 under daylight illumination and with auto white balance setting.

Table 4-16 Color value and color differences of Macbeth color checker (24 patches) captured by Sigma SD9 under daylight illumination and with auto white balance setting.

No	sRGB			X Y Z (CIE)			L* a* b* (CIE D65)			ΔE
	R	G	B	X	Y	Z	L*	a*	b*	
1	109	78	63	9.80	8.90	5.60	35.78	11.51	15.04	2.83
2	187	159	129	37.50	37.70	26.40	67.78	5.69	19.68	9.80
3	57	119	154	14.20	16.50	33.70	47.69	-9.38	-25.42	10.11
4	71	94	56	7.10	9.50	4.80	36.93	-17.55	20.45	6.92
5	122	134	196	26.90	25.60	56.60	57.68	10.91	-33.76	9.13
6	103	206	184	36.89	51.20	54.10	76.78	-35.51	1.56	5.78
7	205	146	47	36.40	34.30	7.00	65.20	13.17	59.90	20.03
8	37	79	164	10.10	8.50	36.90	34.95	17.57	-51.65	12.26
9	181	90	92	24.90	18.00	12.20	49.50	37.72	16.48	7.95
10	62	32	96	4.30	2.50	11.30	18.07	31.51	-35.24	21.47
11	147	179	50	29.20	39.40	8.70	69.02	-29.12	60.49	4.19
12	193	156	39	34.80	35.90	6.60	66.45	2.18	63.51	15.45
13	15	61	151	7.30	5.40	30.50	27.84	23.77	-55.33	4.76
14	72	150	67	14.60	24.00	8.90	56.05	-42.55	37.58	4.01
15	178	46	62	20.30	11.60	5.40	40.59	55.05	24.14	2.16
16	213	192	34	47.10	52.70	8.80	77.71	-8.19	75.04	10.20
17	164	61	137	21.90	13.30	25.50	43.22	51.35	-21.24	9.16
18	23	121	145	11.80	15.80	26.60	46.75	-21.38	-16.78	10.90
19	210	222	216	65.80	71.60	76.10	87.79	-5.06	1.50	8.20
20	173	194	191	46.70	52.10	57.70	77.34	-7.69	-0.93	8.28
21	132	151	153	26.80	29.90	35.10	61.60	-6.41	-3.38	8.48
22	88	101	105	11.20	12.40	15.20	41.84	-4.23	-4.11	10.59
23	47	56	59	3.00	3.40	4.30	21.40	-3.30	-3.46	14.83
24	26	26	28	0.60	0.70	0.80	5.84	0.63	-1.68	17.68

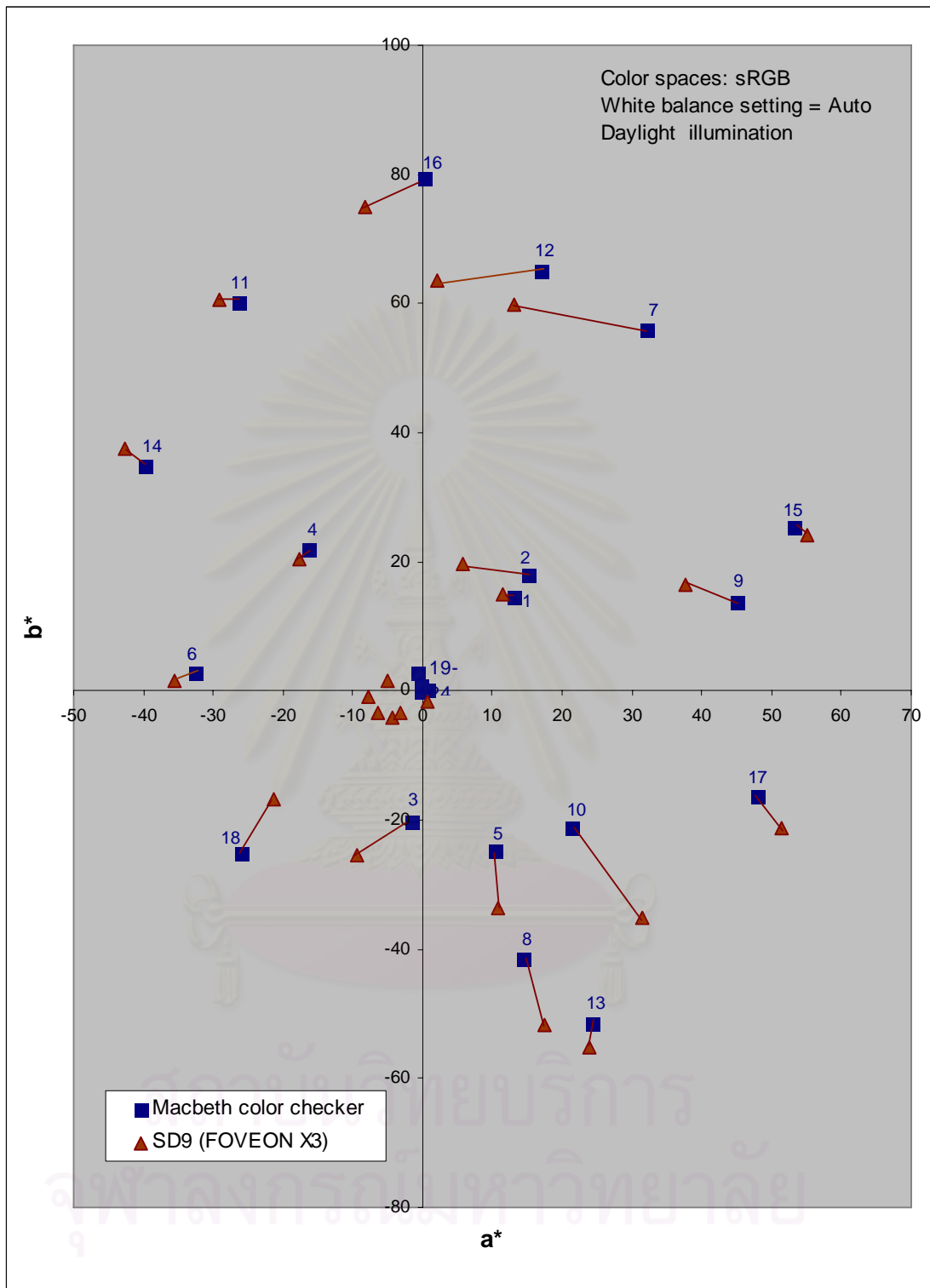


Figure 4-30 Color error in the a^*b^* plane of the CIELAB color space captured by Sigma SD9 under daylight illumination and with auto white balance setting.

4.3.2 The Comparison of the Color Reproduction

In order to compare the color reproduction between original and reproduced image the color of Macbeth color checker are compared in Delta E^*_{ab} .

Table 4-17 Total Delta E^*_{ab} of Macbeth color checker of all digital cameras.

Camera	Total Delta E^*_{ab} *	Total Delta E^*_{ab} of all color (No1-No18)	Total Delta E^*_{ab} of gray scale (neutral tones)
Nikon D100 (True WB)	208.75	173.75	35.00
Fuji S2pro (True WB)	245.07	194.99	50.08
Canon D60 (True WB)	256.60	215.33	41.27
Sigma SD9 (True WB)	238.43	182.15	56.28
Nikon D100 (Auto WB)	234.17	189.29	44.88
Fuji S2pro ((Auto WB)	245.78	188.12	57.66
Canon D60 ((Auto WB)	265.35	222.21	43.14
Sigma SD9 (Auto WB)	235.16	167.11	68.05

The total Delta E^*_{ab} from color value of Macbeth color checker shown in Table 4-17 are not easy to interpret as how advantage and disadvantage in color reproduction hence, the color tone in Macbeth color checker are grouped in Table 4-18 for easier measurement and can be classified into 5 color groups as follow.

1. Gray-scale : White to dark tone in color patch from no.19- no.24.
2. Red tone : Red tone at 315° - 45° of a*b*plane in CIELAB color spaces.
3. Yellow tone : Yellow tone at 45° - 135° of a*b*plane in CIELAB color spaces.
4. Green tone : Green tone at 135° - 225° of a*b*plane in CIELAB color spaces.
5. Blue tone : Blue tone at 225° - 315° of a*b*plane in CIELAB color spaces.

Table 4-18 The classification of CIE color space in the a*b*plane for comparing the color error of normal image sensor.

Gray-scale (No19-No24)	Red tone (315° - 45°)	Yellow tone (45° - 135°)	Green tone (135°-225°)	Blue tone (225°-315°)
white 9.5 (No19)	moderate red (No9)	dark skin (No1)	bluish green (No6)	blue sky (No3)
white 8 (No20)	purple (No10)	light skin (No2)	green (No14)	blue flower (No5)
white 6.5 (No21)	red (No15)	Foliage (No4)	cyan (No18)	purplish blue (No8)
white 5 (No22)	magenta (No17)	orange (No7)		blue (No13)
white 3.5 (No23)		yellow green (No11)		
white 1.5 (No24)		orange yellow (No12)		
		yellow (No16)		

Table 4-19 The average Delta E^*_{ab} calculated from all 5 color groups classified in Table 4-18, show the capability of each image sensor in color reproduction once comparing to an ideal color.

Camera/Average Delta E^*_{ab}	Gray-scale (neutral tones)	All color tone (0°- 360°)	Red tone at (315°- 45°)	Yellow tone (45°- 135°)	Green tone (135°-225°)	Blue tone (225°-315°)
Nikon D100 (True WB)	5.83	9.65	11.80	7.93	11.42	7.21
Fuji S2pro (True WB)	8.35	10.83	18.18	8.74	8.29	6.87
Canon D60 (True WB)	6.88	11.96	10.23	11.62	13.61	10.15
Sigma SD9 (True WB)	9.38	10.12	14.74	7.35	8.37	9.82
Nikon D100 (Auto WB)	7.48	10.52	10.41	8.48	13.31	9.98
Fuji S2pro ((Auto WB)	9.61	10.45	17.27	8.81	5.67	7.89
Canon D60 ((Auto WB)	7.19	12.35	10.86	11.83	13.99	10.54
Sigma SD9 (Auto WB)	11.00	9.28	10.19	8.68	6.90	9.06

From Table 4-19, lower value of average Delta E^*_{ab} (average color error) means better color reproduction.

From comparing between the white balance after adjusting to be auto white balance and the white balance after setting custom, Delta E^*_{ab} from auto white balance are higher. This can be concluded that the white balance after adjusting color temperature to be equal to the light source can provide better software and color reproduction than adjusting color temperature to be equal to auto white balance.

Therefore, this research use the white balance after adjusting color temperature to be equal to the light source for evaluating the average Delta E^*_{ab} of all 5 color groups. The measurement data are as follows.

The average Delta E^*_{ab} of total gray-scale from Sigma SD9, Fuji S2pro, Canon D60 and Nikon D100 are 9.38, 8.35, 6.88 and 5.83, respectively.

The average Delta E^*_{ab} values of all color tone from Canon D60, Fuji S2pro, Sigma SD9 and Nikon D100 are 11.96, 10.83, 10.12 and 9.65, respectively.

The average Delta E^*_{ab} values of Red tone from Fuji S2pro, Sigma SD9, Nikon D100 and Canon D60 are 18.18, 14.74, 11.80 and 10.23, respectively.

The average Delta E^*_{ab} values of Yellow tone from Canon D60, Fuji S2pro, Nikon D100 and Sigma SD9 are 11.62, 8.74, 7.93 and 7.35, respectively.

The average Delta E^*_{ab} values of Green tone from Canon D60, Nikon D100, Sigma SD9 and Fuji S2pro are 13.61, 11.42, 8.37 and 8.29, respectively.

The average Delta E^*_{ab} values of Blue tone from Canon D60, Sigma SD9, Nikon D100 and Fuji S2pro are 10.15, 9.82, 7.21 and 6.87, respectively.

The image sensors and imaging management program got Delta E^*_{ab} differently. Lower Delta E^*_{ab} can theoretically indicate more color effectiveness. If there is lowest color error, the image sensor can most capture the color in each color scale. The comparison result is shown below:

From total gray-scale analysis, Nikon D100 (CCD) has lowest color error while Sigma SD9 (Foveon X3) has highest color error.

From all color tones analysis, Nikon D100 (CCD) has lowest color error while Canon D60 (CMOS) has highest color error.

From red tone analysis, Canon D60 (CMOS) has lowest color error while Fuji S2pro (Super CCD) has highest color error.

From yellow tone analysis, Sigma SD9 (Foveon X3) has lowest color error while Canon D60 (CMOS) has highest color error.

From green tone analysis, Fuji S2pro (Super CCD) has lowest color error while Canon D60 (CMOS) has highest color error.

From blue tone analysis, Fuji S2pro (Super CCD) has lowest color error
which Canon D60 (CMOS) has highest color error.



สถาบันวิทยบริการ
จุฬาลงกรณ์มหาวิทยาลัย

4.4 The Noise and Graininess

4.4.1 The Preparation and Evaluation of the Noise and Graininess

The sequence of images of the Macbeth color checker chart will be used for measure noise levels. The standard deviation of the middle gray patch 100 x 100 pixels of this image sequence is measured by Photoshop histogram.

There are total 4 types of moise which including dark current noise, amplifier noise, shot noise and thermal noise. However, only first 3 types are used to measured in this research because there is no available room in 24 hours temprature control and it is too much time to complete the thermal testing within the specific time of this research.

4.4.1.1 Dark Current Noise

To evaluate dark current noise, the standard deviation of Grey patches from images captured by different setting ISO by each camera were compared in Figure 4-31 to 4-34.

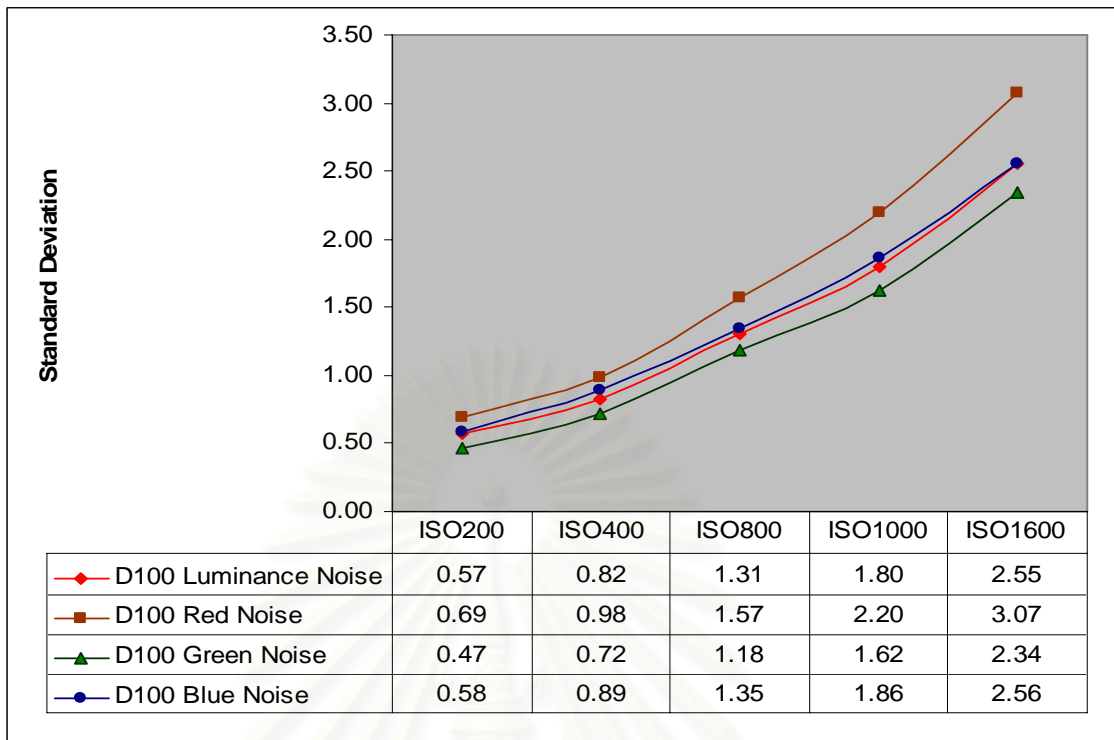


Figure 4-31 Dark current noise- from Nikon D100.

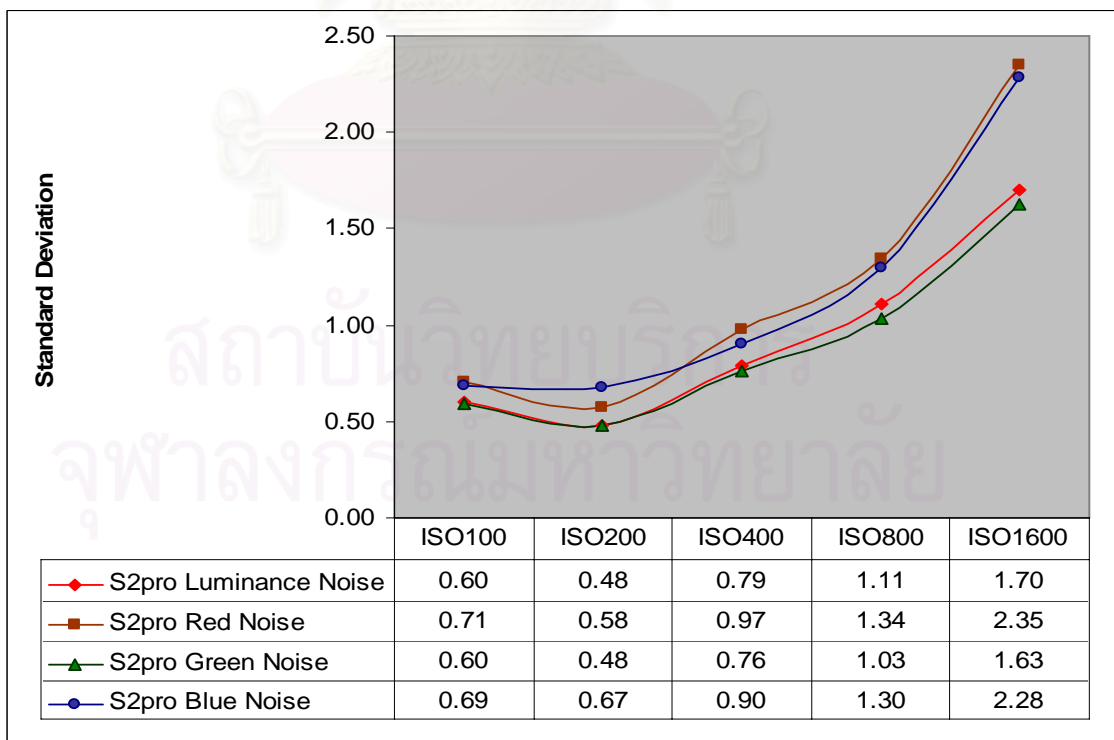


Figure 4-32 Dark Current Noise- from Fuji S2pro.

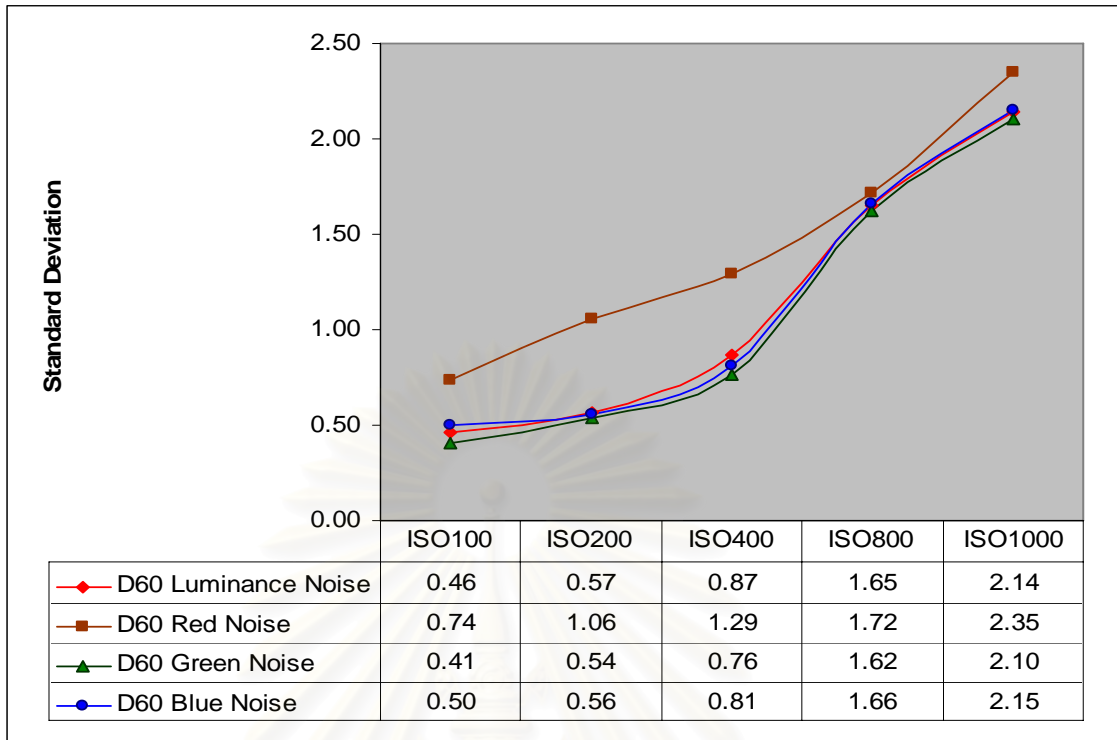


Figure 4-33 Dark Current Noise- from Canon D60.

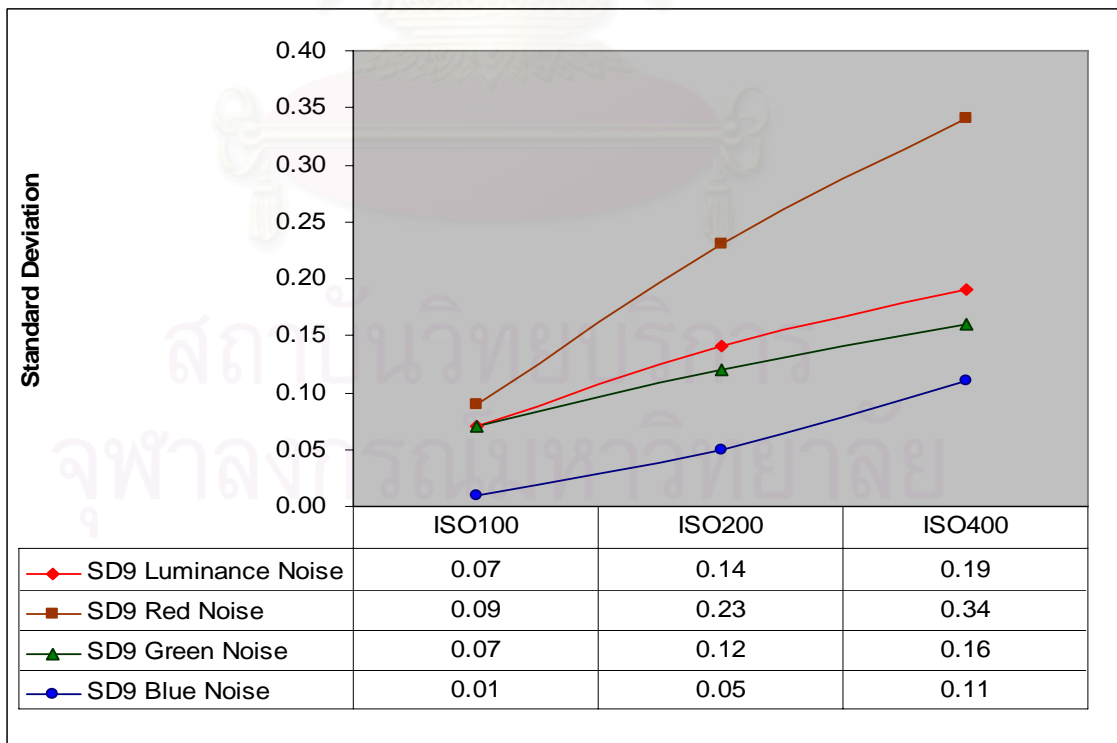


Figure 4-34 Dark Current Noise- from Sigma SD9.

4.4.1.2 Amplifier Noise

To evaluate amplifier noise, the standard deviation of Grey patches from images captured by different setting ISO by each camera were compared in Figure 4-35 to 4-38.

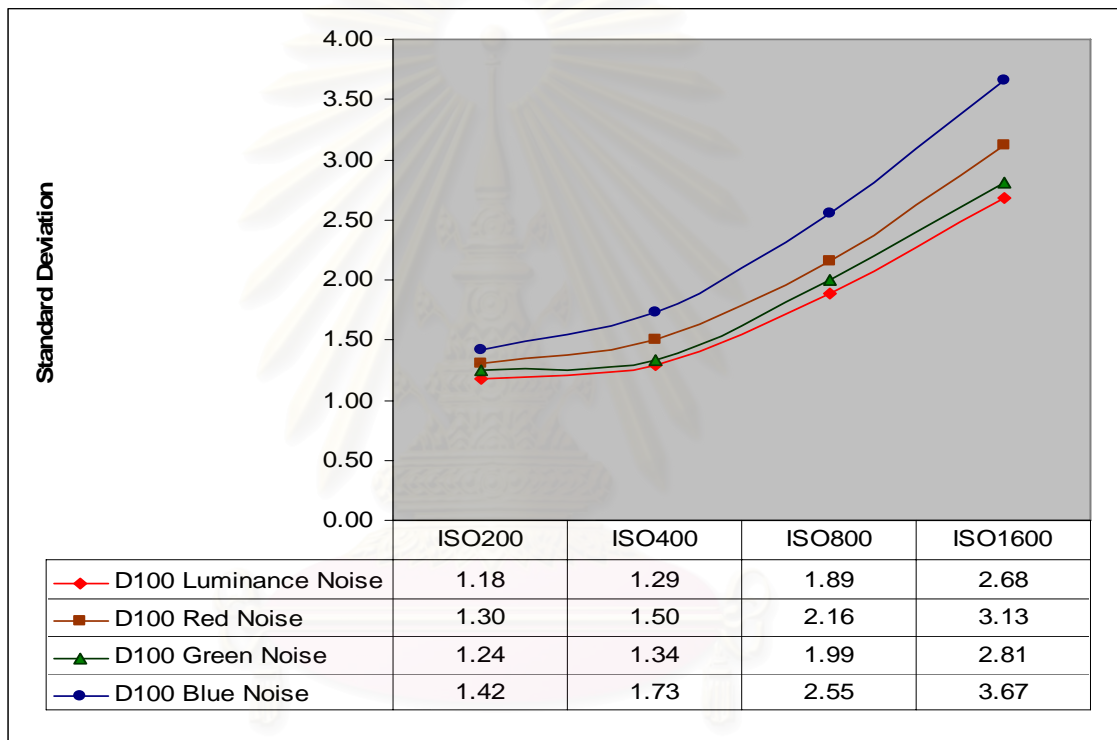


Figure 4-35 Amplifier Noise from Nikon D100.

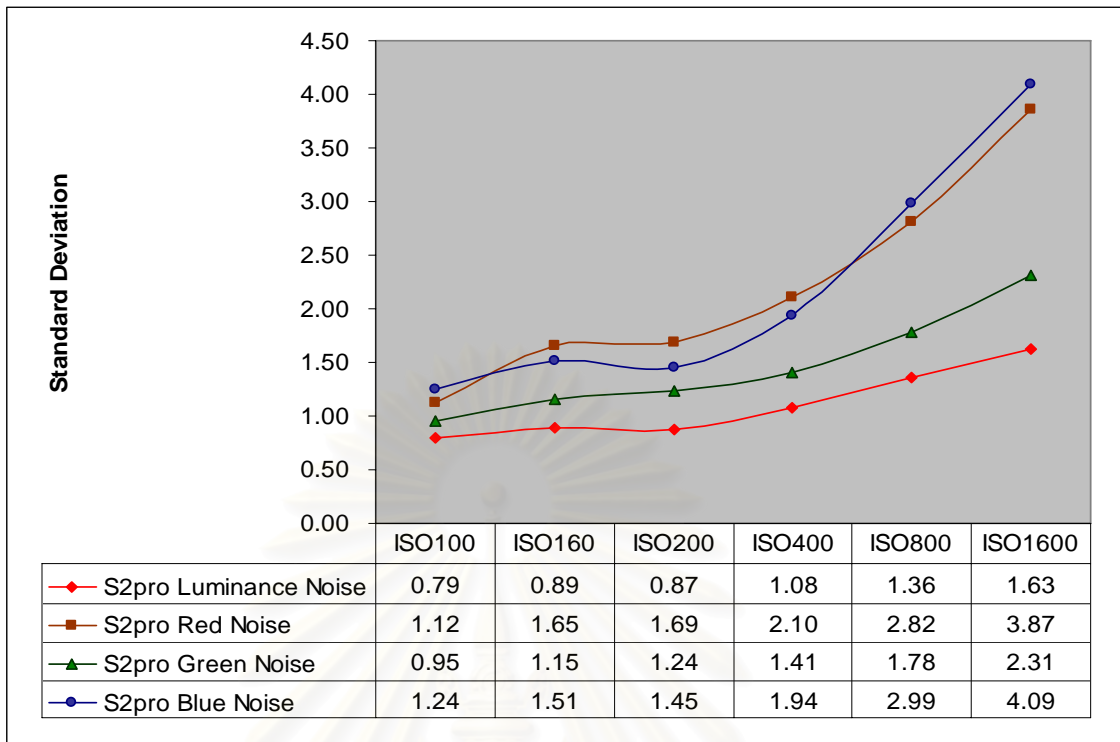


Figure 4-36 Amplifier Noise from Fuji S2pro.

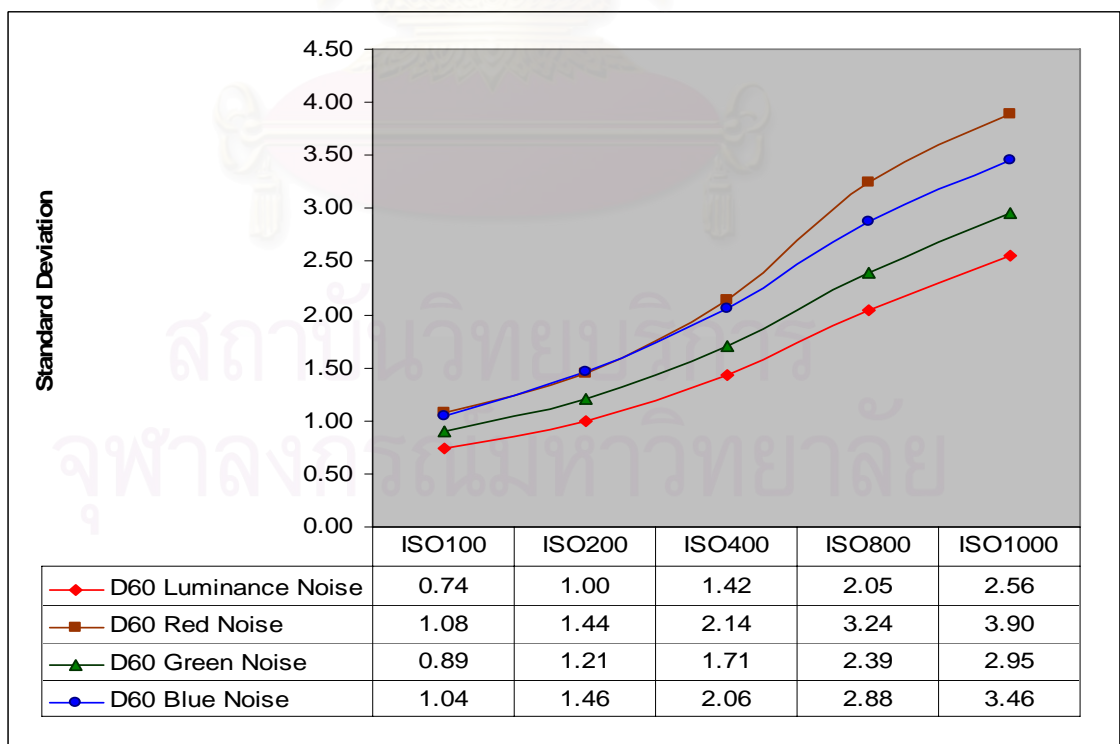


Figure 4-37 Amplifier Noise from Canon D60.

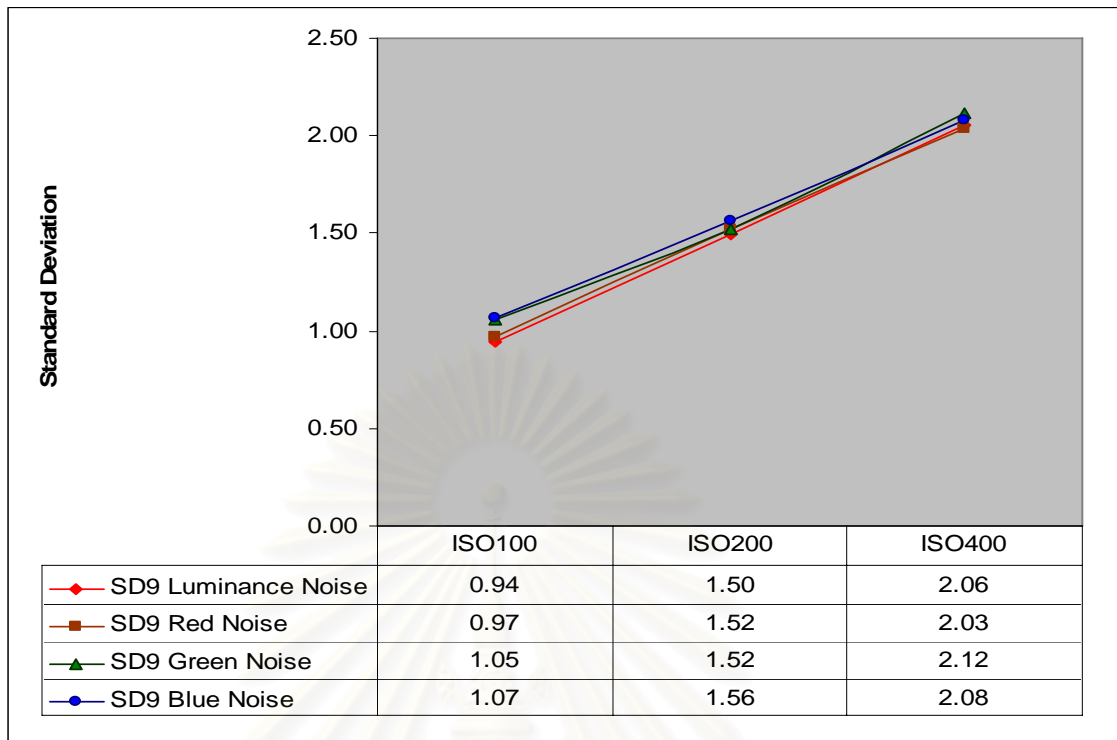


Figure 4-38 Amplifier Noise from Sigma SD9.

4.4.1.3 Shot Noise

To evaluate shot noise, the lowest ISO was set to each camera, then shutter were vary from 30 sec. to 1/1.5 sec. and result are shown in Figure 4-39 to 4-42.

สถาบันวิทยบริการ
จุฬาลงกรณ์มหาวิทยาลัย

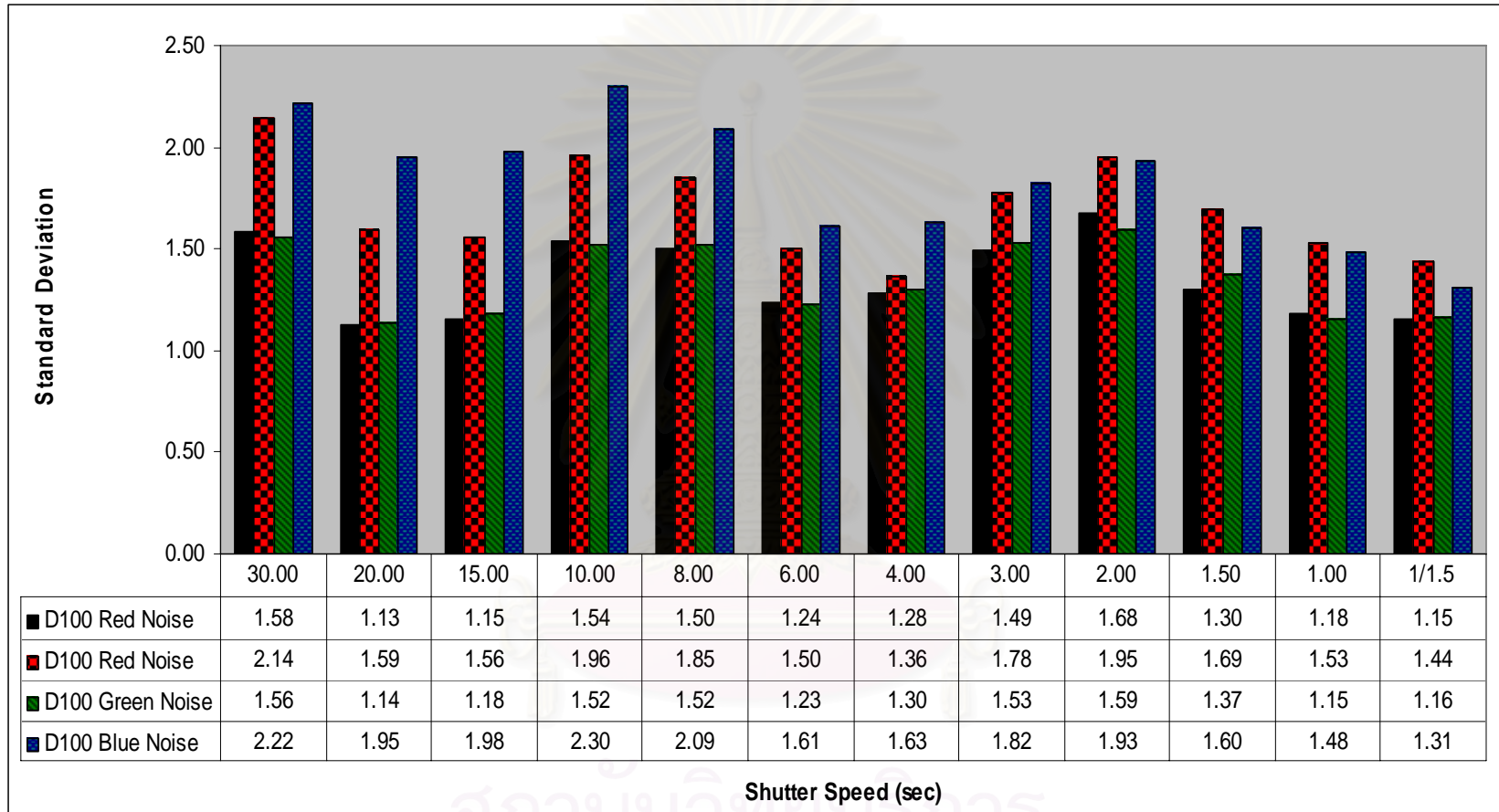


Figure 4-39 Shot Noise from Nikon D100.

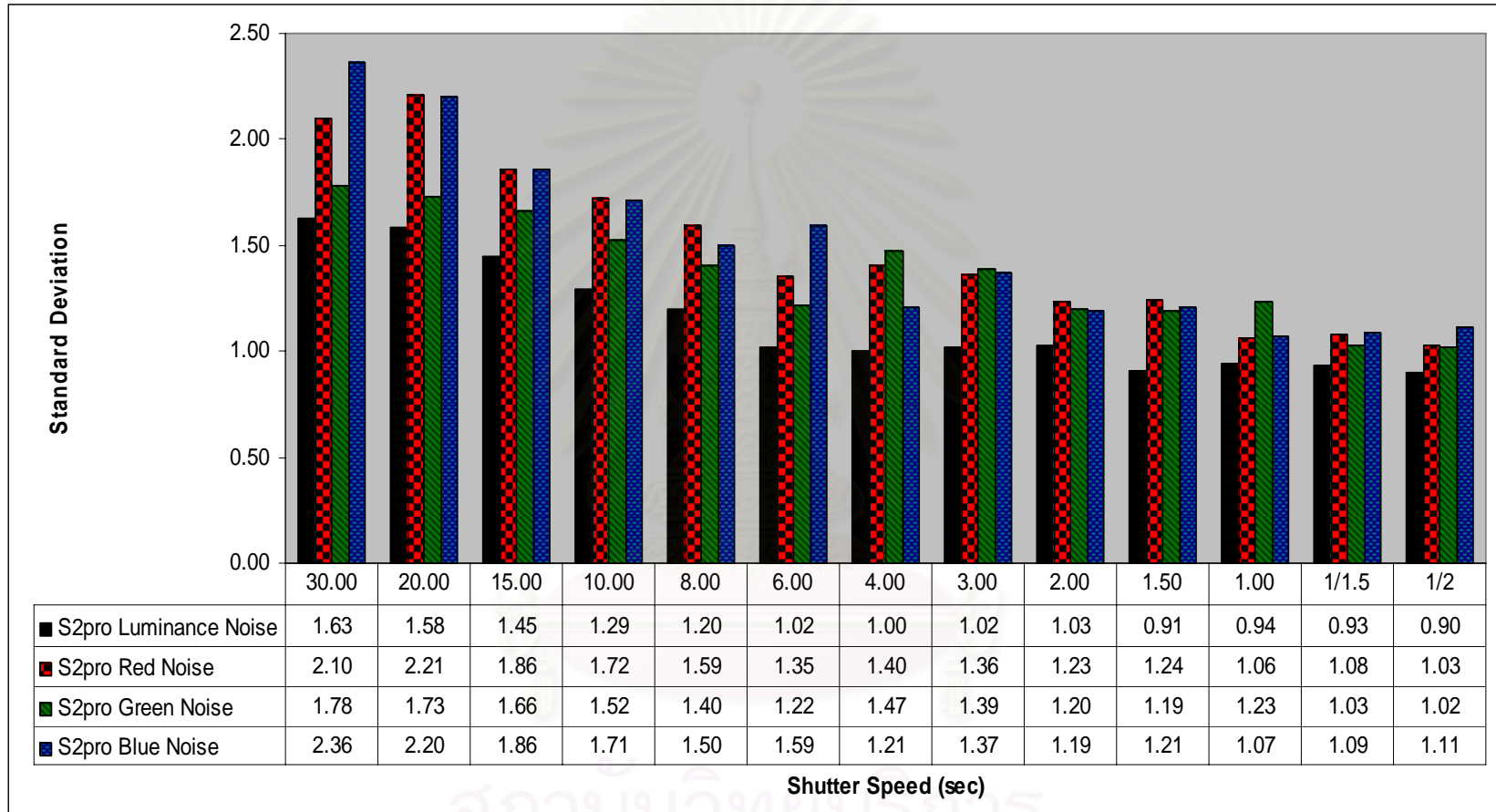


Figure 4-40 Shot Noise from Fuji S2pro.

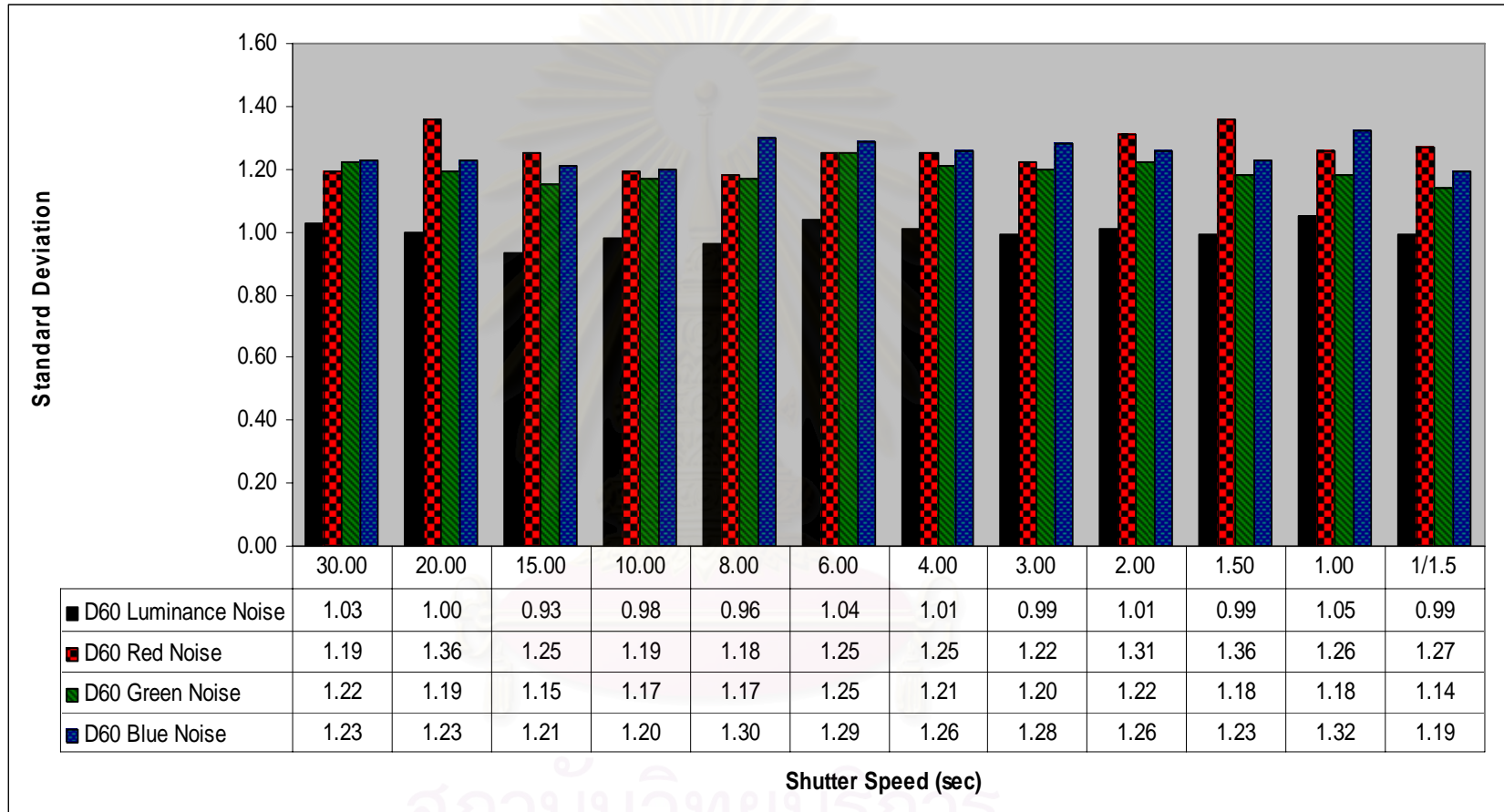


Figure 4-41 Shot Noise from Canon D60.

สถาบันวิทยบริการ
จุฬาลงกรณ์มหาวิทยาลัย

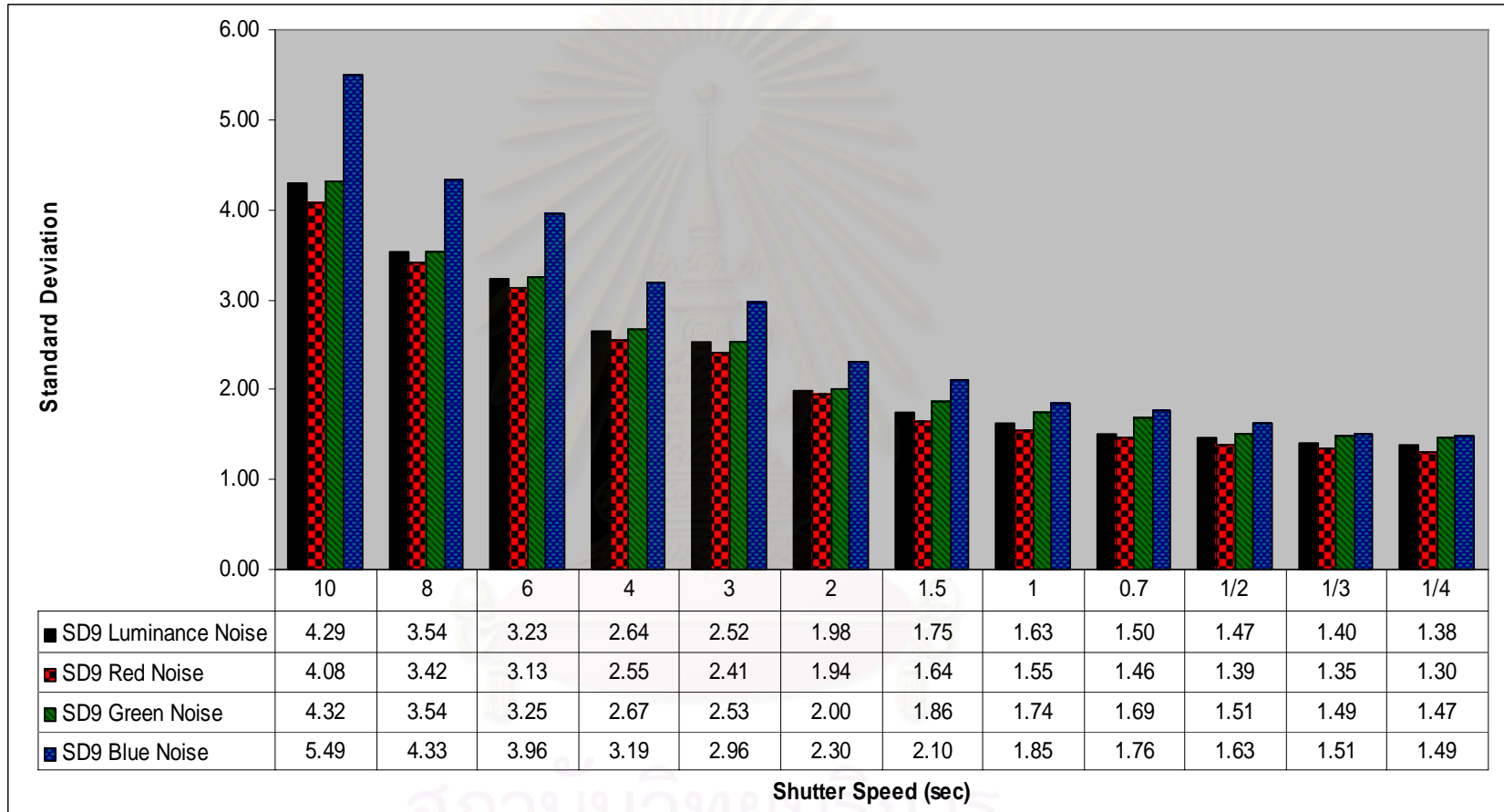


Figure 4-42 Shot Noise from Sigma SD9.

4.4.2 The Comparison of the Noise and Graininess

The standard deviation represents the noise of image signal of each image sensor type. Higher standard deviation means higher noise that is lower the accuracy of image signal.

Figure 4-43 shows the comparison of dark current noise among various image sensor types at red, green, and blue channel. The x axis is the sensitivity of the camera while the y axis is the standard deviation. Due to red, green, and blue value is not easy to be interpreted therefore, the luminance channel will be further used to analyze in Figure 4-44. This is because the luminance channel is closely related to light-dark perception of human's eye and it is the best channel to represent how the eye detects information in typical scenes.

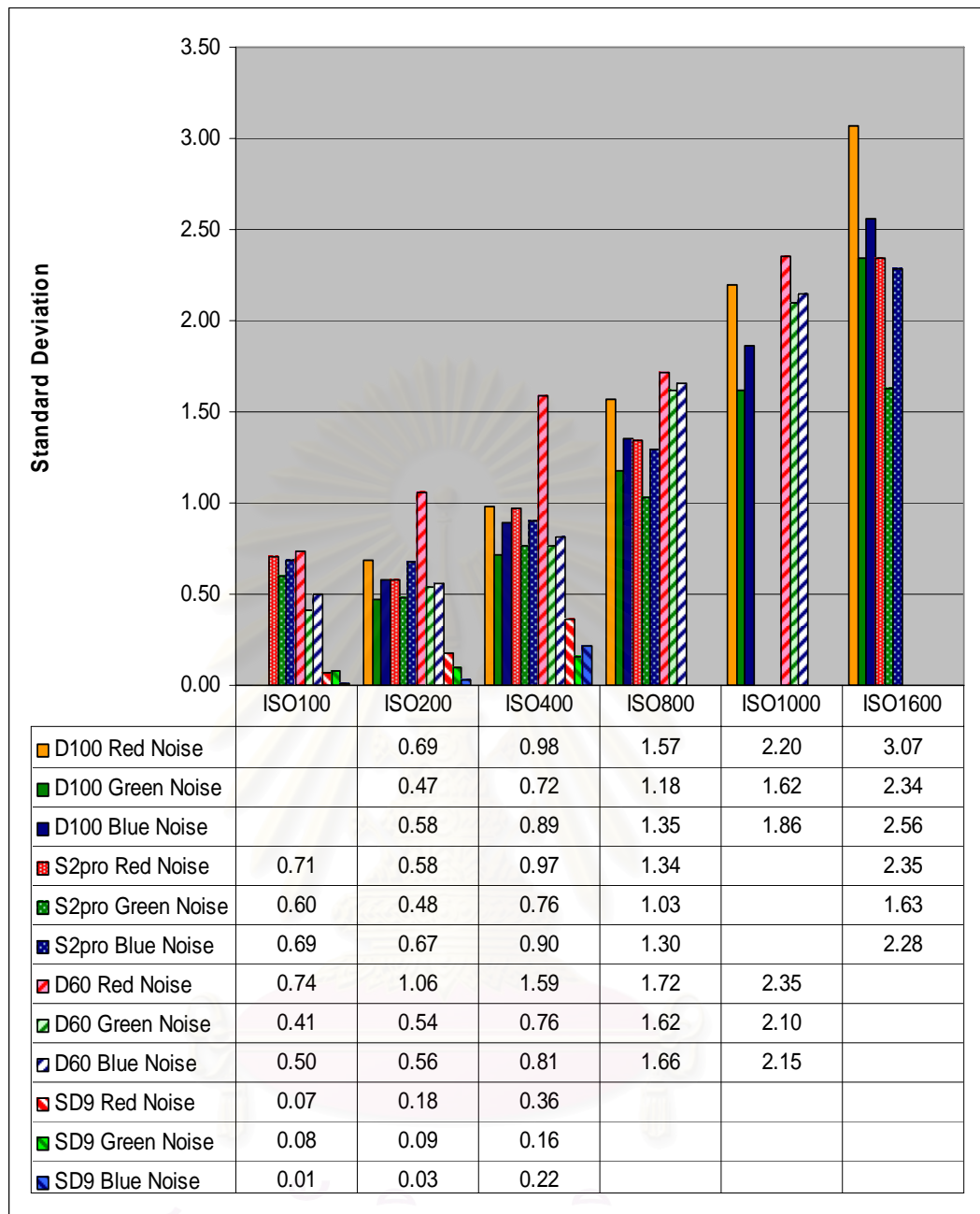


Figure 4-43 Dark current noise of all image sensors in red, green, and blue channel.

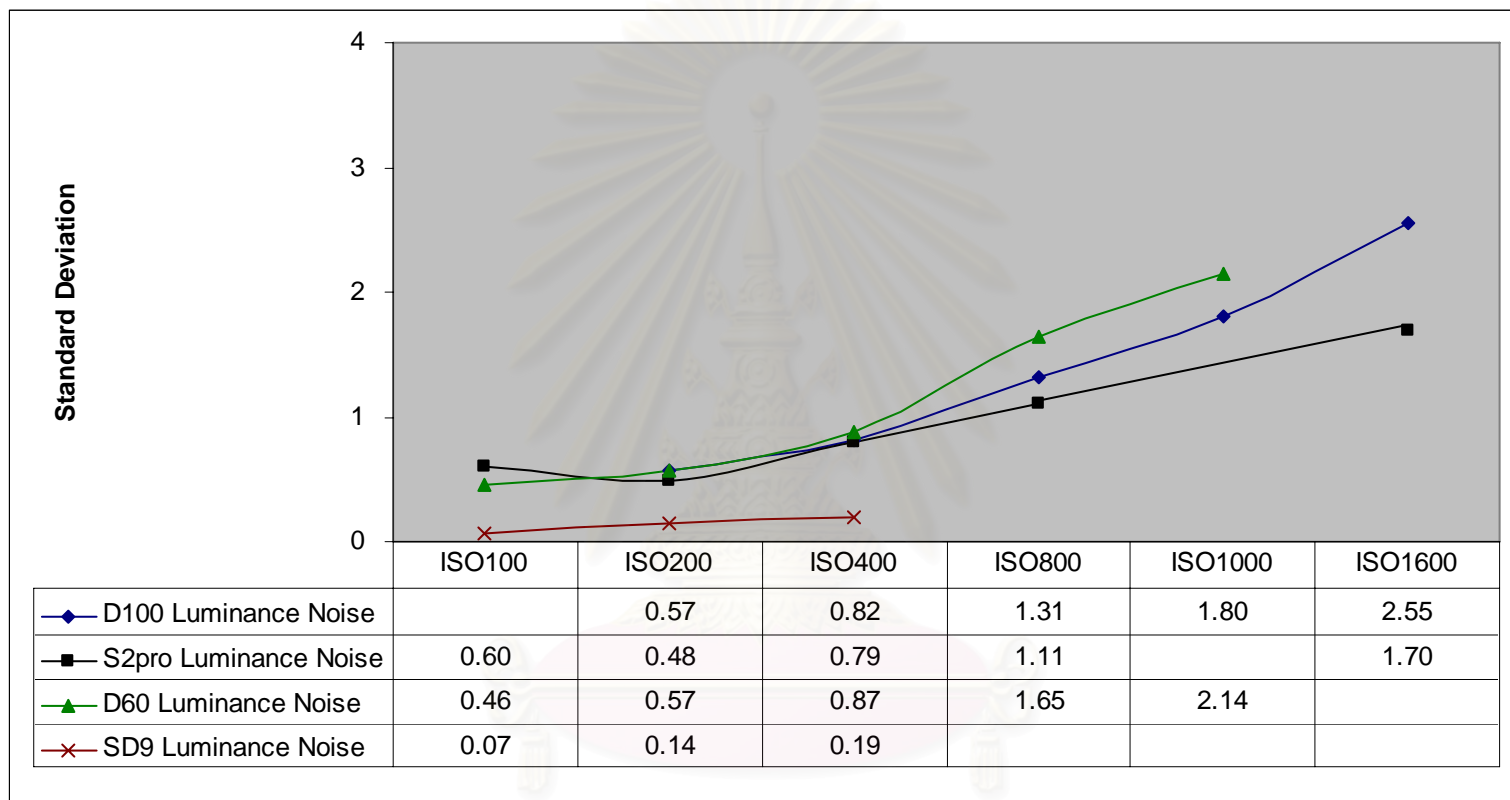


Figure 4-44 Dark current noise of all image sensors in luminance channel.

From Figure 4-44, the results show as follows when camera was set as various ISOs at 100, 200, 400, 800, 1000 and 1600 respectively.

With ISO 100, Fuji S2pro, Canon D60 and Sigma SD9 have standard deviation of 0.06, 0.47 and 0.07 respectively.

With ISO200, Nikon D100, Canon D60, Fuji S2pro and Sigma SD9 have standard deviation of 0.57, 0.57, 0.48 and 0.14 respectively.

With ISO400, Canon D60, Nikon D100, Fuji S2pro and Sigma SD9 have standard deviation of 0.87, 0.79, 0.82 and 0.19 respectively.

With ISO800, Canon D60, Nikon D100 and Fuji S2pro have standard deviation of 1.31, 1.11 and 1.65 respectively.

With ISO1000, Canon D60 and Nikon D100 have standard deviation of 2.14 and 1.8 respectively.

With ISO1600, Nikon D100 and Fuji S2pro have standard deviation of 2.55 and 1.70 respectively.

Dark current noise is the electronic currency formed in the image sensors, where is measured by taking the photo at dark environment, and it can indicate the possibility of amplifier noise that will occurred in each image sensor with the

different sensitivity (ISO). For dark current noise analysis in luminance channel of each image sensor, Sigma SD9 (Foveon X3) has the lowest dark current noise in all sensitivity (ISOs). For other sensors, Canon D60 has the second lowest value at ISO 100 and Fuji S2pro (Super CCD) has the second lowest value at ISO200-ISO1600 while Sigma SD9 (Foveon X3) has the highest value at all ISOs.



สถาบันวิทยบริการ
จุฬาลงกรณ์มหาวิทยาลัย

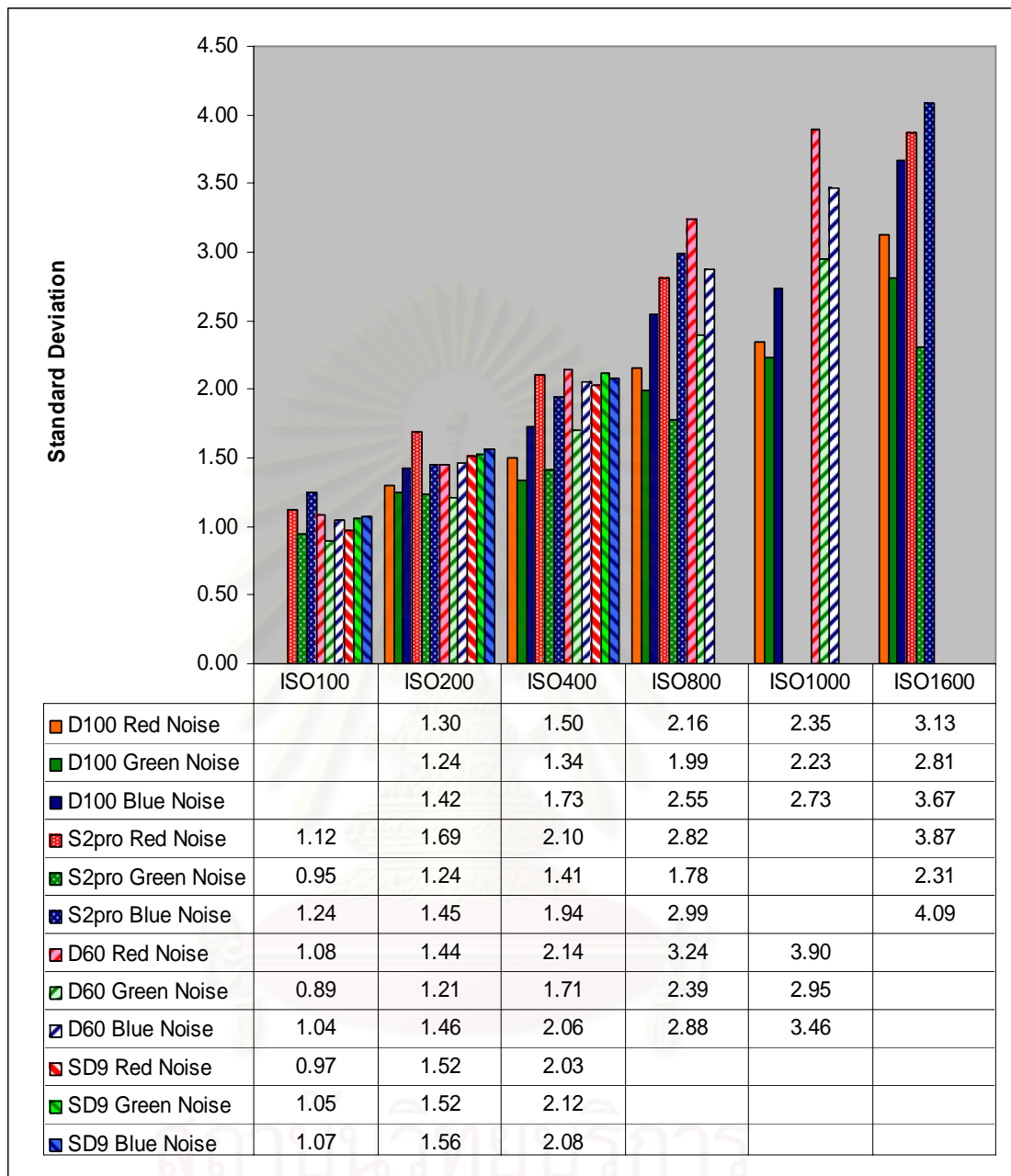


Figure 4-45 Amplifier noise of all image sensors in red, green, and blue channel.

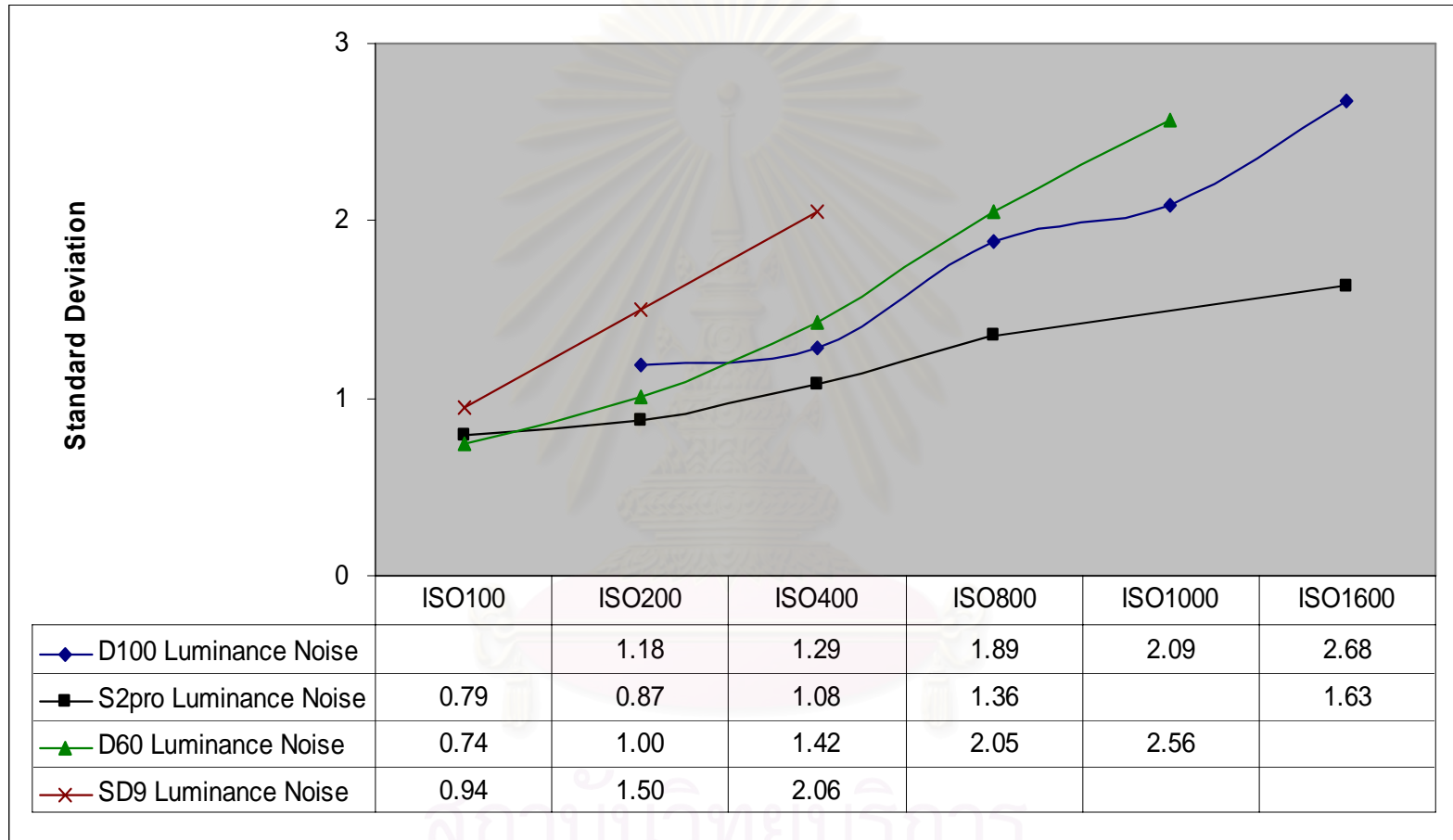


Figure 4-46 Amplifier noise of all image sensors in luminance channel.

Figure 4-45 shows the comparison of amplifier noise among four image sensor types at red, green, and blue channel. The x axis is the sensitivity of the camera while the y axis is the standard deviation.

Figure 4-46 shows the comparison of amplifier noise among four image sensor types at luminance channel. The x axis is for the sensitivity of the camera while the y axis is the standard deviation. The amplifier noises at luminance channel from the represented graph are shown with different ISO level as follows:

With ISO100, Sigma SD9, Fuji S2pro, and Canon D60 have standard deviation of 0.94, 0.79 and 0.74 respectively.

With ISO200, Sigma SD9, Nikon D100, Canon D60, and Fuji S2pro have standard deviation of 1.50, 1.18, 1.00 and 0.87 respectively.

With ISO400, Sigma SD9, Canon D60, Nikon D100, and Fuji S2pro have standard deviation of 2.06, 1.42, 1.29 and 1.08 respectively.

With ISO800, Canon D60, Nikon D100 and Fuji S2pro have standard deviation of 2.05, 1.89 and 1.36 respectively.

With ISO1000, Canon D60 and Nikon D100 have standard deviation of 2.56 and 2.09 respectively.

With ISO1600, Nikon D100 and Fuji S2pro have standard deviation of 2.68 and 1.63 respectively.

Even if the amplifier noise represents the effectiveness of image sensors in enlarging the image signal, noise will be increased subsequently. The data analysis in Figures 4-45 and 4-46 indicate that amplifier noise in red, green and blue channel of each image sensor with the bayer pattern filter array, Nikon D100 (CCD), Fuji S2pro (Super CCD) and Canon D60 (CMOS) have lower noise in green channel than in red and blue channel. For an analysis where is applied with the true color filter array, it shows that Sigma SD (Foveon X3) has similar noise in red, green, blue channel.

For amplifier noise analysis in luminance channel of each image sensor, Canon D60 (CMOS) has lowest noise value at ISO100 and Fuji S2pro (Super CCD) has lowest noise value at ISO200-ISO1600 while Sigma SD9 (Foveon X3) has highest noise value at all ISOs.

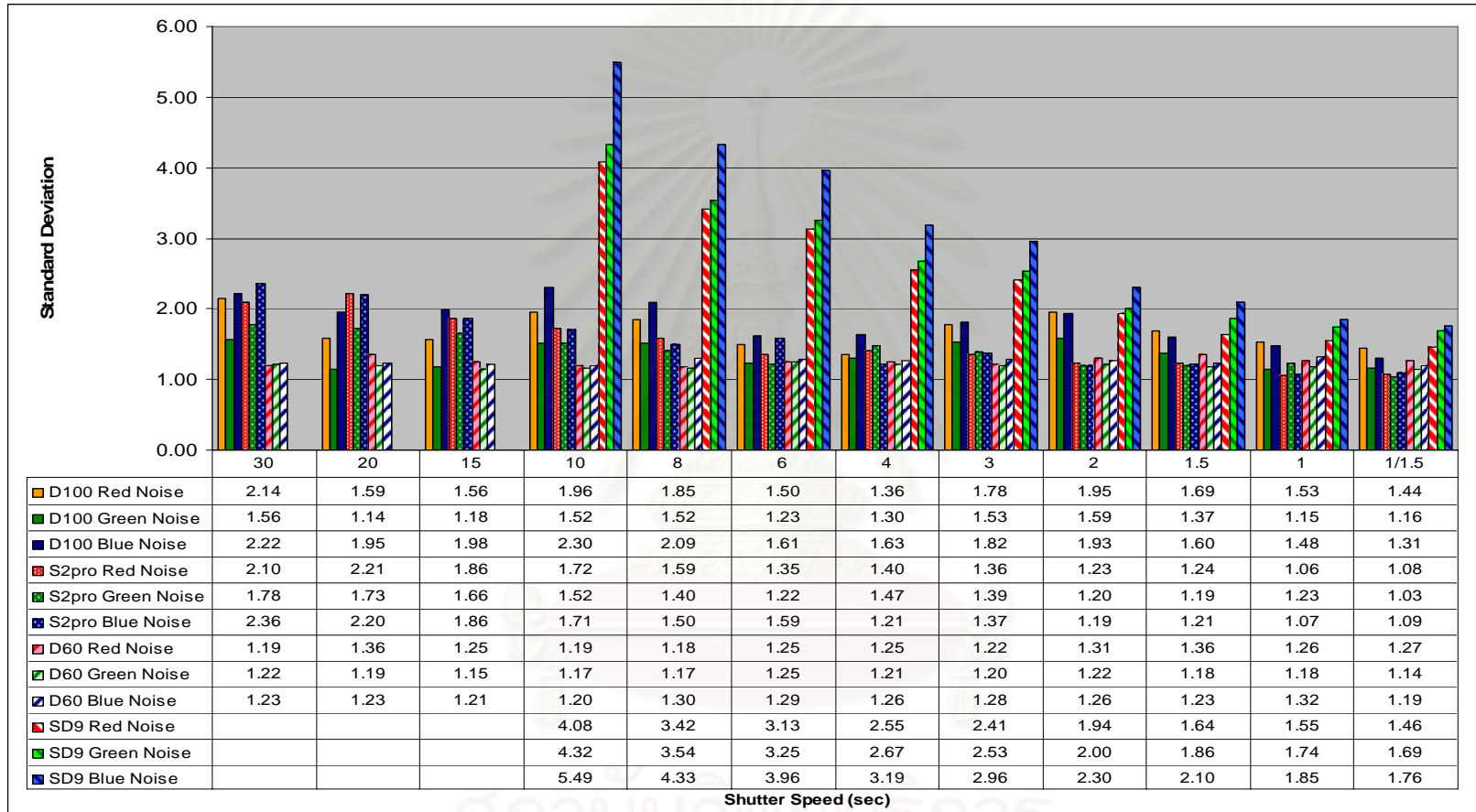


Figure 4-47 Shot noise of all image sensors in red, green, and blue channel.

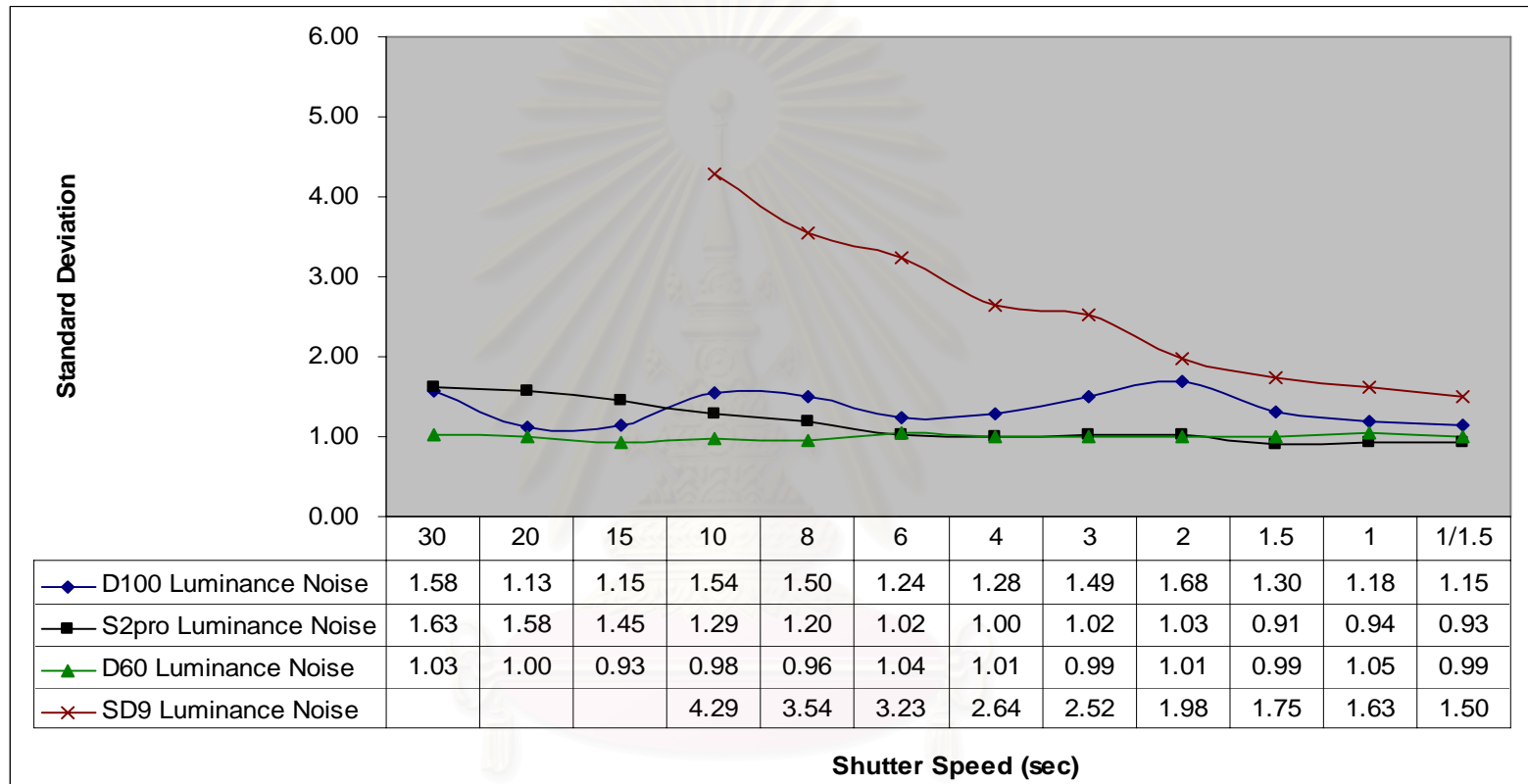


Figure 4-48 Shot noise of all image sensors in luminance channel.

Figure 4-47 shows the comparison of shot noise among four image sensor types at red, green, and blue channel. The x axis is the exposure time of the camera while the y axis is the standard deviation.

Figure 4-46 shows the comparison of amplifier noise among image sensor types at luminance channel. The x axis is the exposure time of the camera while the y axis is the standard deviation.

Sigma SD9 has the highest standard deviation or noise level in every exposure time where its standard deviation is continuously increase from 0.15 to 4.29 at the exposure time from 1/1.5 sec to 10 sec.

Shot noise represents the effectiveness of long exposure capture. The data analysis in Figure 4-47 and 4-48 indicates that noise of Sigma SD9 (Foveon X3) was increasing in each longer exposure time. However, the noise was rarely occurred to Fuji S2pro (Super CCD), Canon D60 (CMOS) and Nikon D100 (CCD) on each longer exposure time.

Hence, Sigma SD9 (Foveon X3) might not have the noise reduction while Fuji S2pro (Super CCD), Canon D60 (CMOS), and Nikon D100 (CCD) might have the noise reduction in their management program.

CHAPTER 5

CONCLUSIONS AND SUGGESTION

5.1 Conclusions

5.1.1 Conclusions of Resolution Measurement

For the measurement of image resolution from all image sensor types in this research, there were two parameters to be compared and evaluated.

The first parameter was the spatial frequency resolution (SFR) which was shown the contrast as a function of spatial frequency in each image sensor and this contrast represents the capability of image sensor to differentiate the dark and white area of the scene. The second parameter was the visual resolution observed from the the captured images.

This research focused on the resolution at 6 mega pixels from all image sensor types. From the comparison between the spatial frequency resolution (SFR) and the visual resolution of each image sensor, Foveon X3 (Sigma SD9) had the highest SFR which represented the best overall contrast result. However, its low number of photosite might cause the low absolute resolution but high extinction resolution. This was because Foveon X3 had no anti-aliasing filter. As a result, Foveon X3 had higher color artifact when the picture was interpolated.

The 50% SFR of Fuji S2pro (Super CCD) was higher than Nikon D100 (CCD) but less than Canon D60 (CMOS). However the absolute resolution and extinction resolution of Fuji S2pro (Super CCD) is the highest among all image sensors. This is because the photo site of Super CCD had 45° diagonal axis and seemed to have more volume despite the fact that it was remain the same.

5.1.2 Conclusions of Tone Reproduction Measurement

Tone reproduction of this research were evaluated by capture the middle gray patch of Macbeth color checker with various shutter speed by all digital cameras with half-stop interval.

From tone reproduction analysis, each image sensor had different capacity in tone reproduction. Canon D60 (CMOS) had the highest dynamic range which meant that CMOS could capture subtle tonal gradation in the shadow, midtone, and highlight details of the scene. Fuji S2pro (Super CCD), Nikon D100 (CCD) and Sigma SD9 (Foveon X3) also had lower dynamic range subsequently.

Testing results indicated that black-gray had dynamic range at 4.94-5.32 while gray-white had different dynamic range at 2.0-2.4. Image sensor that has low dynamic range in this area will fail to 'Blooming'. The results show that Canon D60 (CMOS) had the best dynamic range at 2.4 stop while Sigma SD9 (Foveon X3), Nikon D100 (CCD) and Fuji S2Pro (Super CCD) had lower dynamic range respectively.

5.1.3 Conclusions of Color Reproduction Measurement

Color reproduction is to measure the Delta E^*_{ab} / color error of test chart (Macbeth color checker) captured by each digital camera. The color reproduction is used to evaluate the effectiveness of camera software in reproducing color image to be closely similar to the original color.

The Macbeth color checker was set the white balance to custom white balance. In the meantime, it also was set the white balance to auto white balance. The result of custom white balance was better than the auto white balance and was concluded that the software for the custom white balance was better than software for the auto white balance.

From total gray-scale analysis, Nikon D100 (CCD) had lowest color error which meant that CCD could capture most of the natural color in gray-scale while Sigma SD9 (Foveon X3) had highest color error which meant that Foveon X3 could capture least of the natural color in gray-scale.

From all color tones analysis, Nikon D100 (CCD) had lowest color error which meant that CCD could capture most of the natural color in all color tones while Canon D60 (CMOS) had highest color error which meant that CMOS could capture least of the natural color in all color tones.

From red tone analysis, Canon D60 (CMOS) had lowest color error which meant that CMOS could capture most of the natural color in red tone while Fuji S2pro (Super CCD) had highest color error which meant that Super CCD could capture least of the natural color in red tone.

From yellow tone analysis, Sigma SD9 (Foveon X3) had lowest color error which meant that Foveon X3 could capture most of the natural color in yellow tone while Canon D60 (CMOS) had highest color error which meant that CMOS could capture least of the natural color in yellow tone.

From green tone analysis, Fuji S2pro (Super CCD) had lowest color error which meant that Super CCD could capture most of the natural color in green color tone while Canon D60 (CMOS) had highest color error which meant that CMOS could capture least of the natural color in green tone.

From blue tone analysis, Fuji S2pro (Super CCD) had lowest color error which meant that Super CCD could capture most of the natural color in green tone while Canon D60 (CMOS) had highest color error which meant that CMOS could capture least of the natural color in blue tone.

5.1.4 Conclusions of Graininess/Noise Measurement

Graininess/noise measurement is to measure the standard deviation of middle gray patch where the standard deviation represents noise of image signal. Lower value of standard deviation will show low and high image signal to noise ratio.

When considering the dark current noise and amplifier noise of each image sensor, the dark current noise can indicate the possibility of amplifier noise that will be occurred in each image sensor type with the different sensitivity (ISO) level.

When analyzing amplifier noise in red, green and blue channel of each image sensor type with the bayer pattern filter array, Nikon D100 (CCD), Fuji S2pro (Super CCD) and Canon D60 (CMOS) have lower noise in green channel than in red and blue channel. For an analysis where is applied with the true color filter array, it shows that Sigma SD (Foveon X3) has similar noise in red, green and blue channel.

For amplifier noise analysis in luminance channel of each image sensor type, Canon D60 (CMOS) has lowest noise value at ISO100 and Fuji S2pro (Super CCD) has lowest noise value at ISO200-ISO1600 while Sigma SD9 (Foveon X3) has highest noise value at all ISOs.

For shot noise analysis in luminance channel of each image sensor type, Canon D60 (CMOS) has the lowest and stable standard deviation at every exposure time about 1 ± 0.7 when comparing to the others while Sigma SD9 (Foveon X3) has the highest standard deviation or noise level in every exposure time where its standard deviation was continuously increase from 0.15 to 4.29 at the exposure time from 1/1.5 sec to 10 sec.

As a conclusion, the measurement result of the image quality of each image sensor can be described as follows:

Nikon D100 (CCD)

- Visual resolution (6.0 mp)
 - Horizontal (LW/PH) : Absolute Res. = 1400 and Extinction Res. = 1600
 - Vertical (LW/PH) : Absolute Res. = 1350 and Extinction Res. = 1600
- Spatial frequency response (6.0 mp)
 - Horizontal SFR(L3) : 50% SFR = 0.18 cycle per pixel location
 - Vertical SFR (L4) : 50% SFR = 0.16 cycle per pixel location
- Dynamic range
 - Dark-white(0-255) = 7.55 stop
 - Dark-gray(0-127) = 5.33 stop
 - Dark-white(0-255) = 2.23 stop
- Color reproduction(True WB)
 - Average Delta E^*_{ab} of gray-scale (neutral tones) = 5.83
 - Average Delta E^*_{ab} of all color tone = 9.65
- Amplifier noise (luminance channel)
 - ISO200 = 1.18
 - ISO400 = 1.29
 - ISO800 = 1.89
 - ISO1000 = 2.09
 - ISO 1600 = 2.68

Fuji S2pro (Super CCD)

- Visual Resolution (12 mp)

- Horizontal (LW/PH) : Absolute Res. = 1800 and Extinction Res. = 2000
- Vertical (LW/PH) : Absolute Res. = 1700 and Extinction Res. = 2000
- Visual Resolution (6.0 mp)
 - Horizontal (LW/PH) : Absolute Res. = 1550 and Extinction Res. = 1700
 - Vertical (LW/PH) : Absolute Res. = 1450 and Extinction Res. = 1700
- Spatial frequency response (6.0 mp)
 - Horizontal SFR(L3) : 50% SFR = 0.22 cycle per pixel location
 - Vertical SFR (L4) : 50% SFR = 0.20 cycle per pixel location
- Dynamic range
 - Dark-white(0-255) = 7.61 stop
 - Dark-gray(0-127) = 5.54 stop
 - Dark-white(0-255) = 2.08 stop
- Color reproduction(True WB)
 - Average Delta E^*_{ab} of gray-scale (neutral tones) = 8.35
 - Average Delta E^*_{ab} of all color tones = 10.83
- Amplifier noise (luminance channel)
 - ISO100 = 0.79
 - ISO200 = 0.87
 - ISO400 = 1.08
 - ISO800 = 1.36
 - ISO 1600 = 1.63

Canon D60 (CMOS)

- Visual Resolution (6.4 mp)

- Horizontal (LW/PH) : Absolute Res. = 1450 and Extinction Res. = 1650
- Vertical (LW/PH) : Absolute Res. = 1350 and Extinction Res. = 1600
- Spatial frequency response (6.4 mp)
 - Horizontal SFR(L3) : 50% SFR = 0.28 cycle per pixel location
 - Vertical SFR (L4) : 50% SFR = 0.22 cycle per pixel location
- Dynamic range
 - Dark-white(0-255) = 8.01 stop
 - Dark-gray(0-127) = 5.57 stop
 - Dark-white(0-255) = 2.44 stop
- Color reproduction(True WB)
 - Average Delta E^*_{ab} of gray-scale (neutral tones) = 6.88
 - Average Delta E^*_{ab} of all color tone = 11.96
- Amplifier noise (luminance channel)
 - ISO100 = 0.74
 - ISO200 = 1.00
 - ISO400 = 1.08
 - ISO800 = 2.05
 - ISO1000 = 2.56

Sigma SD9 (Foveon X3)

- Visual Resolution (6.1 mp)
 - Horizontal LW/PH : Absolute Res. = 1300 and Extinction Res. = 1800
 - Vertical LW/PH : Absolute Res. = 1300 and Extinction Res. = 1800
- Visual Resolution (3.4 mp)

- Horizontal (LW/PH) : Absolute Res. = 1200 and Extinction Res. = 1800
- Vertical (LW/PH) : Absolute Res. = 1200 and Extinction Res. = 1800
- Spatial frequency response (6.0 mp)
 - Horizontal SFR(L3) : 50% SFR = 0.32 cycle per pixel location
 - Vertical SFR (L4) : 50% SFR = 0.26 cycle per pixel location
- Dynamic range
 - Dark-white(0-255) = 7.28 stop
 - Dark-gray(0-127) = 4.94 stop
 - Dark-white(0-255) = 2.34 stop
- Color reproduction(True WB)
 - Average Delta E^*_{ab} of gray-scale (neutral tones) = 9.38
 - Average Delta E^*_{ab} of all color tone = 10.12
- Amplifier noise (luminance channel)
 - ISO100 = 0.94
 - ISO200 = 1.50
 - ISO400 = 2.06

5.2 Suggestion for Further Work

In the area of comparison of the image quality of various image sensor types, further studies in the following aspects should be carried out.

- 1) The thermal noise analysis with temperature control of each image sensor types
- 2) The color spaces comparison of different image sensor types

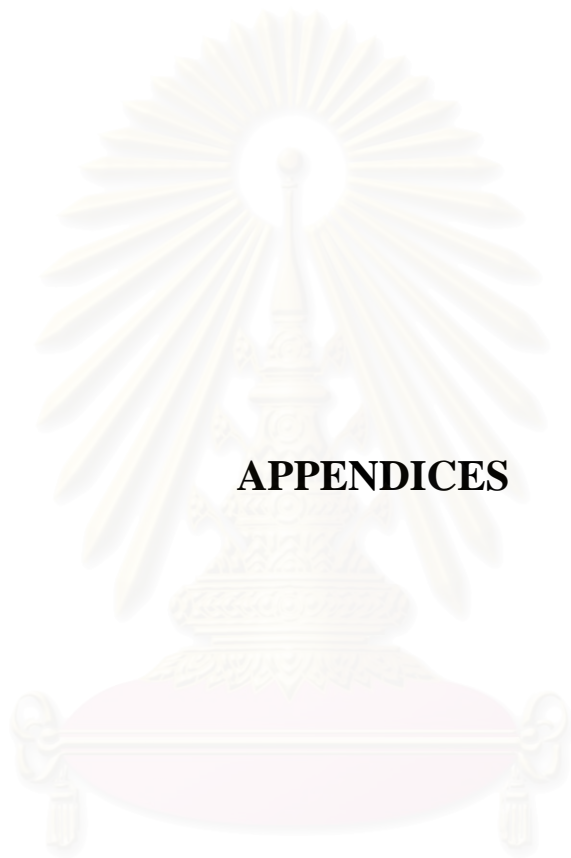
REFERENCES

1. Miyake, Y., Satoh, Y., Yaguchi, H., and Igarashi, T. An Evaluation of Image Quality for Color Images with Different Spatial Frequency Characteristics. *The Journal of Photographic Science*. 38 (1990): 118.
2. Charge Coupled Device (CCD) Image Sensors [Online]. Eastman Kodak Company, NY, 2001. Available from:
<http://www.kodak.com/global/plugins/acrobat/en/digital/ccd/applicationNotes/chargeCoupledDevice.pdf> [2003, June 12].
3. Fujifilm's 3rd Generation Super CCD System [Online]. Fuji Photo Film CO., LTD., 2002. Available from:
http://home.fujifilm.com/photokina2002/data/pr_pdf/di_4a.pdf [2003, June 12].
4. CMOS Sensor Used as a Key Device Applied in Various Equipment [Online]. Canon Inc., 2004. Available from:
<http://www.canon.com/technology/detail/device/cmos/index.html> [2004, June 13].
5. Titus, H. Imaging Sensors That Capture Your Attention [Online]. Eastman Kodak Company, NY, 2001. Available from:

<http://www.kodak.com/global/plugins/acrobat/en/digital/ccd/papersArticles/sensorsCaptureAttention.pdf> [2004, June 03].

6. Bayer, B. Color Imaging Array, *United States Patent*, No. 3, 971, 065, 1975.
7. Hubel, M. P., Liu, J., and Guttosch, J. R. Spatial Frequency Response of Color Image Sensors: Bayer Color Filters and Foveon X3 [Online]. Available from: http://www.foveon.com/X3_tech_papers.html [2004, June 24].
8. ISO12233. *Photography-electronic Still Picture Camera-Resolution Measurements*, 1977.
9. Don, W. Measuring Quality Of Digital Masters [Online]. Available from: <http://lyra2.rlg.org/visguides/visguide2.html> [2004, June 24].
10. ISO 14524. *Photography-Electronic Still Picture Cameras-Methods for Measuring Opto-Electronic Conversion Functions (OECFs)*, 1999.
11. Stokes, M., Anderson, M., Chandrasekar, S., and Motta, R. A Standard Default Color Space for the Internet – sRGB [Online]. 1996. Available from: <http://www.w3.org/graphics/color/srgb.htm> [2003, January 10].
12. Sharma, A. Digital Noise, Film Grain. *Digital Photo Techniques*. (November 2001): 62-63.

13. Uschold, A. Current Capabilities of Digital Cameras and the Comparison of the Classical Architecture of Digital Cameras Based on 35 mm SLR-Systems and a Digital Optimized Architecture [Online]. Available form:
[http://www.uschold.com/pdf/report%20slr%20public %2009. 02%20n.pdf](http://www.uschold.com/pdf/report%20slr%20public%2009.02%20n.pdf)
[2003, January 10].
14. Burns, D. P. and Williams, D. Improved Evaluation of Image Resolution for Digital Cameras and Scanners, *International Conference of Imaging Science*. (2002): 353-354.
15. Roberts, W. J. and Kelley, F. E. Measurements of Static Noise in Display Images, *Electronic Imaging*. (2001): 211-218.
16. Baer, R. L. CCD Requirements for Digital Photography, Image Processing, *Image Quality Image Capture Systems Conference*. (2000): 26-30.
17. Williams, D. SFRwin 1.0 [Computer program]. 2000. Available form:
<http://www.i3a.org/downloads.html> [2003, January 10]
18. Koren, N. SFR Measure Sharpness [Online]. 2004. Available form:
http://www.imatest.com/docs/tour_sfr.html [2004, January 14].



APPENDICES

สถาบันวิทยบริการ
จุฬาลงกรณ์มหาวิทยาลัย

APPENDIX A

SENSOR LINEARIZATION

- **Lookup Table Preparation**

Due to the fact that image sensor does not response to light in a linear manner, therefore, it is necessary to perform linear of an image captured by each image sensor. Kodak grayscale is used to find out the LUT data. This chart has 12 patches at different refecton density as shown in table A-1

Table A-1 The relationship between the density and reflectance of Kodak grayscale and the pixel value of image captured by each image sensor.

Density	Reflectance	Nikon D100 (CCD)	Fuji S2pro (SUPER CCD)	Canon D60 (CMOS)	Sigma SD9 (FOVEON X3)
1.75	0.0178	14.09	25.87	20.20	23.56
1.55	0.0282	28.33	34.91	25.29	33.56
1.40	0.0398	36.99	46.88	33.02	44.08
1.23	0.0589	50.56	57.40	44.05	57.86
1.08	0.0832	67.00	71.35	55.77	73.37
0.92	0.1202	86.74	88.22	71.90	91.21
0.79	0.1622	106.10	105.18	87.77	109.40
0.61	0.2455	131.30	126.88	108.42	132.97
0.47	0.3388	151.26	146.13	125.07	152.74
0.33	0.4677	174.56	163.22	143.60	174.56
0.20	0.6310	192.51	183.85	163.74	194.80
0.04	0.9120	219.05	213.82	188.66	216.54

From table A-1, the density is obtained from measurement of gretag spectrolino and the reflectance is derived from equation A-1.

The optical density is traditionally measured with filter instruments. For a given reflectance, R, the density D is found by:

$$D = -\log R \quad (\text{A-1})$$

where,

- D : Optical density
R : Relative reflectance

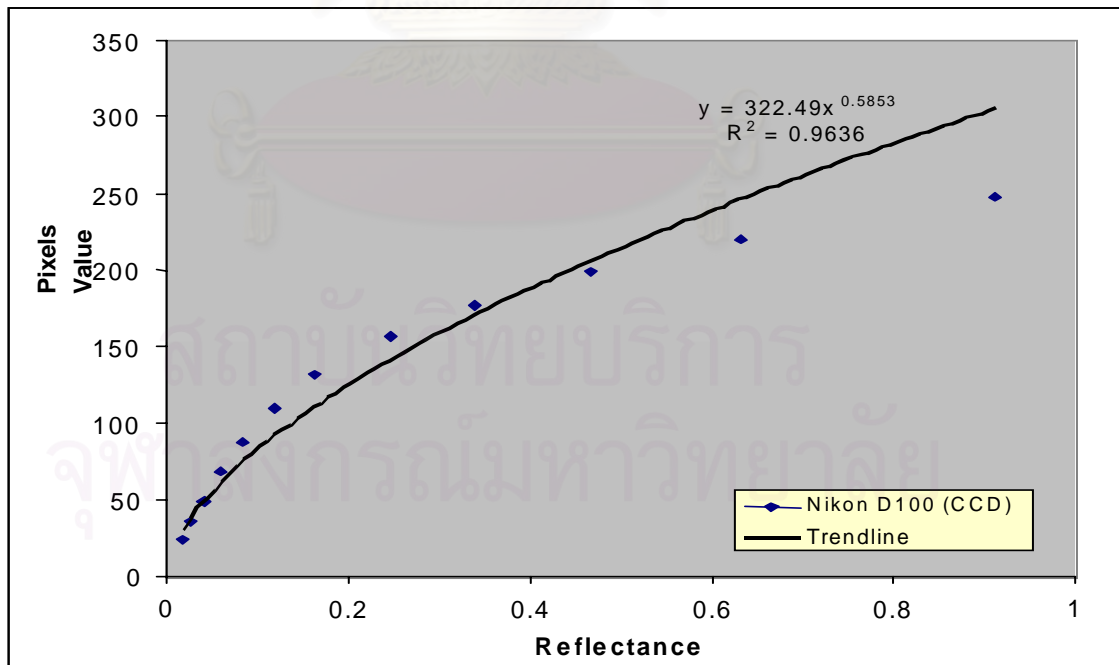


Figure A-1 Tonal response curves for Nikon D100 (CCD).

To prepare LUT as see from figure A-1, the given trendline of regression line approximates is not fitted well with the value from the measurement. Therefore, the darkness point is adjusted to the most at (0, 1) and the whiteness point is adjusted to the most at (255, 256) as be shown in table A-2.

Table A-2 The reflectance and pixel value of Kodak grayscale of each image sensor after adjustment.

Reflectance				Pixels Value			
Nikon D100 (CCD)	Fuji S2pro (SUPER CCD)	Canon D60 (CMOS)	Sigma SD9 (FOVEON X3)	Nikon D100 (CCD)	Fuji S2pro (SUPER CCD)	Canon D60 (CMOS)	Sigma SD9 (FOVEON X3)
1.00	1.00	1.00	1.00	0.00	0.00	0.00	0.00
18.72	13.26	8.70	14.21	13.21	12.26	7.70	13.21
29.49	29.51	20.41	28.11	27.11	28.51	19.41	27.11
46.37	43.78	37.10	46.32	45.32	42.78	36.10	45.32
66.83	62.70	54.84	66.82	65.82	61.70	53.84	65.82
91.39	85.59	79.26	90.39	89.39	84.59	78.26	89.39
115.47	108.60	103.28	114.43	113.43	107.60	102.28	113.43
146.83	138.04	134.54	145.57	144.57	137.04	133.54	144.57
171.66	164.16	159.74	171.70	170.70	163.16	158.74	170.70
200.65	187.35	187.79	200.53	199.53	186.35	186.79	199.53
222.98	215.34	218.28	227.27	226.27	214.34	217.28	226.27
256.00	256.00	256.00	256.00	255.00	255.00	255.00	255.00

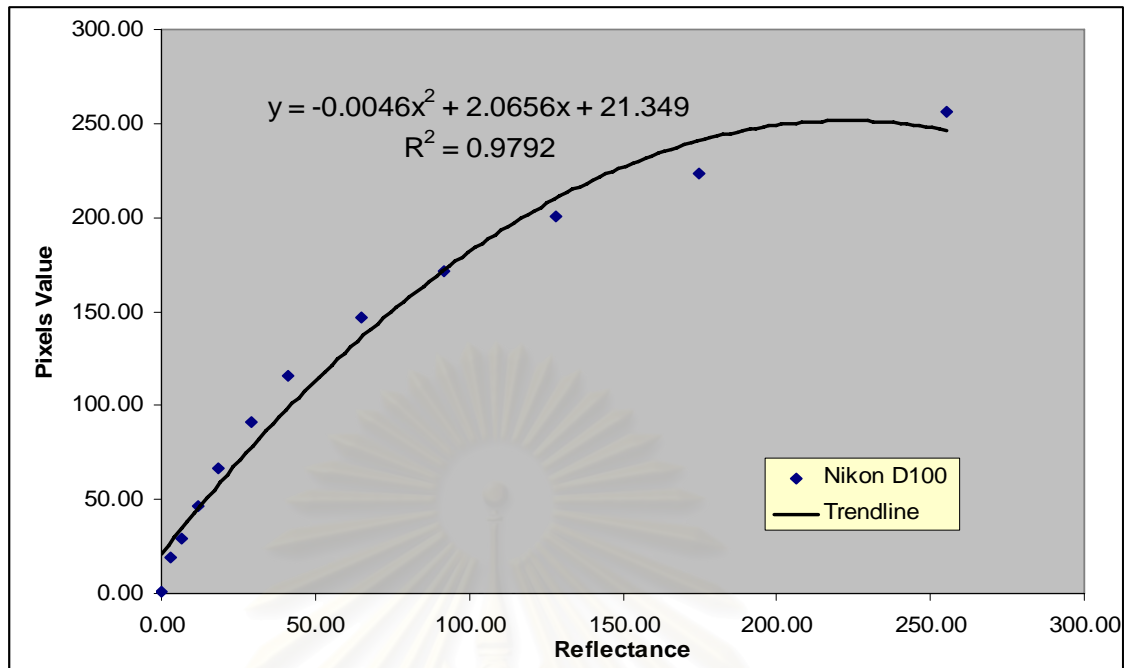


Figure A-2 Tonal response curve for Nikon D100 (CCD) after adjusting the reflectance and pixel value

However, the given trendline of regression line approximates is still not fitted well with the most darkness point at (0, 1) and the most whiteness point at (255, 256). Therefore, the regression line approximates with almost 1 will be separated into 4 parts as be shown in figure A-3 to figure A-6.

From figure A3 to figure A6, the regression line approximates will be calculated for Lookup Table (LUT) of Nikon D100 by putting x and y value in the equation of regression line approximates.

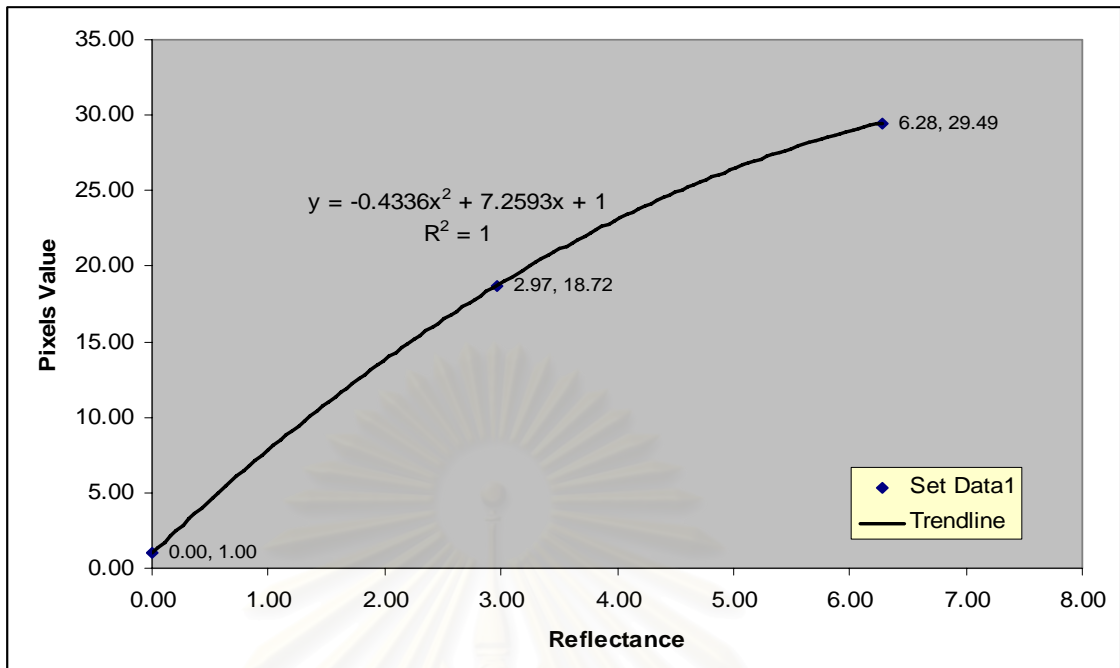


Figure A-3 Tonal response curves for Nikon D100 (CCD) – Set Data 1 after adjusting the reflectance and pixel value of Kodak grayscale

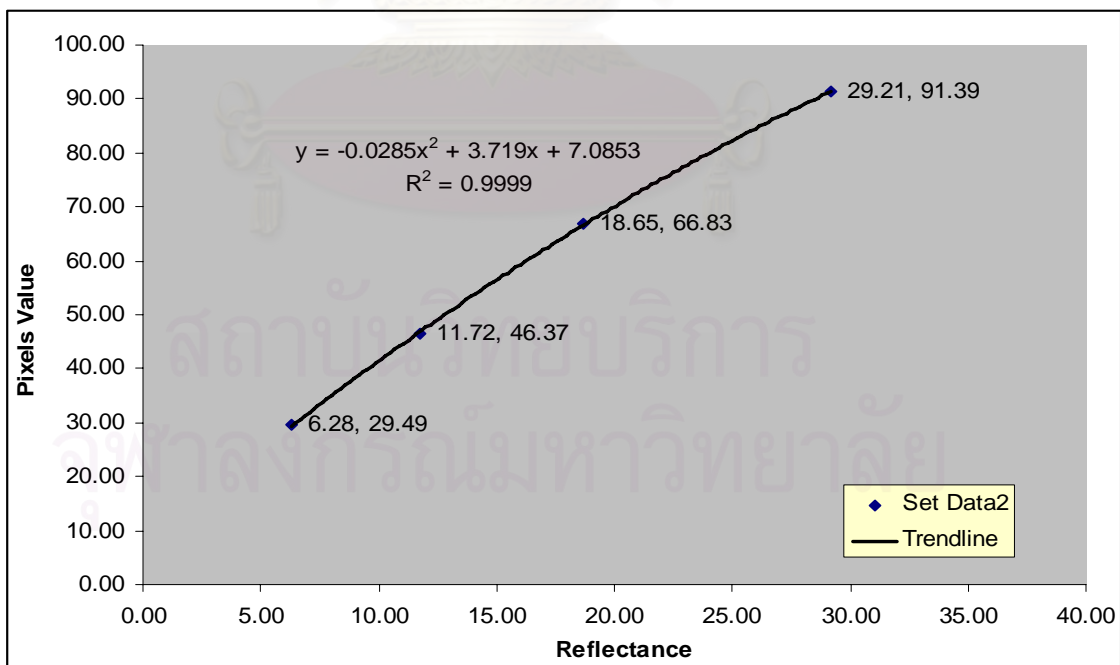


Figure A-4 Tonal response curves for Nikon D100 (CCD) – Set Data 2 after adjusting the reflectance and pixel value of Kodak grayscale

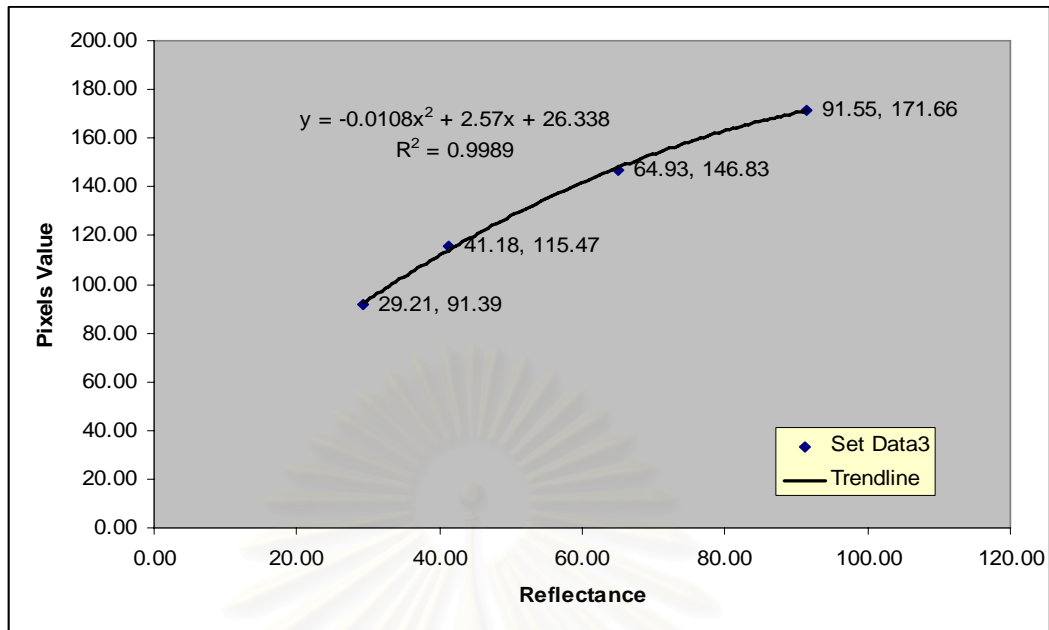


Figure A-5 Tonal response curves for Nikon D100 (CCD) – Set Data 3 after adjusting the reflectance and pixel value of Kodak grayscale

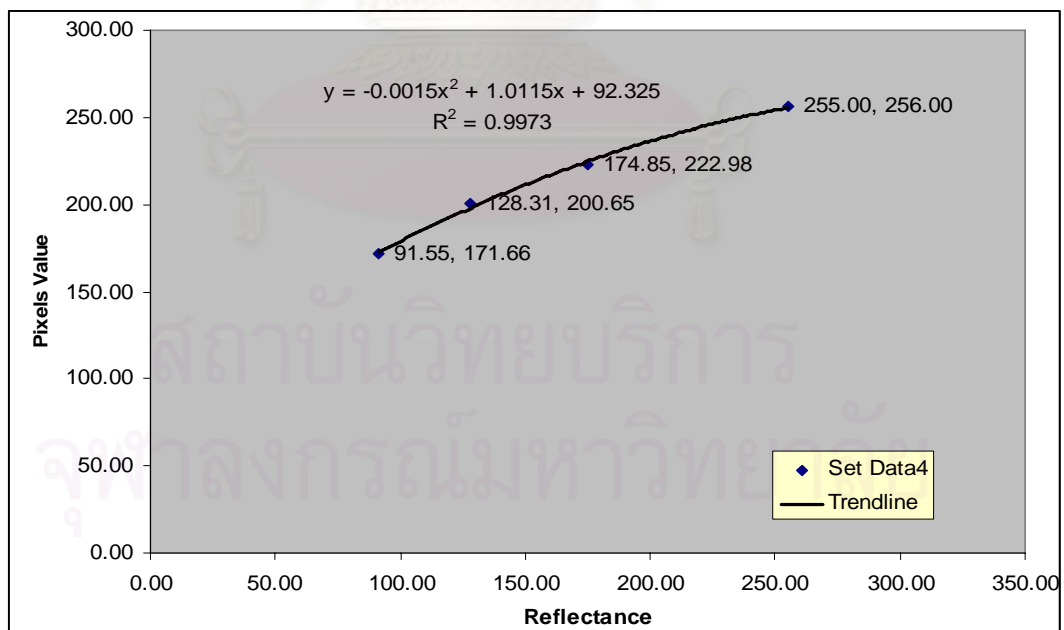


Figure A-6 Tonal response curves for Nikon D100 (CCD) – Set Data 4 after adjusting the reflectance and pixel value of Kodak grayscale

APPENDIX B

TONE REPRODUCTION MEASUREMENT

As a result of the differentiation of shadow details and high light details in each image sensor type, the minimum point of the shadow detail are significant to measure the tone reproduction as be shown in table 4-7 where Δ pixels value equals to 4. The maximum point of high light detail usually is 5% of above fog in this case it was calculated form 95% of maximum pixel value. Thereafter, tone reproductions from pixel value are used to calculate the dynamic range through the equation B-1 and result are represented in figure B-1.

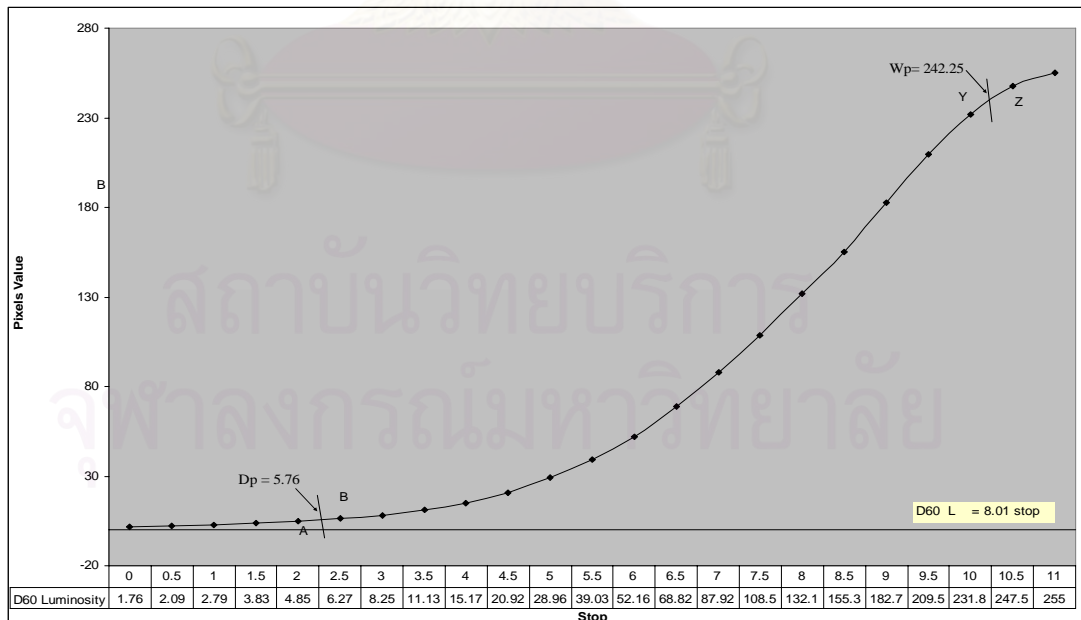


Figure B-1 The dynamic range from calculating tone reproduction at luminosity channel of Canon D60

From figure B-1, the lowest and highest point of dynamic range can be estimated from the interpolation approximation theory. Equation B-2 is calculated from plotting graph at data interval of 0.5 stop.

$$\left[\frac{B - D_p}{B - A} \right] / 2 + [N] / 2 + \left[\frac{Y - W_p}{Z - Y} \right] / 2 = S \quad (B-1)$$

$$D_p = L - L_s \quad (B-2)$$

$$W_p = 0.95U \quad (B-3)$$

where,

D_p : The minimum point of pixels value for dynamic range calculation

W_p : The maximum point of pixels value for dynamic range calculation

L : The minimum point of pixels value of image sensor

L_s : The lowest margin at 4 where shadow details classified with human eye

U : The maximum point of pixels value of image sensor

D_p : The lowest acceptant point of pixels value

W_p : The highest acceptant point of pixels value

A : Prior to the lowest point of pixels value for dynamic range calculation

B : Later to the lowest point of pixels value for dynamic range calculation

Y : Prior to the highest point of pixels value for dynamic range calculation

Z : Pater to the highest point of pixels value for dynamic range calculation

N : Total number of scales counted from B to A

APPENDIX C

SFR MEASUREMENT ALGORITHM C-CODE

```
/*
//sfr_computation.c
//Copyright (c) Polaroid Corporation, 1994,1995          All Rights Reserved.
//
//Portions of this source code were provided by Eastman Kodak Company for use by
//the ISO and have been previously copyrighted by Eastman Kodak Company. All
//remaining source code is Copyright (c) Polaroid Corporation, 1994-1995 All
//Rights Reserved. Requests for permission to duplicate, distribute, publish, or
//otherwise copy
//this code should be directed to Eric W. Higgins or Andrew K. Juenger, Polaroid
//Image Science Laboratory,
//750 Main Street MS-3J, Cambridge, Massachusetts, 02139 USA.
*/
#include "plugin.h"
# include "sfr_computation.h"
# include "io_routines.h"
# include "UserInterface.h"
# include "radiometric_tranform.h"
//.macros
static double dmaxarg1, dmaxarg2;
#define DMAX(a,b) (dmaxarg1=(a), dmaxarg2=(b),( dmaxarg1) > ( dmaxarg2)?\
    (dmaxarg1) : (dmaxarg2))

static double dminarg1, dminarg2;
#define DMIN(a,b) (dminarg1=(a), dminarg2=(b),( dminarg1) < ( dminarg2)?\
    (dminarg1) : (dminarg2))

static double sqrarg;
#define SQR(a) ((sqrarg=(a)) == 0.0? 0.0 : sqrarg * sqrarg)
short sfrProc (GHdl globals, dblHandle FreqHdl, dblHandle dispString)

{
    unsigned short    i, j, nSamplesPerPixel, tmpalpha, err = 0;
    long              pcnt, pcnt2, col, ww_in_pixel;
    double            dt, dtl, sfr, tmp, tmp2, slope;
    OSErr             erro = 0;
    Unsigned long     size_x, size_y;

    uHandle            area=nil;
}
```

```

dbHandle
darea=nil,temp=nil,shifts=nil,edgex=nil,Signal=nil;
dbHandle          AveEdge=nil,AveTmp=nil,farea=nil;
longHandle        counts=nil;
size_x = gStuff->inRect.right - gstuff->inRect.left;
size_y = gStuff->inRect.bottom - gstuff->inRect.top;
nSamplesPerPixel = gstuff->imageMode;
ww_in_pixels = size_x;

//Verify input selection dimensions are EVEN
if (fmod((double)size_x,2.0) !=0.00)
    { ShowAlertText(SHOWALERTSTOP,SFRERR,5);
      gResult = 1;
      return 1;
    }
if (fmod((double)size_y,2.0) !=0.00)
    { ShowAlertText(SHOWALERTSTOP,SFRERR,6);
      gResult = 1;
      return 1;
    }
}
//Allocate memory
    This code not shown
//Load the image data into the "area" array
if (TestAbort 0) {
    gResult = 1;
    return 1;
}
    err = load_area_array(globles, area); if (err !=0) {
    gResult = 1;
    return 1;
}
if (TestAbort 0) {
    gResult = 1;
    return 1;
}
    err = radiometric_conversion(globles, area, darea); if (err !=0) {
    gResult = 1;
    return 1;
}
//Extract first color channel (luminance)
-for (j=0; j<size_y; j++) {
    for ((i=0; i<size_x; i++) {
        (*farea)[((j*(long)size_x)+i)] =
            (*darea)[(nSamplesPerPixel*((j*(long)size_x)+i))+OL];
    }
}
err = check_image_data(globles, farea, darea);
if (err != 0) {
    gResult = 1;
    return 1;
}

```

```

    }
    if (TestAbort ()) {
        gResult = 1;
        return 1;
    }
    err = locate_centroids(globals, farea, temp, shifts); if (err != 0) {
        gResult = 1;
        return 1;
    }
//Calculate the best fit line to the centriods
    err = fit(size_y, temp, shifts, &slope);
    if (err != 0) {
        gResult = 1;
        return 1;
    }
    if (fabs(slope) < (1.0/(double)size_y) || slope > (double)(1.0/4.0)) {
        ShowAlertText(SHOWALERTSTOP, SFRERR,4);
        gResult = 1;
        return 1;
    }
}
/*****
/* Figure out how many lines to use for size_y; new window will start at top and go
down that number of lines <size_y such that an integer number of x-transitions are
made by the edge; for example, if we had a slope of 10 (the edge goes down 10 lines
before jumping over one pixel horizontally), and size_y = 35, the new size_y is going
to be 30 (an integer multiple of 10, less than 35). */
size_y = (unsigned short)(long)(size_y*slope)*(1.0/slope));

//refernce the temp and shifts values to the new y center
col = (long) size_y/2;
for (i = 0; i < size_y; i++) {
    (*temp)[i] = (double)i-(double)col;
}

//Instead of using the values in shifts, synthesize new ones based on the best fit line.
for (i = 0; i < size_y; i++) {
    (*shifts)[i] = slope * ((*temp)[i]);
}

//compute the global MAX and MIN
dt = 99999999.9;
dtl = -99999999.9;
pcnt = 0;
for (j = 0; j < size_y; j++) {
    for (i = 0; i < size_x; i++){ dt = DMIN(dt, (*farea)[pcnt]);
    dtl = DMAX(dtl, (*farea)[pcnt]); pcnt++;
    }
}

```

```

if (TestAbort ()) {
    gResult = 1;
    return 1;
}

//Calculate a long paired list of x values and signal values
pcnt 0;
for (j = 0; j<size_y; j++) {
    for (i = 0; i<size_x; i++) {
        (*edgex)[pcnt] = (double)I - (*shifts)[j];
        (*Signal)[pcnt] = (((*farea)[((j*(long)size_x)+i)]) - dt)/(dtl-dt);
        pcnt++;
    }
}
tmpalpha = (unsigned short)ALPHA;
err = bin_to_regular_xgrid(globals, &tmpalpha, edgex, Signal, AveEdge, counts,
size_y); if (err != 0) {
    gResult = 1;
    return 1;
}
calculate_derivative (globals, (unsigned short) ALPHA, AveTmp, AveEdge);
locate_max_PSF(globals, (unsigned short) ALPHA, AveEdge, size_x, &pcnt2);
apply_hamming_window (globals, (unsigned short) ALPHA, (unsigned
short)ww_in_pixels, Aveedge, &pcnt2);

tmp = 1.0;
tmp2 = 1.0/((double)size_x*ALPHA);

if (TestAbort ()) {
    gResult = 1;
    return 1;
}
//ftwos (nx, dx, lsf(x), nf, df, sfr(f)
(void) ftwos(globals, (long) ALPHA *size_x, &tmp, AveEdge,
(long)(size_x*ALPHA/2.0), &tmp2, AveTmp);
if (TestAbort ()) {
    gResult = 1;
    return 1;
}
for(i = 0; i<(long)((double)size_x*ALPHA/2.0); i++)
{
    sfrc = (*AveTmp)[i];
    (*FreqHdl)[i] = ((double)i/(double)size_x;
    (*dispString)[i] = (double) (sfrc/(*AveTmp)[0]);}
//I/O code calls here...
if (TestAbort ()) {
    gResult = 1;
    return 1;
}
return(0);

```

```

}

#pragma mark --- pre-check the data ---
/*****/
unsigned short check_image_data(GHdl globals, dblHandle farea, dblHandle temp) {
    long j = 0;
    double dt, dt1, dt2, dt3;
    unsigned short size_x, size_y;
    OSErr erro = 0;
// --> check to make sure there is a clear black to white or white to black
// transition on both the bottom and the top of the image
// --> if there is not at least 20% difference between the left and right side of the
// image box, return with an error of 5: calling program will display an error
// message.
// --> If the transition left -> right is white-> black, flip the data left to right
// (the rest of the routine assume a black to white transition from left to right)

size_x = gStuff -> inRect.right - gStuff -> inRect.left;
size_y = gStuff -> inRect.bottom - gStuff -> inRect.top;

//Get averages of 4 pixels in each corner of the input image */
//upper right corner
dt = (*farea)[(size_x-1)] + (*farea)[(size_x-2)];
dt = dt + (*farea)[2*size_x-1] + (*farea)[2*(long)size_x-2];
dt = dt/4.0;

//lower right corner
dt1 = (*farea)[(size_x*(long)size_y)] + (*farea)[(size_x*(long)size_y-2)];
dt1 = dt1 + (*farea)[((size_y-1)*(long)size_x-1)] + (*farea)[((size_y-1)*(long)size_x-2)];
dt1 = dt1/4.0

//lower left corner
dt2 = (*farea)[((size_y-1)*(long)size_x)] + (*farea)[((size_y-1)*(long)size_x+1)];
dt2 = dt2 + (*farea)[((size_y-2)*(long)size_x)] + (*farea)[((size_y-2)*(long)size_x+1)];
dt2 = dt2/4.0

//upper left corner
dt3 = ((*farea)[0] + (*farea)[1] + (*farea)[size_x] + (*farea)[size_x+1])/4.0;

// If there is not at least 20% difference between the left and right sides of the
// image box, return with an error of 5: calling program will display an error
// message.

if (fabs(dt-dt3) < 0.20) j = 1;
if (fabs(dt1-dt2) < 0.20) j = 1;
if (j) {
if (ShowAlertText(SHOWALERTWARN, SFRERR, 2) == 2) {
gResult = 1;
}
}
}

```



```

        return 5
    }
}

//If the transition left -> right is white -> black, flip the data left to right // (the rest of
the routine assumes a black to white transition from left to right )
flip_image_data_horiz(globals, farea, temp, &dt, &dt1,&dt2, &dt3);
return 0;
}

/*****
void flip_image_data_horiz(GHdl globals, dblHandle farea, dblHandle darea, double
* dt, double*dt1,double *dt2,double *dt3)
{
    unsigned long i, j;
    unsigned short size_x, size_y;

    size_x = gStuff->inRect.right - gStuff->inRect.left;
    size_y = gStuff->inRect.bottom - gStuff->inRect.top;

//If the transition left -> right is white -> black,
//flip the data left to right
    if ( ((*dt) < (*dt3)) D ((*dt1) < (*dt2) ) ) {
        for (I = 0; i < size_y; i++) {
            for (j = 0; j < size_x; j++) {
                (*darea)[j] = (*farea)[(i*(long)size_x)+(size_x-1L)-j]; }
            for (j = 0; j < size_x; j++) {
                (*farea)[i*(long)size_x+j] = (*darea)[j];
            }
        }
    }
}

#pragma mark ---- vector processing routines----
/*****
unsigned short locate_centroids(GHdl globals, dblHandle farea, dblHandle temp,
dblHandle shifts) {
    unsigned long i, j;
    double dt, dt1, dt2;
    unsigned short size_x, size_y;
    size_x = gStuff->inRect.right - gStuff->inRect.left; size_y = gStuff->inRect.bottom -
gStuff->inRect.top;

//Compute the first difference on each line. Interpolate to find the centroid of the first
derivatives.
    for (j = 0; j < size_y; j++) {
        dt = 0.0;
        dt1 = 0.0;
        for (i = 0; i < size_x-1; i++) {

```

```

        dt2 = (*farea)[((j*(long)size_x)+ i)+1] - (*farea)[((j*(long)size_x)+ i)]; dt +=
dt2 * (double)I;
        dt1 += dt2;
    }
    (*shifts)[j] = dt/dt1;
    if (TestAbort ()) {
        gResult = 1;
        return 1;
    }
}

// check again to be sure we aren't too close to an edge on the corners. If the
// black to white transition is closer than 2 pixels from either side of the
// data box, return an error of 5; the calling program will display an error
// message (the same one as if there were not a difference between the left and
// right sides of the box)
if ((*shifts)[size_y-1] < 2) {
    ShowAlertText(SHOWALERTSTOP, SFRERR, 3);
    return 5;
}

    if (fabs((*shifts)[0] - size_x) < 2 ) {
        ShowAlertText(SHOWALERTSTOP, SFRERR, 3);
        return 5;
    }
        // Reference shifts to the vertical center of the data box
j = size_y/2;
dt = (*shifts)[j];
for (i = 0; i < size_y; i++)
    {
        (*temp)[i] = (double)i - (double)j;
        (*shifts)[i] = dt;
    }
    return = 0;
}
/*****
/unsigned short fit(unsigned long ndata, db1Handle x, db1Handle y, double * b)
{
    unsigned long i;
    double t, sxoss, sx =0.0, sy = 0.0, st2 = 0.0, ss, sigdat, chi2, a, siga, sigb;

    *b = 0.0;
    for (i =0; i < ndata; i++) {
        sx += (*x)[i];
        sy += (*y)[i];
    }
    ss = (double)ndata;
    sxoss = sx/ss;
    for (i = 0; i < ndata; i++) {
        t = (*x)[i] - sxoss;

```

```

    st2 += t*t;
    *b += t* (*y)[i];
  }
  *b/ = st2; // slope
  a = (sy - sx*(*b))/ss; // offset
  siga = sqrt((1.0 + sx*sx/(ss*st2))/ss);
  sigb = sqrt(1.0/st2);
  chi2 = 0.0;

  for (i = 0; i < ndata; i++) chi2 += SQR((*y)[i] - a - (*b) * (*x)[i]); sigdat =
sqrt(chi2/(ndata - 2));
  siga *= sigdat;
  sigb *= sigdat;
  return 0;
}

/*****
/* Notes: this part gets averages and puts them in a number of bins, equal to size_x
times alpha. Next a long check is done in case one bin gets no values put into it: if this
is the case, it will keep checking previous bins until it finds one with non-zero counts
and will use that value as its current bin average. If the first bin has zero counts the
program checks bins in the forward rather than reverse direction. If, in any case, the
end of the array of bins is reached before finding a non-zero count, the program starts
checking in the opposite direction. A bin with zero counts must be avoided because
each bin will be divided by counts at the end. */

unsigned short bin_to_regular_xgrid(GHdl globals, unsigned short *alpha, dblHandle
edgex, dblHandle Signal, dblHandle AveEdge, longHandle counts unsigned long
size_y)
{
  long i, j, k, bin_number;
  unsigned short size_x;
  size_x = gStuff->inRect.right - gStuff->inRect.left;

  for (i = 0; i < (size_x * (*alpha)); i++) {
    (*AveEdge)[i] = 0;
    (*counts)[i] = 0;
  }
  for (i=0; i < (size_x * (long)size_y; i++) {
    bin_number = (long) ((*alpha) * ((edgex)[i]));
    if (bin_number >= 0 {
      if (bin_number <= (size_x * (*alpha) - 1)) {
        if (bin_number == 0) {
        }
        (*AveEdge)[bin_number] = (* AveEdge)[bin_number] + (* Signal)[i];
      }
    }
  }
  if (TestAbort () ) {gResult = 1; return 1;
}
}

```

```

for (i= 0; i<size_x>(*alpha); i++) {
if (TestAbort()) {
    gResult = 1;
    return 1;
    }
    j = 0;
    k = 1;
    if ((*counts)[i] == 0) {
    if (i = 0) {
        while (!j) {
            if ((*counts)[i+k] != 0) {
                (*AveEdge)[i] =
(*AveEdge)[i+k]/((double)(*counts)[i+k]);
                j = i;
            }
            else k++;
        }
        } else {
while (!j &&((i - k)>= 0))
{
    if ((*counts)[i-k] != 0) {
        (*AveEdge)[i] = (*AveEdge)[i-k]/((double)(*counts)[i-k]);
        j = 1;
    } else k++;
    }
    if ((i-k) < 0) {
        k = 1;
        while (!j) {
            if ((*counts)[i+k] != 0) {
                (*AveEdge)[i] = (*AveEdge)[i+k]/((double) *
(*counts)[i+k]);
                j = 1;
            } else k++;
        }
    }
} else (*AveEdge)[i] = ((*AveEdge)[i]/((double)(*counts));
}
return 0;
}

```

```

/*****/
void calculate_derivative(Ghdl globals, unsigned short alpha, dblHandle AveTmp,
dblHandle AveEdge)
{
    unsigned long I;
    unsigned short size_x;
    size_x = gStuff -> inRect.right - gStuff -> inRect.left;
    for (i=0; i< (size_x*alpha; i++) (*AveTmp)[i] = (*AveEdge)[i];

```

```

        for (i=1;i<(size_x*alpha-1); i++){(*AveEdge)[i] = ((*AveTmp)[i+1] -
(*AveTmp)[i-1])/2.00;
        (*AveEdge)[0] = (*AveEdge)[1];
        (*AveEdge)[size_x*alpha-1] = (*AveEdge)[size_x*alpha -2];
    }
/*****/
void locate_max_PSF(GHdl globals, unsigned short alpha, dblHandle AveEdge, long
size_x, long *pcnt2) {
    unsigned long i;
    double dt = 0.0, dt_new = 0.0;
    long scnt2 = OL, left = -1L, right = -1L;
// find maximum value in Point Spread Function array */
    for (i=0; i<size_x*alpha; i++) {
        dt_new = fabs((*AveEdge)[i]);
        if (dt_new > dt) {
            (*pcnt2) = (long) i;
            dt = dt_new;
        }
    }
//find leftmost and rightmost occurrence of maximum */
    for (i=0; i<size_x*alpha; i++) {
        dt_new = fabs((*AveEdge)[i]);
        if (dt_new == dt) {
            if (left < 0) = left = i;
            right = i;
        }
    }
//find center of maxima */
    (*pcnt2) = (right + left)/2;
}

/*****/
void apply_hamming_window(GHdl globals, unsigned short alpha, unsigned short
newxwidth, dblHandle AveEdge, long *pcnt2)
{
    long i, j, begin, end, edge_offset;
    double sfrc;
    unsigned short size_x;
    size_x = gStuff -> inRect.right - gStuff -> inRect.left;
//Shift the AveEdge [i] vector to center the lsf in the transform window
edge_offset = (*pcnt2) - (size_x*alpha/2);
if (edge_offset != 0) {
    if (edge_offset < 0) {
        for (i=size_x*alpha-1; i> -edge_offset-1; i--)
(*AveEdge)[i+edge_offset];
        for (i=0; i<-edge_offset; i++) (*AveEdge)[i] = 0.00; /* must be last
operation */
    } else {
        for (i=0; i<size_x*alpha-edge_offset; i++){(*AveEdge)[i] =
(**AveEdge)[i+edge_offset];

```

```

        for (i=size_x*alpha-edge_offset; i<size_x*alpha; i++) (*AveEdge)[i] =
0.00;
    }
}
//Multiply the LSF data by a Hamming window of width NEWXWIDTH*alpha
begin = (size_x*alpha/2)-(newxwidth*alpha/2);
if (begin < 0)begin = 0;
end = (size_x*alpha/2)+(newxwidth*alpha/2);
if (end > size_x*alpha) end = size_x*alpha;
for (i=0; i<begin; i++)(*AveEdge)[i] = 0.0;
for (i=end; i<size_x*alpha; i++)(*AveEdge)[i] = 0.0;

for (i=begin, j= -newxwidth*alpha/2; i<end; i++, j++) {
    sfrc = 0.54 + 0.46*cos((PI*(double)j)/(newxwidth*alpha/2));
    (*AveEdge)[i] = ((*AveEdge)[i])*sfrc;
}
}

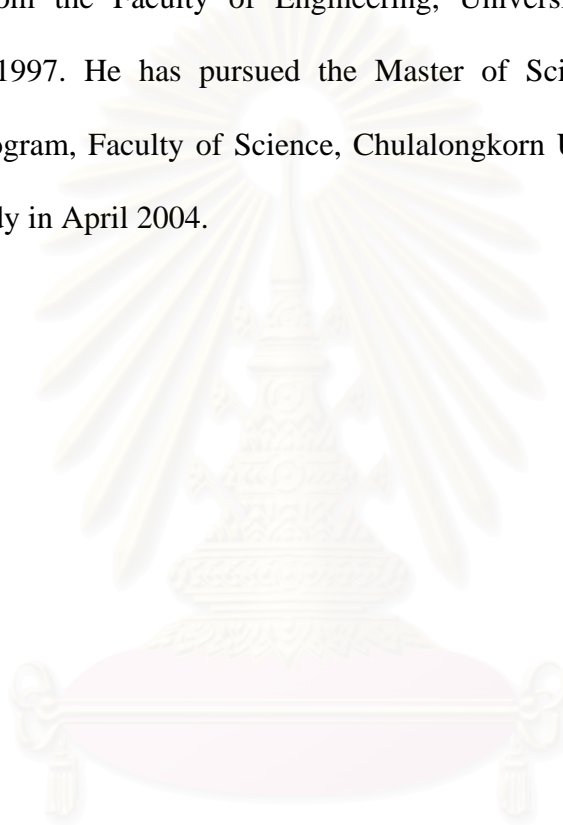
/*****
unsigned short ftwos(GHdl globals,long number, double*dx, dblHandle lsf, long ns,
double *ds, dblHandle sfr)
{
    double a, b, twopi, g, *ind = nil;
    long i, j;

    twopi = 2.0 *PI;
    for (j = 0; j < ns; j++) {
        g = twopi * (*dx) * (*ds) * (double)j;
        for (i=0, a = 0, b = 0; i< number; i++) {a += (*lst[i] * cos(g *
(double) i);
            b += (*lst[i] *sin(g * (double) i); }
        (*sfr)[j] = sqrt(a * a + b * b); if (TestAbort ()) {
            gResult = 1;
            return 1;
        }
    }
    return 0;
}

```

VITA

Mr. Viriya Pornkulvilai was born on January 8, 1975 in Bangkok, Thailand. He graduated with a Bachelor of Degree in Industrial Engineering Department, from the Faculty of Engineering, University of Thai Chamber of Commerce in 1997. He has pursued the Master of Science Degree in Imaging Technology Program, Faculty of Science, Chulalongkorn University since 2001 and finished his study in April 2004.



สถาบันวิทยบริการ
จุฬาลงกรณ์มหาวิทยาลัย